NATIONAL LIBRARY
OTTAWA

BIBLIOTHÈQUE NATIONALE
OTTAWA

CANADA

8490

NAME OF AUTHOR...Rumfeldt, R.C.

TITLE OF THESIS...The radiation chemistry of hydrogen halides.

UNIVERSITY...U of A at Calgary

DEGREE FOR WHICH THESIS WAS PRESENTED...Ph.D.

YEAR THIS DEGREE GRANTED...1963

Permission is hereby granted to THE NATIONAL LIBRARY OF CANADA to microfilm this thesis and to lend or sell copies of the film.

The author reserves other publication rights, and neither the thesis nor extensive extracts from it may be printed or otherwise reproduced without the author's written permission.

(Signed) Robert C. Rumfeldt

PERMANENT ADDRESS:

DEPT. OF CHEMISTRY
U. of WINDSOR
WINDSOR, ONTARIO

DATED...Mar. 31/71...19

NL-91 (10-68)

THE UNIVERSITY OF ALBERTA

THE RADIATION CHEMISTRY OF HYDROGEN HALIDES

A THESIS

SUBMITTED TO THE FACULTY OF GRADUATE STUDIES IN PARTIAL
FULFILMENT OF THE REQUIREMENTS FOR THE DEGREE OF DOCTOR
OF PHILOSOPHY

DEPARTMENT OF CHEMISTRY

by

R.C. RUMFELDT, B.Sc.

CALGARY, Alberta

JUNE, 1963

© R.C. Rumfeldt 1971

UNIVERSITY OF ALBERTA

FACULTY OF GRADUATE STUDIES

The undersigned certify that they have read, and recommend to the Faculty of Graduate Studies for acceptance, a thesis entitled

THE RADIATION CHEMISTRY OF HYDROGEN HALIDES

submitted by R.C. Rumfeldt in partial fulfilment of the requirements for the degree of Doctor of Philosophy

D.A. Armstrong
(Supervisor)

Peter J. Krueger

(External Examiner)

Date. Jun. 19th, 1963

ABSTRACT

The Co^{60} γ-radiolyses of HCl and HBr in the liquid (-79°C) and in the solid (-196°C) phases were investigated. Hydrogen yields for the pure liquids ($G(H_2)_{HCl} = 6.5_3 \pm 0.1_0$ and $G(H_2)_{HBr} = 12.4_2 \pm 0.06$) were independent of dose. G-values for the solid phase irradiation at doses in excess of $\sim 2 \times 10^{18}$ ev/gm were $G(H_2)_{HCl} = 3.3_6 \pm 0.1_0$ and $G(H_2)_{HBr} = 10.5_0 \pm 0.1_0$, however for smaller doses these values increase. The true initial values of $G(H_2)$ for the solid phase radiolyses appeared to be nearly identical with the liquid phase values.

The addition of low concentrations of bromine or ethylene caused a reduction in the hydrogen yield from liquid HCl. These results were interpreted in terms of the formation of hydrogen in the reactions

$$H + HCl \longrightarrow H_2 + Cl \qquad [10]$$

and

$$H(hot) + HCl \longrightarrow H_2 + Cl \qquad [10^*]$$

The reduction of the hydrogen yields was attributed to the reactions

$$H + S \longrightarrow \text{product} \qquad [15]$$

and

$$H(hot) + S \longrightarrow \text{product} \qquad [15^*]$$

or

$$HCl^* + S \longrightarrow HCl + S^* \qquad [28]$$

The rate constant ratios calculated were shown to be characteristic of hydrogen atom reactions and the values of G_H and G_{H^*} were found to be 2.4±0.2 and 4.1±0.2 respectively. These results were consistent with a mechanism which predicted the formation of thermal hydrogen atoms from the reaction

$$e + H\text{-}Cl\text{--}H\text{-}Cl \longrightarrow H + Cl^-\text{--}H\text{-}Cl \qquad [7a]$$

The addition of increasing amounts of HBr to HCl (-79°C) caused only a gradual rise in the hydrogen yield. The use of bromine as a scavenger in HCl - HBr mixtures indicated that track recombination reactions were not important and that the higher yields for HBr must be

attributed to a greater initial sensitivity of the HBr to radiation. From the mixture studies, a value of $G_H = 4.0$ for HBr was found, however a direct determination in pure HBr was precluded due to deviations from hydrogen atom kinetics. An alternate electron scavenging mechanism has been considered.

A brief investigation of the radiation-induced addition of HBr to ethylene was made. The results were consistent with a long chain free radical mechanism. 1-Bromopropane was the principal product of the radiolysis of HBr - propylene mixtures which further confirmed the free radical character of the radiation-induced addition of HBr to olefins.

The results of the radiolysis of solid hydrogen halides indicated that hydrogen was being formed during the radiolysis by at least two different species. The first species did not exhibit hydrogen atom characteristics and it was suggested that this was an electron which formed hydrogen by recombination with the parent ion. Molecular halogen produced during the radiolysis appeared to scavenge these electrons. Calculations showed that electrons in the solid hydrogen halides were migrating distances in excess of 30Å from the parent ion.

ACKNOWLEDGEMENTS

The author wishes to express his appreciation to the Atomic Energy of Canada Ltd. for a summer appointment in 1960. He also wishes to acknowledge the ready assistance of the staff members of the University of Alberta, Calgary, Chemistry Department, especially Dr. F.C. Adam.

Particular appreciation is owing to the author's Research Director Dr. D.A. Armstrong for his guidance, advice, and unfailing support in all aspects of this research program.

Finally, sincere gratitude is expressed to my wife, Mary, for her patience and continued enthusiasm which were constant sources of encouragement.

TABLE OF CONTENTS

Page

INTRODUCTION

1. General 1
2. Elementary Processes in the Absorption of Radiation 3
    - 2.1. Electromagnetic radiations 3
        - 2.1.1. Photoelectric effect 3
        - 2.1.2. Compton Recoil Effect 4
        - 2.1.3. Pair production 4
    - 2.2. Fast electrons 5
    - 2.3. Heavy particles 6
    - 2.4. Secondary electrons 7
3. Primary Products 8
    - 3.1. Excitation 9
    - 3.2. Positive ions 10
    - 3.3. Electrons 11
4. Radiolysis of Water 16
    - 4.1. Molecular and radical yields 17
    - 4.2. Track effect 19
    - 4.3. Electrons as reactive intermediates in irradiated aqueous solutions 21
5. Previous Studies of the Radiolysis of Hydrogen Halides 23
6. Purpose and Scope of the Present Work 26

EXPERIMENTAL 28

1. Apparatus 28
    - 1.1. Preparation line 28
    - 1.2. Hot filament apparatus 30
    - 1.3. Analysis line 33
    - 1.4. Low temperature spectrometer 33

1.5. Co^{60} sources 35

1.5.1. 100 curie source 35

1.5.2. 1000 curie source 35

1.5.3. 12,000 curie source 35

1.5.4. 200 curie source 35

1.6. Irradiation cells 36

2. Materials 38

3. Dosimetry 40

4. Irradiation Techniques 41

4.1. Cell preparation 41

4.2. Sample preparation 43

4.3. Irradiation proceedures 43

5. Analyses 44

5.1. Hydrogen yields 44

5.2. Halogen yields 44

5.3. Olefins reactions 45

5.3.1. HBr - ethylene 45

5.3.2. HBr - propylene 45

RESULTS 46

1. The Liquid Phase 46

1.1. HCl 46

1.1.1. Pure HCl 46

1.1.1.1. Hydrogen yields 46

1.1.1.2. Halogen yield 46

1.1.2. HCl - bromine 46

1.1.3. HCl - sulphurhexafluoride 48

1.1.4. HCl - ethylene - nitric oxide 48

1.2. HBr 53

1.2.1. Pure HBr 53

1.2.1.1. Hydrogen Yields 53
1.2.1.2. Halogen Yields 53
1.2.2. HBr - bromine 59
1.2.3. HBr - sulphurhexafluoride 59
1.2.4. HBr addition to ethylene 59
1.2.4.1. Thermal reaction 62
1.2.4.2. Radiation-induced reaction 62
1.2.5. HBr addition to propylene 62
1.2.5.1. Thermal reaction 66
1.2.5.2. Radiation-induced reaction 66
1.3. HCl - HBr mixtures 66
1.3.1. Hydrogen yields 66
1.3.2. HCl - HBr - bromine 71
2. The Solid Phase 71
2.1. HCl 71
2.1.1. Hydrogen yields 71
2.1.2. Hot filament reaction 74
2.2. HBr 74
2.2.1. Hydrogen yields 74
2.2.2. Hot filament reaction 75
2.3. HCl - HBr mixtures 75
DISCUSSION 79
1. The Liquid Phase 79
1.1. Ionic reactions 79
1.2. Free radical reactions 84
1.3. Pure hydrogen halide 85
1.4. Scavenger studies: HCl 87
1.5. HCl - HBr mixtures 95
1.6. Scavenger studies: HBr 100

1.7. Hydrobromination of ethylene 103

1.8. Hydrobromination of propylene 105

2. The Solid Phase 106

2.1. Pure hydrogen halide 106

2.2. The identity of H' 108

2.3. The electron return model 112

2.4. HCl - HBr mixtures 116

BIBLIOGRAPHY 120

APPENDIX 1 126

LIST OF TABLES

Table No.	Title	Page
I	Examples of some of the dose rates employed.	42
II	Absorption maxima and extinction coefficients of halogen molecules in vaious solvents.	47
III	Hydrogen yields from γ-irradiated solutions of bromine in HCl at -79°C.	50
IV	Hydrogen yields from γ-irradiated solutions of sulphurhexafluoride in HCl at -79°C.	52
V	Hydrogen yields from γ-irradiated solutions of ethylene (0.1 mole % nitric oxide added) in HCl at -79°C.	54
VI	Hydrogen yields from γ-irradiated HBr at -79°C.	55
VII	Hydrogen yields from γ-irradiated solutions of scavengers in HBr at -79°C.	60
VIII A	Spontaneous addition of HBr to ethylene at -79°C.	63
VIII B	Effect of nitric oxide on γ-irradiated mixtures of HBr and ethylene at -79°C.	63
IX	Rates of radiation-induced addition of HBr to ethylene at -79°C.	64
X A	Spontaneous addition of HBr to propylene at -79°C.	67
X B	Effect of nitric oxide on γ-irradiated mixtures of HBr and propylene at -79°C.	67
XI	1-Bromopropane yields from γ-irradiated mixtures of HBr and propylene at -79°C.	68
XII	Hydrogen yields from γ-irradiated HCl - HBr mixtures at -79°C.	70

XIII Hydrogen yields from γ-irradiated solutions of bromine in HCl - HBr mixtures at -79°C. 72

XIV Hydrogen yields from γ-irradiated solid HCl - HBr mixtures at -79°C. 77

XV Values of kinetic parameters obtained from scavenger studies of γ-irradiated HCl at -79°C. 91

XVI Values of kinetic parameters obtained from scavenger (bromine) studies of γ-irradiated HCl - HBr mixtures at -79°C. 98

XVII True G-values for γ-irradiated solid (-196°C) HCl and HBr. 109

XVIII Some kinetic parameters of hydrogen atom reactions. 127

LIST OF FIGURES

Figure No.	Title	Page
1	Potential energy curves for the bromine molecule and the bromine molecule ion.	13
2	Potential energy curves for the chlorine molecule and the repulsive state of molecule-ion.	14
3	Potential energy curves for hydrogen halide molecules and molecule-ions.	14
4	Sample purification line.	29
5	Sample measuring apparatus.	31
6	Hot filament apparatus.	32
7	Hydrogen analysis line.	34
8	Sample vessel for hydrogen analysis.	37
9	Sample vessel for spectral analysis.	37
10	The dependence of hydrogen yields on dose.	49
11	The variation of $G(H_2)$ from γ-irradiated HCl (-79°C) with scavenger concentration.	51
12	Spectra of solutions of bromine in HBr(-79°C).	56
13	Optical densities of 300$m\mu$ and 400$m\mu$ peaks as a function of radiation time.	58
14	The variation of $G(H_2)$ from γ-irradiated HCl - HBr mixtures (-79°C) with bromine concentration.	61
15	First order plots for ethylene consumption.	65
16	Logarithmic plots of reaction rates versus dose rates.	65

17 The variation of $G(H_2)$ from γ-irradiated HCl - HBr mixtures as a function of electron fraction HBr. 69

18 The variation of $G(H_2)$ from γ-irradiated solid samples (-196°C) as a function of dose. 73

19 The variation of hydrogen pressure (P_{H_2}) with reaction time. 76

20 Kinetic plot of the effect of halogens on the hydrogen yield from γ-irradiated HCl (-79°C). 89

21 Kinetic plot of the effect of ethylene on the hydrogen yield from γ-irradiated HCl (-79°C). 89

22 Kinetic plot of the effect of bromine on the hydrogen yield from γ-irradiated HCl - HBr mixtures (-79°C). 97

23 Kinetic plot of the effect of bromine on the hydrogen yield from γ-irradiated HBr (-79°C). 101

24 Kinetic plot of the effect of halogen on the hydrogen yield from γ-irradiated solid hydrogen halide (-196°C). 110

25 Effect of phase transition on the hydrogen yields from γ-irradiated HCl - HBr mixtures. 118

INTRODUCTION

1. General

Radiation chemistry is the study of the chemical effects induced in matter by the actions of ionizing radiation. Although chemical reactions produced by electrical discharges in gases were known in the eighteenth century, radiation chemistry is generally acknowledged to have begun with the discovery of radioactivity by Becquerel (1) in 1896. Within a few short years it was found that α-particles, principally from radon or radium salts would effect chemical changes in numerous systems. For instance, Giesel (2) in 1900 reported that water could be converted into its elements by the action of radium and a year later Curie and Debierne(3) observed the continuous evolution of hydrogen and oxygen from aqueous solutions of radium salts. In 1910 Lind (4) commenced the first systematic study of gas phase irradiations and later concluded that ions were the major chemically reactive species formed.

The contemporary development of the chemistry of free radicals finally culminated in the proposal by Eyring, Hirshfelder and Taylor (5) of the classic mechanism for the radiation-induced formation and decomposition of hydrogen bromide (HBr). Their theory was based on the postulate that both ions and excited molecules reacted to form free radicals which subsequently gave rise to products. Indeed this concept has become an essential feature of almost all mechanisms of radiation induced reactions.

With the advent of the nuclear reactor, radiation chemistry entered an era of rapid scientific progress. The study of radiation damage to materials used both in reactor construction and in the handling of radioactive substances provided great impetus. Likewise, the widespread use of X-rays and radioisotopes in medicine prompted careful investigation of the effects of radiation on living systems. The increased availability of isotopes such as Co^{60} also encouraged researches into the industrial uses of high energy radiations. Underlying these major applications of radiation is the fundamental problem of elucidating the complex mechanisms associated with the interactions of ionizing radiations with matter. Thus it is, that the radiation chemistry of relatively simple systems has become such an increasingly important part of chemical kinetics.

2. Elementary Processes in the Absorption of Radiation

The principal chemical effects produced in attenuating media by high energy radiations result from the interactions of fast charged particles. These particles may constitute the incident radiation such as α or β-rays or be produced by the primary interaction of uncharged species such as γ-rays, X-rays or neutrons. It is outside the scope of this thesis to present a detailed discussion of the radiation physics of all types of radiations. However, the primary energy loss processes of electromagnetic radiation, fast electrons and heavy particles are pertinent to this investigation; thus a brief description of the essential features of each follows.

2.1. Electromagnetic Radiations

Electromagnetic radiation is attenuated in matter by the transfer of either part or all of its energy to atomic electrons. The energy imparted to these electrons will exceed their binding energies, and since the resultant ejected electrons have only a limited range in condensed phases, this excess energy will usually be entirely expended in the medium. The total energy absorbed by a system is given essentially by the sum (6), $\tau_a + \sigma_a + \kappa_a$, of the absorption coefficients which refer to the photoelectric, Compton recoil, and pair production processes, respectively.

2.1.1. Photoelectric Effect

In this process all of the photon energy is transferred to a single bound electron (6,7,8). The absorption coefficient, Ta, varies approximately as $\lambda^3 Z^4$ (where λ is the wavelength of the photon and Z is the atomic number of the attenuating atom) and falls off rapidly with increasing photon energy. Thus, the photoelectric effect is most important for low energy photons and is usually the predominant process at photon energies comparable to the electron binding energies in atoms.

2.1.2. Compton Recoil Effect

In the Compton effect the photon energy is large enough that the binding energy of the electron can be neglected. Only part of the photon energy is transferred to the electron with the remaining energy being carried off by the scattered photon. Applying the ordinary laws of conservation of energy and momentum, it can be shown that the difference in wavelengths of the incident and scattered photon will be given by the equation: (6)

$$\Delta\lambda = \frac{h}{mc}(1-\cos\phi)$$

where ϕ is the angle between the direction of the two photons. The recoil electron energies will be continuous over a range given by:

$$\epsilon = h\nu\frac{\delta\lambda}{\lambda+\delta\lambda}$$

where the maximum is at $\delta\lambda = \frac{2h}{mc}$ (i.e. ϕ = 180°).

From the formula developed by Klein and Nishina (9) it can be assumed that for high photon energies and intermediate Z materials absorption by the Compton process will be directly proportional to the electron density. This postulate is particularly significant for dose rate calculations in the present investigation where hydrogen halides have been irradiated with Co^{60} γ-rays.

2.1.3. Pair Production

The energy associated with an electron at rest M_0C^2 is 0.511 Mev (8). Photons with energies equal to at least $2M_0C^2$ can interact with a strong electric field converting part of the energy (1.02 Mev) into mass and producing an electron-positron pair. The photon energy in excess of the threshold energy will appear as kinetic energy of the particles produced. Recombination of the positron and an electron will lead to annihilation with the subsequent emission of two 0.511 Mev photons in such directions that momentum is conserved.

The absorption coefficient for pair production varies approximately as Z^2 and is a monotonically increasing function of the incident photon energy. Thus, this process would not contribute significantly to the total energy absorption except in the case of relatively high energy photons (i.e. 2 Mev) and high atomic weight materials.

2.2. Fast Electrons

Whether the incident radiation is a high energy electromagnetic radiation or a β-particle, the species which acts to transfer energy to the medium is the same, that is, a swiftly moving electron. The energy transfer mechanism can be envisaged by considering the electric field produced by the charged particle at an atom lying near the trajectory of the electron. Although the field will be time-dependent if the particle velocity is sufficiently high, the resultant electric pulses will contain appreciable intensities in the correct frequency range in which the medium absorbs (8). The rate at which this electron loses energy is variously called the stopping power or linear energy transfer (LET) and is denoted by -dE/dx.

For non-relativistic velocities the simple equation:

$$-\frac{dE}{dx} \approx \frac{2\pi e^4 Z^2}{m V^2} \ln \frac{m V^2}{4I}$$

can be developed using the electron velocity, V, the mean ionization-excitation potential, I, and the classical Rutherford (10) scattering equation. For electrons at relativistic velocities Bethe (7,8) has developed the stopping power formula given by:

$$-\frac{dE}{dx} = \frac{2\pi e^4 ZN}{m V^2}\left[\phi - 2\ln I\right]$$

where ϕ is a complex function of β where $\beta = \frac{V}{c}$. Values for I can be obtained from the relationship given by Bloch: (11)

$$I = 13.5 \times Z$$

when Z is less than 10 and

$$I = 9 \times Z$$

when Z is greater than 10.

According to the Bragg Law of Additivity of Stopping Powers (12), the stopping power of an element is independent of its state of chemical combination. For instance, the stopping power of a hydrogen halide is equivalent to the sum of the stopping powers of an equimolar mixture of hydrogen and halogen.

Other contributions to the LET such as the emission of Bremsstrahlung and polarization effects are not included in the Bethe equation. Since these processes only become important at energies above 1 Mev (8) they will not be considered here.

2.3. Heavy Particles

The LET equation (7) for heavy particles:

$$-\frac{dE}{dx} \approx \frac{4\pi e^4 z^2 NZ}{mV^2} \ln \frac{2mV^2}{I}$$

developed by Bethe is similar to that presented for the energy loss of an electron. Conservation of energy and momentum requires that the maximum energy transferred to an atomic electron is given by 4mE/M where M is the mass of the heavy particle. For a 1Mev proton or a 4Mev α-particle this corresponds to about 2,000 ev. This can be compared with the analogous case for high velocity electrons where all the energy can be transferred to the atomic electron. Since the impinging and ejected electrons are indistinguishable, then by assuming that the faster electron after a collision was also the incident particle, the apparent maximum energy which can be transferred is seen to be half that of the incident particle energy.

A distinct feature of multiple charged heavy particle irradiation is the dependence of the LET on the square of the charge of the particle.

From the above equations it can be seen, for instance, that the rate of energy loss for an α- particle will be greater than that of an electron with equivalent kinetic energy. However, other effects such as electron capture by the heavy charged particle can lead to reductions in the mean LET.

The neutral heavy particle, the neutron, interacts by producing high velocity charged recoil particles (7). For example, in the case of a collision with a hydrogen atom sufficient energy would be transferred to effect ionization and the resultant proton will ionize and excite the medium in the usual manner.

2.4. Secondary Electrons

Ions and excited molecules are formed along the tracks of the charged particles and many of the electrons ejected by the incident fast particle will possess sufficient energy to cause additional ionizations and excitations. Since these electrons will have relatively low velocities, their rate of energy loss will be high (13). For secondary electrons with less than 100ev, the formation of several ion-pairs will suffice to reduce the electron to subexcitation energies (usually about 5ev). Since the mean energy necessary to form an ion-pair (i.e. W) is approximately 30±10ev (7), the physical picture following the moderation of a 100ev secondary electron will be a cluster of about three ion-pairs and perhaps several excited molecules. For low LET primary particles, these clusters or spurs will appear as widely separated beads along the particle track (14). For a densely ionizing radiation, such as an α-particle, these clusters will be formed so close together that they will produce a columnar envelope of ion-pairs.

Secondary electrons formed with kinetic energy in excess of 100ev can produce true tracks which diverge from the direction of the primary. These secondary electrons are known as delta-rays.

3. Primary Products

The primary products formed by the interaction of an ionizing radiation with matter are electronically excited molecules, ions, and electrons. In condensed media, little is known of the exact nature of these species and the most common approach thus far has been to attempt to gain insight from conventional gas phase spectroscopic techniques. Thus, it is assumed that those ions which appear most abundant in the mass spectrometer will be the most probable species formed during the radiolysis. Likewise, ultra-violet spectroscopy can offer useful information regarding excited states which might be formed by irradiation. However, at present optical spectra cannot accurately predict which excited states will be formed.

The initial transfer of energy from the swiftly moving charged particle to the absorbing molecule occurs in less than 10^{-16} sec. (15) which is several orders of magnitude less than the time for one vibration, so that the Franck-Condon principle is applicable. For high energy particles, the spectroscopic selection rules will apply. However, at low energies, electron exchange excitation becomes possible, giving rise to spectroscopically forbidden transitions. When the energy transferred to a molecule greatly exceeds its ionization potential then ionization should occur directly. However, as Platzman (16) has described, the possibility may exist that an intermediate superexcited state will be formed. In this case the molecule will possess an energy in excess of its ionization potential, without undergoing immediate ionization. The superexcited state may undergo pre-ionization which entails ejection of an electron after a brief period of time. If this superexcited state can lose sufficient energy to fall below the ionization potential, then more normal excited states will evolve. This primacy of superexcited states could be an important factor in the relationship between the total energy absorbed by a medium and the ratio of ionization to excitation.

In the following discussions the primary products of the radiolytic interaction will be considered mainly with respect to their importance in determining the subsequent chemical reactions.

3.1 Excitation

Two types of excited states may be formed, one a repulsive state and the other an attractive state. Since the potential curves for repulsive states are often quite steep, a transition from the ground state to such a state will lead to immediate dissociation to radical fragments possessing excess kinetic energy. If an attractive state is formed, dissociation will not occur spontaneously unless the potential curve intersects a repulsive one, in which case predissociation may ensue.

For excited states which do not disappear by immediate dissociation, the excitation energy may be transferred to another molecule or emitted as light. The latter process may arise as a result of change in multiplicity, in which case it is termed phosphorescence (17). When no change of multicity occurs, the process is known as fluorescence (18). These types of degradations of excited states are more commonly associated with solids and complex organic molecules.

Recently the importance of energy transfer mechanisms has been stressed by numerous authors. For instance, Forester (19) has indicated that exciton migration can occur over distances exceeding 50Å. Magee (20) and others (21), using more refined models of Davydov (19) coupling, predict that the efficiency of dissociative excitation can be markedly affected by the presence of strong vibronic coupling of the molecules of the medium. For a weakly coupled system, the excited molecule can be considered as an isolated species. In strongly coupled systems the excitation may be completely dissipated by the coupled chain thus precluding dissociation. The energy might also be transmitted a considerable distance to another kind of molecule which might then undergo a detectable chemical reaction.

The products formed by the dissociation of an excited molecule may possess considerable excess kinetic energy. Epithermal (or "hot-radical") reactions resulting from such products would be relatively insensitive to temperature changes and perhaps phase changes also (22). Since these hot atoms would react rapidly, they would be difficult to detect as intermediates by normal scavenging techniques. Thus, the so-called "molecular yield" from some irradiated systems may be the result of hot-atom reactions.

In condensed phases the compact structure of the medium would tend to impede the diffusion of reactive intermediates. Since not all radical pairs formed from dissociative excited states possess sufficient energy to undergo immediate reaction or escape the site of their formation, the probability may be high for initial radical recombination within the confines of the solvent cage. This tendency of condensed systems to promote re-formation of the original molecules by a cage effect is known as the Franck-Rabinowitch effect (23).

3.2. Positive Ions

The ions formed by irradiation of condensed media are generally assumed to be simple cations of unit charge. Other species, such as multiple charged ions, anion-cation pairs, radical-ion pairs, et cetera, are known from mass spectrometry (24). In general, the cross-section for the ejection of a single electron from a neutral molecule is larger than that for the other processes. This fact coupled with probable solvent stabilization favors the formation of the simple ion described above.

A collision between the ion and a neutral molecule can cause charge transfer. The resonance criterion for this process is that the ionization potentials of the two species be nearly the same (25). Also under normal conditions the ionization potential of the neutral molecule cannot be greater than that of the original ion.

From the work of Schissler and Stevenson (26), and others (25,27), it can be concluded that for molecular ions, ion-molecule reactions are extremely probable. Indeed, in many irradiated systems these reactions may precede neutralization which normally is the ultimate fate of all the ions produced. Neutralization by ion-electron recombination will result in the formation of highly excited neutral molecules. The possible reactions of such species have already been discussed. The alternate cation-anion neutralization may simply be the reverse of the self-ionization reaction and therefore produce non-dissociative neutral products.

$$\text{e.g.}\quad H_3O^+ + OH^- \rightleftharpoons 2H_2O$$

3.3 Electrons

If the kinetic energy of the electron is sufficiently high then it will interact by exciting and ionizing molecules along its path. After the energy has fallen below the lowest excitation potential of the medium, further energy loss occurs by excitation of oscillational modes or dipolar relaxation (28). Since this subexcitation electron will dissipate its energy slowly, it can travel relatively large distances. Thus, the overall distance that the electron travels before thermalization may exceed 10^3 Å. However, due to the random walk type diffusion path, the final intercharge distance between the electron (29) and the parent ion should be much smaller than this.

The ultimate fate of the electron will be a capture reaction either with a neutral molecule or by a positive ion. The case of the ion-electron recombination was considered previously.

Electron capture by a neutral molecule may produce a stable negative molecule-ion intermediate. On the other hand, electron capture might proceed via a dissociative mechanism (30). Figure 1 depicts an example of negative-ion formation by the capture of an electron by a bromine molecule. Curves A and B represent the actual (31,32) potential energy curves of the neutral and negatively charged bromine molecules respectively. It can be seen from Figure 1 that the formation of a negative molecule-ion by the thermal capture process is dependent upon an energy loss in excess of E^{1} by a single quantum emission. Such a contingency reduces the probability of this process and unless an efficient energy loss mechanism is available this reaction may be entirely negligible (33). Similar arguments can be offered to suggest the improbability of forming a stable negative molecule-ion with chlorine.

Dissociative electron capture can occur readily provided that the electron affinity of the ion formed is greater than the energy of the bond being broken. It can be seen from Figures 1 and 2 that this condition is satisfied for both chlorine and bromine. However, to satisfy the Franck-Condon principle, the threshold energy for electron capture by chlorine (curve E, Figure 2) is approximately 1.6ev, whereas bromine (curve C, Figure 1) has a zero energy threshold.

Electron resonance capture can occur for endothermal reactions (where the bond dissociation energy exceeds the electron affinity of the ion formed) if the kinetic energy of the electron is nearly equal to the endothermicity plus an increment imposed by the Franck-Condon principle. An example of such a capture process is illustrated in Figure 3, where HX represents either HCl or HBr. The probability of

FIGURE 1

FIGURE 1

Potential Energy Curves for the Bromine Molecule and the Bromine Molecule-Ion (Br_2^-) (see references (31) and (32).

A -- Potential Energy Curve for Br_2

B -- Potential Energy Curve for Br_2^-

C -- Repulsive Negative Ion Curve

E'-- Vertical Excitation Energy

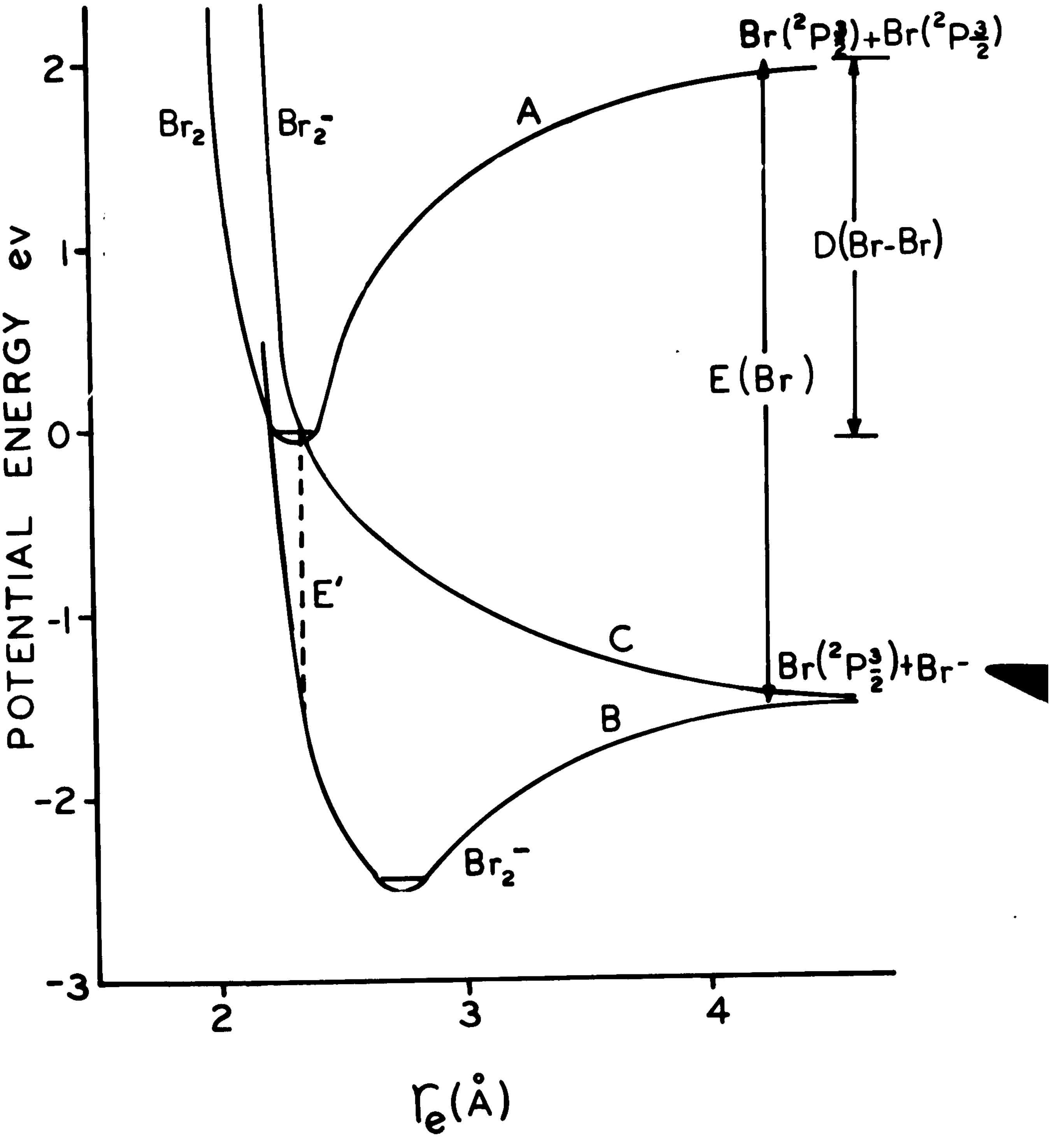
POTENTIAL ENERGY ev
2
1
0
-1
-2
-3
Br_2
Br_2^-
A
$Br(^2P_{\frac{3}{2}})+Br(^2P_{\frac{3}{2}})$
D(Br-Br)
E(Br)
E'
C
$Br(^2P_{\frac{3}{2}})+Br^-$
B
Br_2^-
2
3
4
r_e(Å)

FIGURE 2

FIGURE 3

FIGURE 2

Potential Energy Curves for the Chlorine Molecule and the Repulsive State of the Molecule-Ion (Cl_2^-) (see reference (32)).

D -- Potential Energy Curve for Cl_2

E -- Repulsive Negative Ion Curve

FIGURE 3

Potential Energy Curves for Hydrogen Halide Molecules and Molecule-Ions (see reference (32)).

F -- Potential Energy Curve For HX

G -- Repulsive Negative Ion Curve

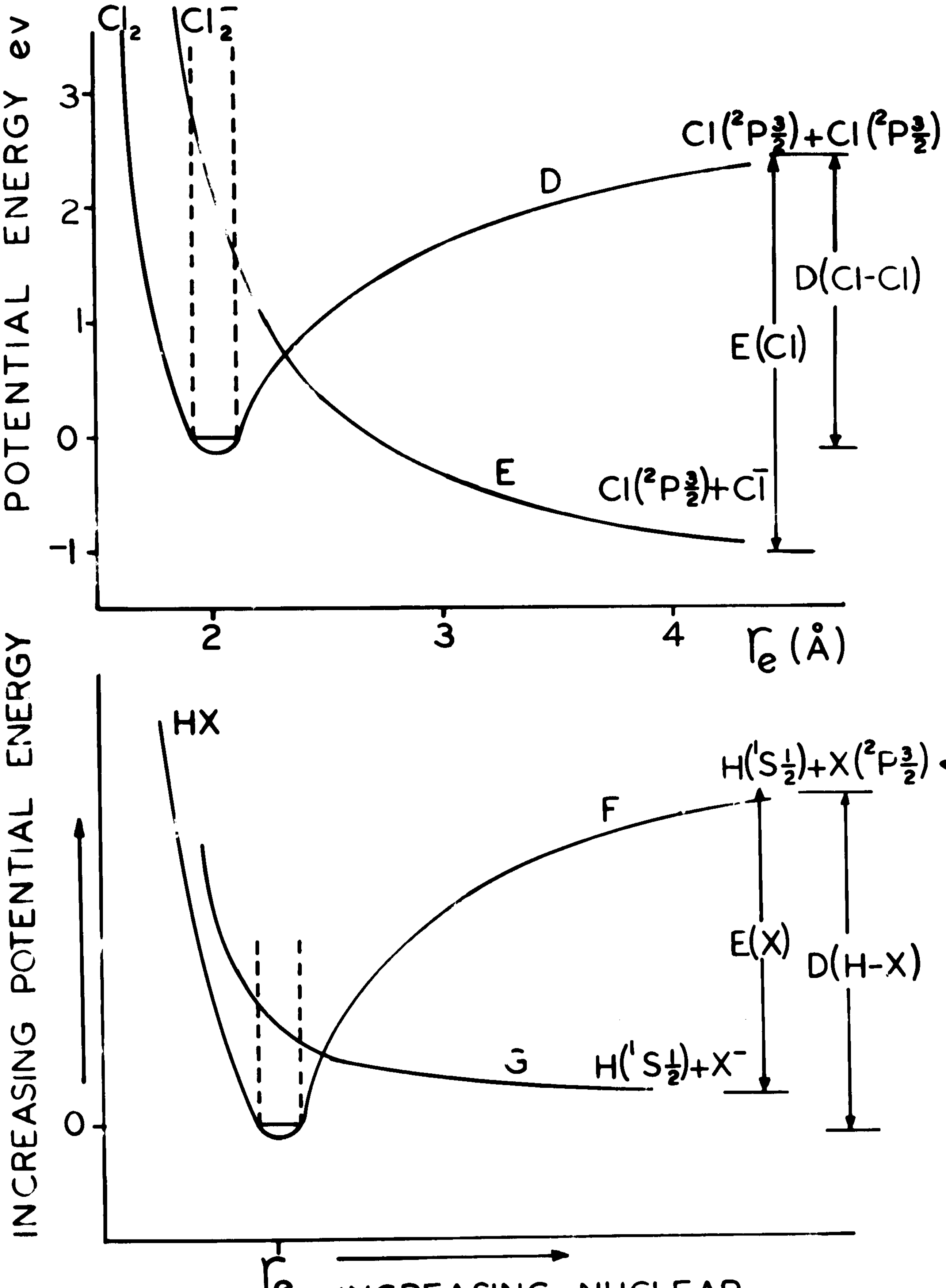
POTENTIAL ENERGY ev
Cl_2
Cl_2^-
3
2
1
0
−1
D
E
$Cl(^2P_{\frac{3}{2}}) + Cl(^2P_{\frac{3}{2}})$
$Cl(^2P_{\frac{3}{2}}) + Cl^-$
D(Cl-Cl)
E(Cl)
2
3
4
r_e (Å)
INCREASING POTENTIAL ENERGY
HX
F
G
0
$H(^1S_{\frac{1}{2}}) + X(^2P_{\frac{3}{2}})$
$H(^1S_{\frac{1}{2}}) + X^-$
E(X)
D(H-X)
r_e
INCREASING NUCLEAR SEPARATION

electron capture by a neutral molecule in irradiated systems depends significantly on the threshold energy. Since the rate of energy loss of a subexcitation electron decreases with decreasing electron energy, molecules which possess high capture threshold energies may not be able to compete with electron moderation processes (34). Thus, those molecules which can capture electrons over lower energy ranges will have the highest probability of undergoing electron attachment reactions.

4. Radiolysis of Water

The radiolysis of water must be recognized as one of the best understood topics in the radiation chemistry of condensed systems. For this reason and since many of the processes occuring in irradiated water are relevant to the system investigated here, a brief resume of some of the essential features of the radiolysis of water is presented.

The initial experiments with water revealed that with high LET irradiations the decomposition products, H_2, O_2, and H_2O_2 were readily detectable (35). However, for X-rays or γ-rays no measurable decomposition was evident (36) unless the water was irradiated in a vessel having a large evacuated volume over the water (37). The early work of Fricke initiated the development of the modern radiation chemistry of water. Fricke noted that whereas X-rays had little effect on pure water, considerable chemical reaction could ensue in the presence of dissolved solutes (38). He assumed that irradiation produced "activated" water. Ultraviolet light of wave-lengths below 1900Å produced many of the reactions characteristic of the X-ray irradiations, but not all of the reactions were the same. From this it was concluded that two kinds of "activated water" were formed (39).

From studies made during the war years, it was concluded that irradiated water yielded both molecular and free radical products. The overall decomposition might thus be represented by the equation:

$$H_2O \longrightarrow H,\ OH,\ H_2,\ H_2O_2$$

The apparent stability of water to X-rays was found to be due to the attack of the free radicals on the molecular products to reform water by the chain reaction (40):

$$OH + H_2 \longrightarrow H + H_2O$$

$$OH + H_2O_2 \longrightarrow HO_2 + H_2O$$

$$H + H_2O_2 \longrightarrow OH + H_2O$$

The following reactions were also shown to occur:

$$OH + H_2O_2 \longrightarrow HO_2 + H_2O$$

$$HO_2 + HO_2 \longrightarrow H_2O_2 + O_2$$

$$H + O_2 \longrightarrow HO_2$$

4.1 Molecular and Radical Yields

Radiolytic yields expressed in terms of the number of molecules formed or decomposed for every 100ev of energy absorbed are called G-values. The total amount of water decomposed is denoted as G $(-H_2O)$, whereas quantities such as the hydrogen atom yield are signified by the formula as a subscript (i.e. G_H).

The stoichiometry for the decompostion of water is given by the equation (40):

$$G(-H_2O) = G_H + 2G^M_{H_2} = G_{OH} + 2G^M_{H_2O_2}$$

where the superscript 'M' denotes molecular yield. The standard technique in determining the yields of each of the reaction products (H, H_2, OH, and H_2O_2) employs the use of scavengers. For example, hydrogen yields can be obtained by intercepting the hydroxyl radicals before they can react with the molecular hydrogen. The bromide ion is an example of one such scavenger, although many others have been employed (41). Thus the reaction:

$$OH + Br^- \longrightarrow OH^- + Br$$

protects the molecular hydrogen from the hydroxyl radicals. The hydrogen yield obtained in this way for $Co^{60}\gamma$-radiolysis is $G^M_{H_2} = 0.45$ (41).

Another example of the use of a scavenger in an aqueous system is the determination of G_H in aerated 0.8 H_2SO_4 by ferrous ion oxidation (34). Each hydroxyl radical will oxidize one ferrous ion,

$$OH + Fe^{++} \longrightarrow OH^- + Fe^{+++},$$

and each peroxide molecule will remove two ferrous ions,

$$H_2O_2 + Fe^{++} \longrightarrow Fe^{+++} + OH^- + OH$$

$$OH + Fe^{++} \longrightarrow Fe^{+++} + OH^-$$

Hydrogen atoms will add to dissolved oxygen to form the radical HO_2 which will subsequently cause the oxidation of three ferrous ions for each initial hydrogen atom,

$$H + O_2 \longrightarrow HO_2$$

$$HO_2 + Fe^{++} \longrightarrow HO_2^- + Fe^{+++}$$

$$HO_2^- + H^+ \longrightarrow H_2O_2$$

The observed G-value for ferric ion formation is 15.6, thus the over-all yield can be represented by:

$$G(Fe^{+++}) = 2G^M_{H_2O_2} + 3G_H + G_{OH} = 15.6$$

From the stoichiometry of the reaction, $G(Fe^{+++})$ can be shown to equal $2G^M_{H_2} + 4G_H$ and by substituting $G^M_{H_2} = 0.45$ then $G_H = 3.65$.

This particular system is the most commonly used chemical dosimeter and is known generally as the Fricke dosimeter. Several independent determinations (42) of $G(Fe^{+++})$ for this system have been made. Thus the value of $G(Fe^{+++}) = 15.6 \pm 0.2$ is accepted as a dosimetry standard for Co^{60} γ-irradiations.

The extensive use of the above solutes and many other scavengers has lead to the following calculated yields for the γ-radiolysis of neutral water (40): $G_H = 2.9$, $G_{H_2} = 0.45$, $G_{OH} = 2.4$, $G_{H_2O_2} = 0.71$, and $G(-H_2O) = 3.80$. These may be compared with the similar yields from 0.8N H_2SO_4: $G_H = 3.65$, $G_{H_2} = 0.45$, $G_{OH} = 2.95$, $G_{H_2O_2} = 0.80$, and $G(-H_2O) = 4.55$. However these G-values refer only to low LET irradiations such as Co^{60}. The radical yields G_H and G_{OH} decrease with increasing LET whereas $G^M_{H_2}$ increases. Although $G^M_{H_2O_2}$ also increases, it does not appear to be as sensitive to LET as $G^M_{H_2}$. $G(-H_2O)$ in neutral solutions at first decreases and then reverses and increases with increasing LET. In 0.8N H_2SO_4 solutions $G(-H_2O)$ appears to exhibit only a downward trend for increasing LET.

4.2. Track Effects

The first quantitative approach to the variation of yields with LET was made by Samuel and Magee. They considered that for low LET irradiations, the ion clusters would be sufficiently far apart that each could be treated as an isolated system. Their model employs the premise that the secondary electron will always return to neutralize the parent ion:

$$H_2O \rightsquigarrow H_2O^+ + e$$

$$H_2O^+ + H_2O \longrightarrow H_3O^+ + OH$$

$$H_3O^+ + e \longrightarrow H + H_2O$$

The distribution of radicals was thus described by a Gaussian function of modulus 10Å - 20Å. The molecular yields would result from recombination reactions of like radicals within the spurs. Of course, unlike radical recombinations would lead to the formation of water molecules which would be indistinguishable from the other molecules of the medium. Those radicals which escape recombination by diffusing out of the spurs constitute the radical yield.

If W is taken as approximately 28 for water (6) and the mean energy deposited per spur is about 100ev, then the radical concentration within the cluster would be sufficiently low to permit a relatively large number of radicals to escape recombination. With densely ionizing radiations the clusters will be formed so close together that after an interval of about 10^{-11} seconds, the track could be envisaged as a columnar envelope enclosing a high concentration of radicals. Thus, the probability of radicals escaping from the tracks of high LET radiations will be relatively much smaller than for the case of separated clusters from fast electrons.

Although the Samuel-Magee model has been widely accepted, an alternate proposal has been advanced by Platzman (34). By assuming that the secondary electron may become solvated, Platzman suggests that hydrogen atoms can be formed by the reaction:

$$e_{aq} + H_2O \longrightarrow H + OH^{-}_{aq}$$

This reaction implies that hydrogen atoms would tend to be formed in higher concentrations at the periphery of the spurs than at their centres.

For both models, diffusion out of the spurs will compete with the recombination reactions, and the yields of the various products can be predicted on the basis of diffusion kinetics. For solutions containing an active solute, the rate at which radicals would disappear is given by:

$$\frac{\partial R}{\partial t} = D\nabla^2 R - k R^2 - k_S R S$$

Where D is the diffusion coefficient, ∇ the Laplacian operator, R the concentration of the radicals, k the rate constant for recombination, S the active solute concentration, and k_S the rate constant for the reaction between R and S. This non-linear differential equation cannot be solved analytically and requires detailed computer calculations. Flanders and Fricke (43) achieved reasonable results assuming a one-radical model based on the initial Gaussian distribution described by Samuel and Magee. Dyne and Kennedy (44) also assumed a Gaussian distribution but made a distinction between the hydrogen and hydroxyl radicals. By suitable adjustment of the numerous variable parameters, these and many other calculations based on the diffusion model have produced values in good agreement with experimental results. By far the majority of solutions assume conditions which are consistent with the Samuel-Magee model, however, this does not invalidate the Platzman model as indeed the latter can also predict reasonable results. (45)

The most serious criticism of the diffusion model is the necessity of employing numerous parameters of unknown values in order to achieve quantitative results. Thus, by a suitable adjustment of these values, it should almost always be possible to obtain a reasonable fit with the experimentally observed results. A second and equally serious criticism involves the exclusive choice of the free radicals H and OH as the reacting species. Reactions other than those considered by the diffusion model can be occuring during the spur expansion. Such reactions principally involve electrons as the reactive intermediates.

4.3 Electrons As Reactive Intermediates in Irradiated Aqueous Systems

Although the reducing species in irradiated water was normally considered to be a hydrogen atom, early experiments by Hochanadel (46) indicated discrepancies in this theory. For instance, hydrogen atoms produced by the reaction:

$$OH + H_2 \longrightarrow H_2O + H$$

react much more slowly with hydrogen peroxide than with molecular oxygen. (15) The "hydrogen atom" produced by radiolysis of water, however, reacts at comparable rates with both reagents (47,48). Allen (47) has suggested that the hydrogen atom in irradiated aqueous systems can exist in the forms represented by the equilibria:

$$e \overset{H^+}{\rightleftharpoons} H \overset{H^+}{\rightleftharpoons} H_2^+$$

where the basic form is simply a solvated electron. Dainton (49) has demonstrated that the basic form of the "hydrogen atom" has unit negative charge. Further studies by Dainton and Peterson (50) with nitrous oxide solutions tend to confirm the existence of the solvated electron.

Numerous other data are presently available to support these conclusions.

Additional evidence supporting the importance of discrete reactions of electrons in aqueous media can be obtained from solid phase studies. Irradiation of aqueous glasses at liquid nitrogen temperatures (-196°) produce hydrogen atoms which are immobile (51). The direct formation of molecular hydrogen under these conditons may support a mechanism suggested by Haissinsky and Magat (52) who proposed that the electron could attach itself directly to the oxygen of a water molecule, thereby liberating a hydrogen molecule and an oxygen atom-ion:

$$e + H_2O \longrightarrow O^- + H_2$$

Dainton and Jones (53) have also demonstrated that while hydrogen cannot diffuse in aqueous glasses at liquid nitrogen temperatures, the secondary electron can travel along preferred paths to react with solutes at least 50Å from the parent ion.

It is worthwhile noting that though the Samuel-Magee model initially rejects the solvated electron, its existence might only require an alteration of the time scale employed but not necessarily a rejection of the entire theory. It still remains the best working model for irradiated aqueous solutions.

5. Previous Studies of Radiolysis of Hydrogen Halides

The radiation chemistry of hydrogen halides has attracted some interest in the past. As early as 1911, Lind (54) had irradiated liquid HBr with α-particles from radon. The decomposition of the HBr was reported in terms of the ion-pair yield, that is, the total number of molecules of HBr converted (M) divided by the total number ion-pairs formed (N). The calculated value was $-M_{HBr}/N = 2.2$ If the energy necessary to form one ion-pair, W, is between 20 and 25ev then $G(-HBr) \approx 10$. Since Lind lacked an accurate method of dosimetry these values may not be too reliable. Furthermore, his yields appeared to be based on irradiations which were allowed to proceed to at least 5% decomposition. Thus, these would not necessarily represent the true initial yields.

The three hydrogen halides HCl, HBr and HI have all been studied in the gas phase (55, 56, 57, 58). The sensitivity to radiation-induced decomposition increases with the atomic weight of the halogen atom (i.e. $-M_{HCl}/N = 3.3$, $-M_{HBr}/N = 5$, and $-M_{HI}/N = 6$). Once again there is uncertainty as to whether these yields represent the true initial yields, since the importance of possible back reactions due to the accumulation of products seems not to have been fully appreciated. Experiments currently in progress in this laboratory tend to show higher yields for the HCl and HBr gas phase irradiations (59).

The data of Lind and Livingston (60) on the α-particle induced synthesis and decomposition of HBr was used by Eyring, Hirschfelder, and Taylor (5) to test their free radical theory of radiation induced reactions. They proposed the following reactions:

$$HBr \rightsquigarrow HBr^{+} + e$$

$$e + HBr \longrightarrow H + Br^{-}$$

$$Br^- + HBr^+ \longrightarrow H + 2Br$$

$$H + HBr \longrightarrow H_2 + Br$$

$$2Br + M \longrightarrow Br_2 + M$$

This mechanism predicts an ion-pair yield of 4.0, and to explain the difference they proposed the alternate ionic reactions:

$$HBr^+ + HBr \longrightarrow H_2Br^+ + Br$$

$$H_2Br^+ + Br^- \longrightarrow 2H + 2Br$$

Zubler, Hamill, and Williams (57) preferred to attribute the excess yield above 4.0 to dissociative excitations.

Recently, Armstrong (61) investigated the Co^{60} γ-radiation induced decomposition of liquid HCl at -79° and reported that $G(-HCl) = 2G(H_2) = 13.0$. It was shown that this value represented the true initial yield and since it is larger than Lind's value for HBr it suggests that either the trend in sensitivities exhibited in the gas phase is not maintained in the liquid phase or that Lind's value is too low. By employing a scavenger, Armstrong was able to detect two hydrogen forming species. The more readily scavenged was considered to be a thermal hydrogen atom with $G_H = 2.3$. The second species was described as a hot-hydrogen atom with $G_{H^*} = 4.2$. Armstrong also irradiated HCl as a solid at -196°C and found that for moderate doses $G(H_2) = 3.3$.

Several investigations have been made of the radiation-induced addition of HBr to ethylene. Hamill and Young (62) observed the addition reaction initiated by bromine radicals formed from the nuclear isomeric transitions of Br^{80*}. A thorough kinetic investigation of the Co^{60} γ-ray induced addition of HBr to ethylene was made by Armstrong and Spinks (63). The ion-pair yield of the single major product, ethyl bromide, was of the order of 10^5 indicating a long chain reaction. For high concentrations of HBr, the reaction rate showed a first order dependence on ethylene concentration, second order dependence on HBr concentration, and a first order dose rate dependence. For higher concentrations of ethylene, the dose rate exponent decreased to 0.5. These data are consistent with a free radical chain mechanism.

Irradiation of similar systems in condensed phases also indicated free radical chain reactions (64). Mitchell et al. (65) detected ethyl radicals by electron spin resonance in irradiated solid mixtures of HBr and ethylene. The ethyl radicals were thought to arise from hydrogen atom scavenging by the olefin.

6. Purpose and Scope of the Present Work

One of the principal chemical responses of hydride molecules to the absorption of energy from an ionizing radiation is the formation of a radical pair. In its simplest form this can be represented by the general reaction:

$$RH \rightsquigarrow R\cdot + \cdot H$$

As indicated earlier when R = OH, the subsequent free radical reactions will be diffusion controlled due to the inertness of the medium. The problems and uncertainties of establishing a model have already been described. When R is an organic radical, diffusion controlled processes are often unimportant. However, a new problem, that of material balance and product analyses, is encountered. Fragmentation of the R group can lead to several new reactive intermediates. Thus, for an organic system such as n-hexane, analysis shows fragments containing all numbers of carbon up to twelve.

The simplest possible compounds for radiation chemical study should be unsymmetrical reactive diatomic molecules. The hydrogen halides constitute such a group and the relatively well-established kinetics of the synthesis and decomposition of the hydrogen halides, HCl and HBr, recommend these materials for study.

The reactivity of both HCl and HBr towards hydrogen atoms should ensure that they would be scavenged by the medium rather than undergoing diffusion controlled reactions, such as exhibited in irradiated water. Since the products of radiolysis can only be hydrogen and halogen molecules, the problems of analysis and material balance are relatively simple.

It is the principal aim of this investigation to attempt to gain insight into the primary act and mechanisms occurring in irradiated condensed hydrogen halides. The relationship between the primary radiolytic products (excited molecules, ions, and electrons) andfree radicals is a leading problem in radiation chemistry. The Eyring, Hirschfelder, and Taylor theory offers a realistic approach to this problem for the gas phase radiolysis of hydrogen halides and it is of considerable interest to test this theory for the analogous condensed systems. With the establishment of mechanisms for all three phases, it may then be possible to correlate some features of the primary products with such variables as density, temperature and phase structure.

EXPERIMENTAL

1. Apparatus

The principle pieces of apparatus employed in this investigation were two vacuum systems, a modified version of the Klein-Scheer hot-filament apparatus (67), a spectrophotometer adapted for low temperature use, a variety of irradiation cells, and several Co^{60} γ-radiation sources. A brief description of these and other associated apparatus follows:

1.1. Preparation Line

A mercury-free vacuum system was constructed for purification and preparation of samples. A Duo-Seal forepump and a V.M.F. oil diffusion pump constituted the pumping system and were capable of producing a vacuum of $4\text{x}10^{-6}$ mm Hg. High vacuum measurements were made with a Balzers HV-2 high vacuum gauge head. Mercury was excluded from the system in order to prevent undesirable reactions between the hydrogen halides or the halogens handled in the system.

Figure 4 shows the portion of the line used for purification and storage of sample materials. Gases were introduced into the system through the stopcock at B and frozen in the adjacent trap with liquid nitrogen. Bulbs C, D, and B were used for bulb-to-bulb distillations and C contained a copper mesh filter. The long bulb F represents one of a number of storage traps. Since both HCl and HBr tended to react with the stopcock grease after extended contact, storage in the solid state in liquid nitrogen traps was preferred to gas phase storage. G represents a stopcock with a $^{10}/_{30}$ $\$$ outer joint for removing samples.

The samples were measured in the gas phase using standard volumes and a mercury manometer connected to the mercury-free line by a dia-

FIGURE 4

FIGURE 4

Sample Purification Line.

A -- Main Manifold

B -- Sample Inlet

C -- Copper Mesh Filter

D -- Drying Taps

E -- Holding Bulbs

F -- Liquid Nitrogen Storage Trap

G -- Sample Outlet

H -- High Vacuum Gauge Head

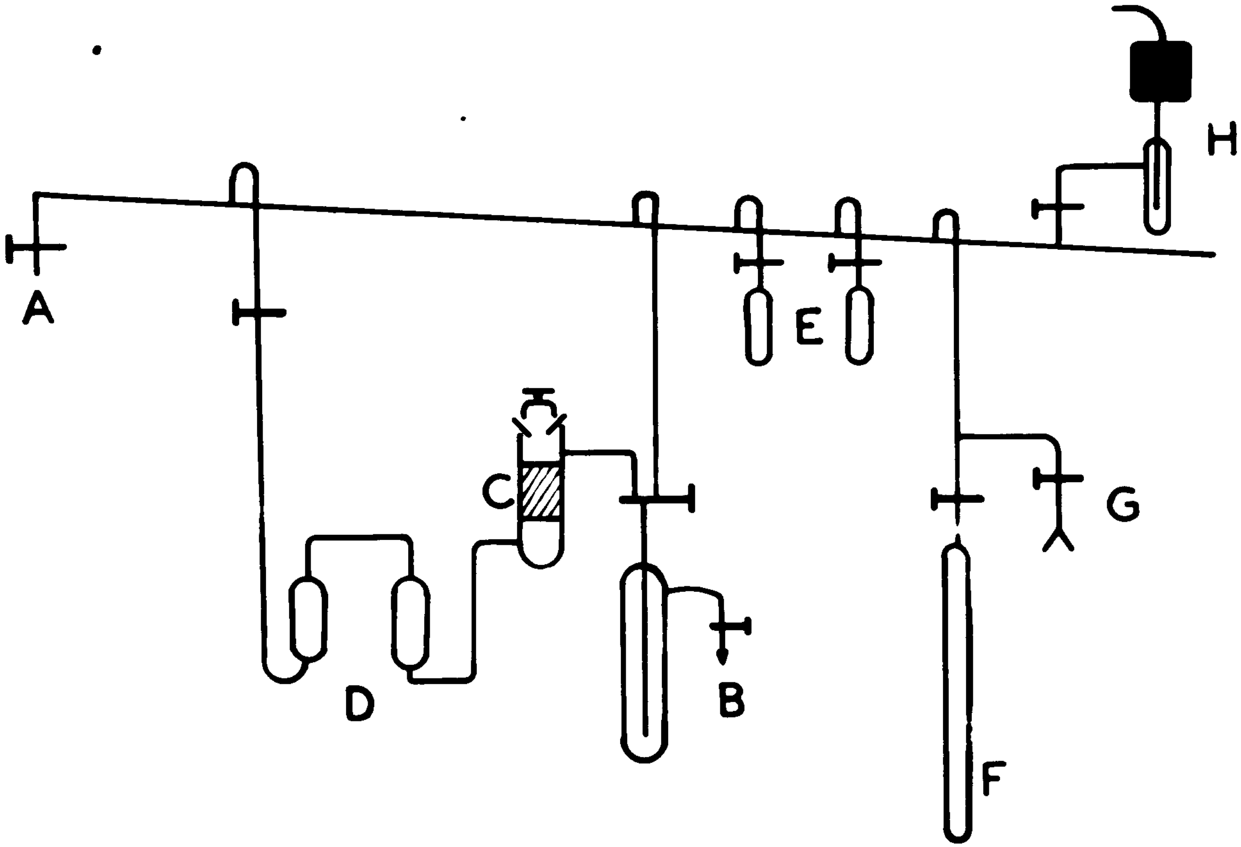
H
A
E
G
C
D
B
F

phragm gauge. The standard volumes I, J, and K shown in Figure 5 were calibrated using water with corrections being made for buoyancy effects. The volumes calculated were 52.4, 305.2, and 511.0 cc for bulbs I, K, and J respectively. A smaller detachable bulb of 1.33_2 cc was calibrated with mercury. The dead space, determined by pressure-volume data, was found to be 105.2 cc.

The diaphragm gauge L was constructed of stainless steel on the gas measuring side and brass on the reference side. The diaphragm itself was made of stainless steel. Distortions of the diaphragm due to pressure inequality were measured by means of the variation in capacitance of the two chambers of the gauge. Linearity in the response of the gauge was maintained up to a pressure differential of approximately 50 mm Hg. At maximum gain the sensitivity of the instrument was ±0.1 mm. The over-all reproducibility of sample measurements for volume J and pressures above 500 mm Hg was within 0.1%.

1.2. Hot Filament Apparatus

The apparatus shown in Figure 6 was attached to an auxiliary manifold of the main vacuum system via Stopcock A. Both the cold finger B and the filament C could be rotated such that either could be set at the centre of the spherical reaction vessel. The filament was made of 1/4000 inch diameter tungsten wire and the power was supplied from a 6 V storage battery.

The hydrogen halide (HCl or HBr) was distilled into the flask and condensed on the tip of the cold finger. The flask was then immersed in liquid nitrogen and the refrigerant rapidly removed from the cold finger. After the hydrogen halide had been deposited as thin film over the walls of the reaction vessel, a small amount of hydrogen was introduced into the flask. The reactions:

FIGURE 5

FIGURE 5

Sample Measuring Apparatus

A -- Main Manifold

I -- 52.4 cc Bulb

J -- 511.0 cc Bulb

K -- 305.2 cc Bulb

L -- Diaphragm Gauge

M -- Hg Manometer

N -- Reference Pressure Control

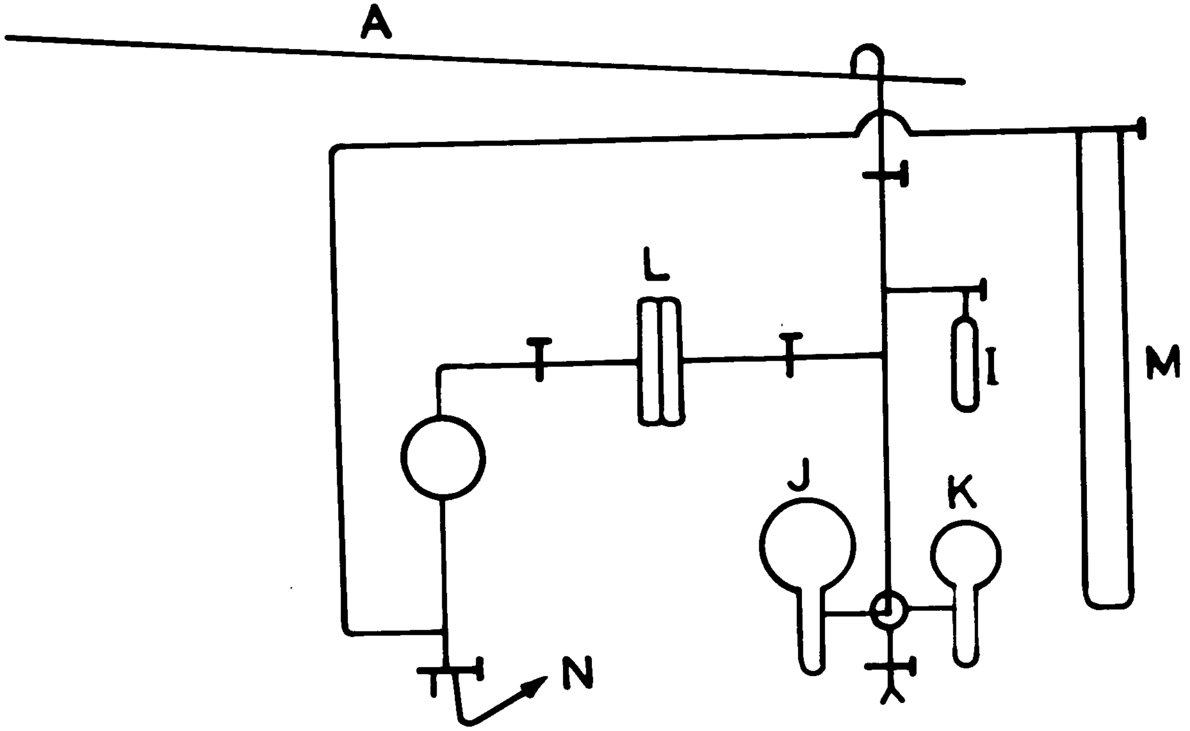
A
L
I
M
J
K
N

FIGURE 6

FIGURE 6

Hot Filament Apparatus

A -- To the Main Manifold

B -- Cold Finger

C -- Filament

D -- Pirani Gauge

E -- Electrical Leads

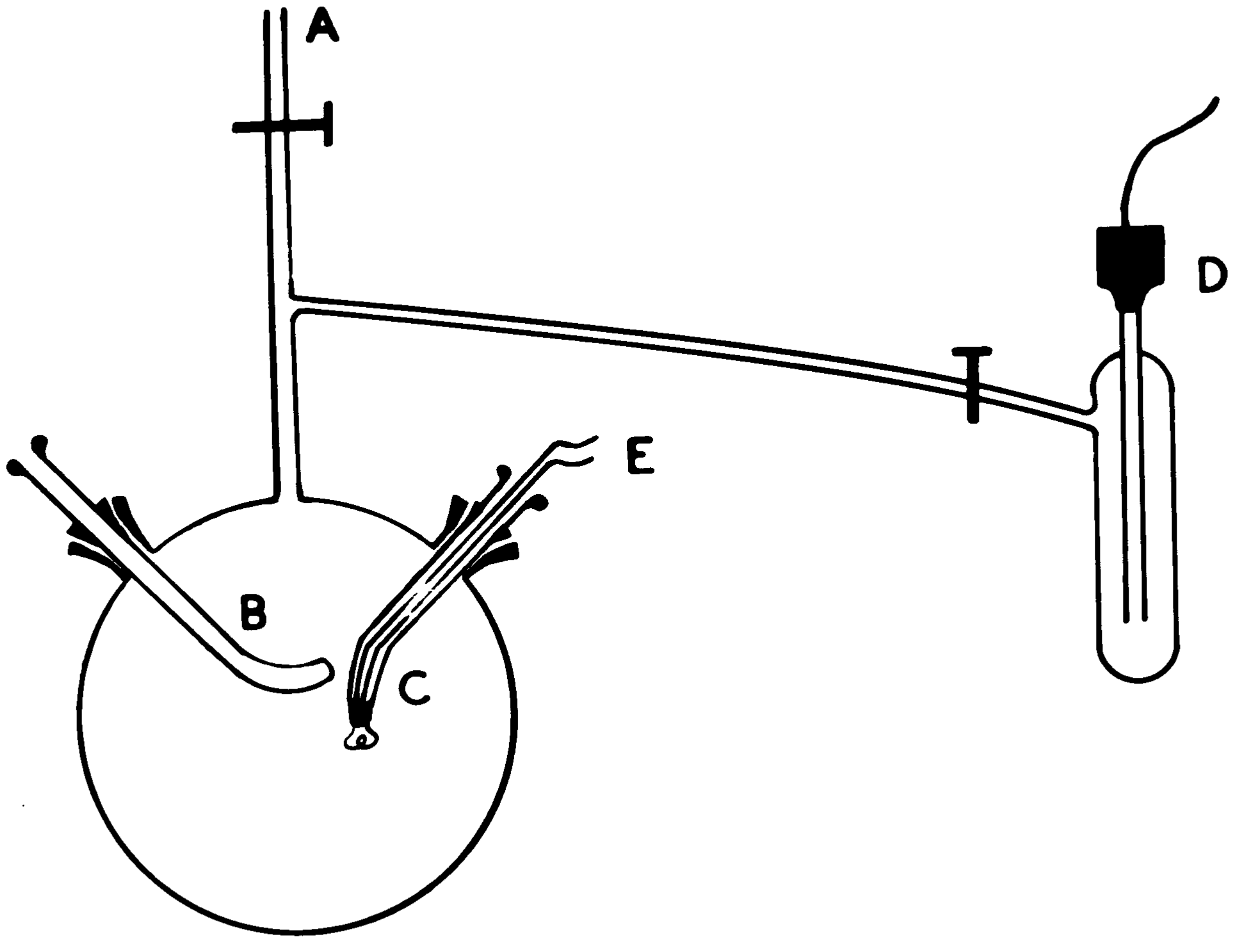

A
D
E
B
C

$$H_2 \xrightarrow[\text{Filament}]{\Delta} H + H$$

$$H + HX \longrightarrow H_2 + X$$

were initiated by passing current through the filament. The increase in hydrogen pressure was measured by the pirani gauge D.

1.3. Analysis Line

The hydrogen analysis system (Figure 7) was similar to that described by Allen (68) except that the combustion apparatus was here replaced by a palladium thimble. A Duo-Seal forepump and an all glass two-stage mercury diffusion pump were employed. The volume of the McLeod gauge and associated dead space (B in Figure 7) was 394 cc. Pressures of hydrogen as low as $7.3\text{x}10^{-4}$ mm Hg were measured. The liquid nitrogen trap E prevented the distillation of mercury from the Toepler pump D into the sample through F.

1.4. Low Temperature Spectrophotometer

A Beckmann model D.U. spectrophotometer was modified for observing spectra at approximately -80°C. A specially built low temperature cell compartment was mounted between the spectrometer and the phototube housing. This compartment which was insulated with styrofoam was made of an aluminium block machined to accept a 1 cm optical cell. The optical path bored through the block was closed at both ends with quartz windows. The lower part of the block could be partially immersed in liquid nitrogen. By controlling the liquid nitrogen level, it was possible to maintain the cell compartment within a few degrees of -80°C. Jets of dry nitrogen gas were passed over the optical cell faces and the quartz windows of the compartment to prevent condensation. The temperature of the cell compartment was monitored with a chromel-alumel thermocouple.

FIGURE 7

FIGURE 7

Hydrogen Analysis Line.

A -- Main Manifold

B -- McLeod Gauge

C -- Palladium Thimble

D -- Toedler Pump

E -- Hg Pump

F -- Sample Inlet

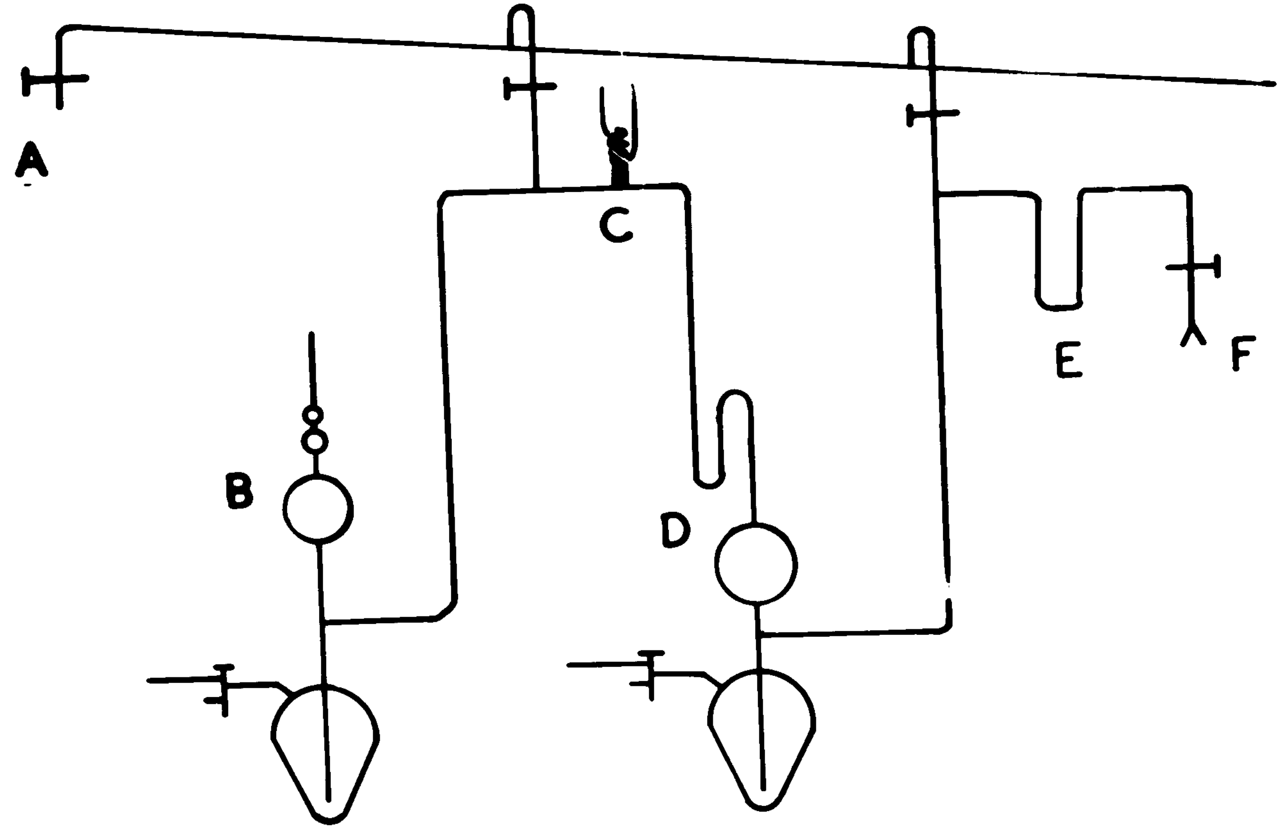
A
B
C
D
E
F

1.5. Co^{60} Sources

Four Co^{60} sources were employed of which three were located at the Atomic Energy Project at Chalk River, Ontario. These were of approximately 100, 1,000, and 12,000 curies respectively, and were used only in the investigation of the radiation induced addition of HBr to ethylene and propylene. The other source (200 curies) was at the University of Alberta, Calgary, and was the only source used to determine hydrogen and halogen yields from irradiated hydrogen halide systems. A brief description of each source follows:

1.5.1. 100 curie Source

The Co^{60} was contained in a capsule kept below floor level and shielded by several layers of lead. Compressed air was used to bring the capsule up into a lead castle. Inside the castle there was a brass spacer with a number of holes which allowed for exact repositioning of samples. Irradiations were timed with a stopwatch.

1.5.2. 1,000 curie Source

The isotope was housed in a lead castle and samples to be irradiated were placed in an aluminium cylinder which could be lowered into the castle. By putting spacers in the bottom of this cylinder, various dose rates were achieved. Four such dose rates were obtained with this source. Radiation times were again measured with a stopwatch.

1.5.3. 12,000 curie Source

This source was an A.E.C.L. Gamma-Cell. Samples were placed in a specially-built brass plunger which was lowered into the Gamma-Cell by remote control. Only one sample position was used and radiation times were recorded automatically.

1.5.4. 200 curie Source

The Co^{60} when in the shielded or off position was in a lead castle mounted into the side of a concrete cave. The cave door was fixed on a trolley which moved into the cavity. The source was activated by lowering the isotope into the cave from its shielded position. The Co^{60} could not be lowered when the cave door was open, nor could the door be opened unless the Co^{60} was inside the castle. Samples to be irradiated were placed in special containers (see Figure 8) bolted to the trolley. Reproducibility of dose rates assured the exact repositioning of samples. Radiation times were measured with a stopwatch.

1.6. Irradiation Cells

When hydrogen yields were to be determined, cells similar to the one depicted in Figure 8 were used. After admitting the sample into the cell, the capillary could be collapsed, thus sealing the cell under vacuum. The sealed tip $^{10}/_{30}$ ₮ inner joint, B, fitted a mated outer joint attached to a stopcock. The tip was drawn so that it fitted into the barrel of the stopcock. When connected to the hydrogen analysis line this cell could be opened under vacuum simply by turning the stopcock and breaking the tip. Other modifications of this type of cell were also used. They differed only in the number of "break-off" tips. Some cells had as many as six such tips, each of which could be resealed under vacuum; thus permitting several consecutive irradiations of the same cell. The large bulb attached to the cell served in bulb-to-bulb distillation of the post-irradiated sample. This effected the release of any hydrogen occluded in the sample.

When the irradiated solutions were to be analysed spectroscopically, cells such as the one represented by Figure 9 were used. After radiolysis, the solution could be poured from the reaction bulb A into the 1 cm path length quartz cell B. If the sample was to be analysed for hydrogen as well, then a "break-off" tip was also attached.

FIGURE 8

FIGURE 9

FIGURE 8

Sample Vessel For Hydrogen Analysis

A -- Sample Bulb

B -- 10/30 $\overline{\$}$ Break Off Tip

C -- Seal Off Capillary

D -- Bulb for Bulb-to-Bulb Distillation

E -- Spacer

F -- Positioning Container Fixed to the Trolley

H -- Dewar Flask

I -- Port for Admitting Refrigerants

FIGURE 9

Sample Vessel For Spectral Analysis

A -- Sample Bulb

B -- 1cm Path Length Quartz Cell

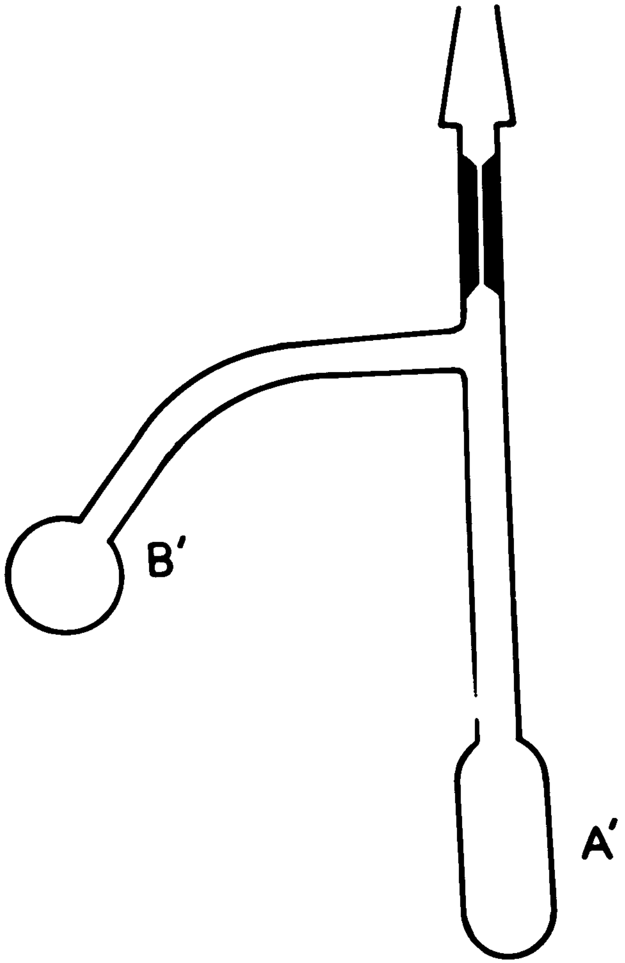
B′
A′

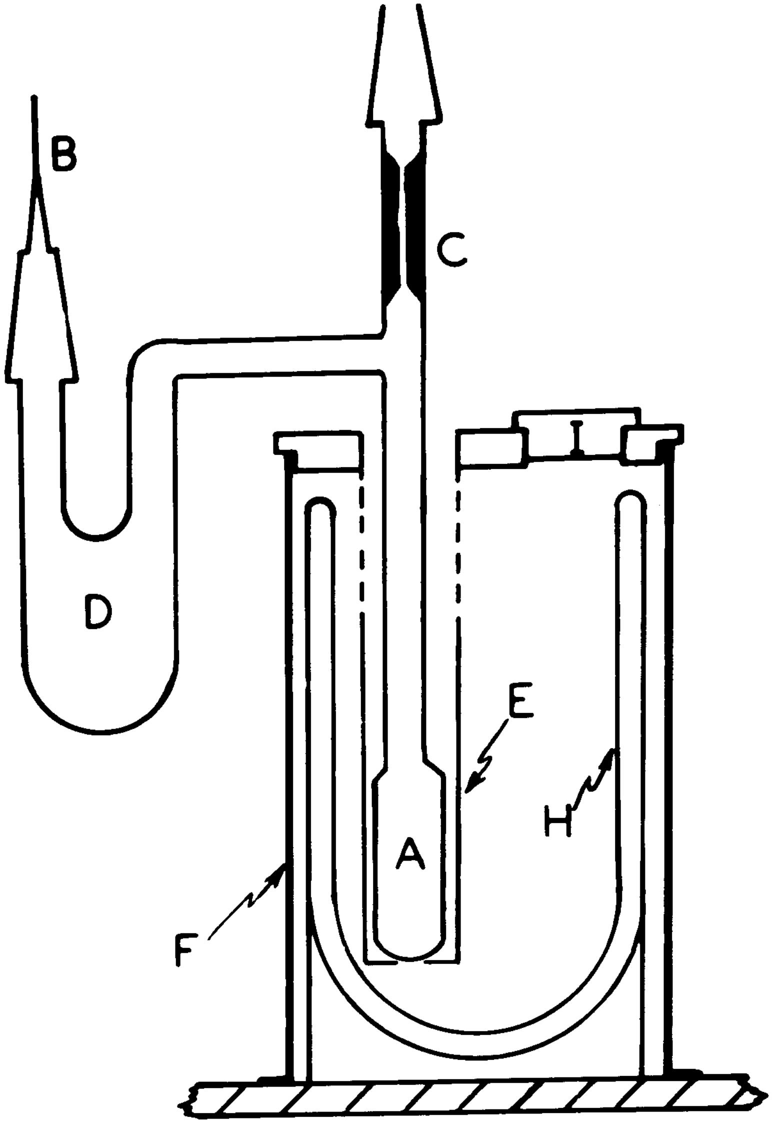
B
C
I
D
E
H
A
F

The radiation cell used in studying the radiation induced addition of HBr to ethylene and propylene was simply a round bottom tube 24 cm in length, 8 mm in inside diameter, and closed by a stopcock. An inner $^{10}/_{30}$ ₮ joint by which the cell could be connected to the vacuum system was attached to the stopcock.

2. Materials

Hydrogen Bromide

Anhydrous HBr of 99.0% minimum purity (the Matheson Co.) was introduced into the system under vacuum and condensed in a liquid nitrogen trap. Non-condensible gases were pumped off. Additional drying of the gas was achieved by either of two methods. The first involved liquefying the HBr over P_2O_5, whereas the second entailed sublimation of the HBr through dry ice traps. Although hydrogen yields from samples dried by either method were identical, the latter technique was favored as it did not involve the risk of depositing P_2O_5 throughout the system. The thoroughly dried gas was subjected to several bulb-to-bulb distillations through a copper mesh filter. Traces of bromine in HBr were easily removed by the copper. Initial and final fractions of the distillate were discarded. After this preliminary purification, the HBr was irradiated for approximately 36 hours at -79°C. The above purification cycle was then repeated.

Hydrogen Chloride

Anhydrous HCl of 99.0% minimum purity (the Matheson Co.) was further purified by the methods described for HBr. Additional drying of the HCl was achieved by passing the gas through traps surrounded by ethanol-liquid nitrogen slurries (approximately -100 to -120°C). Traces of HBr as an impurity in the HCl were equally well oxidized to bromine by either the addition of a small quantity of chlorine or pre-irradiation. Both techniques were employed.

Bromine

Reagent grade bromine (Baker and Adamson) was dried, degassed, and fractionally distilled in a grease-free and mercury-free auxiliary line attached to the main preparation vacuum system. The bromine was first refluxed to remove trapped gases, then distilled from approximately -10°C to -79°C with the end bromine fraction being discarded. The bromine was then liquefied over anhydrous $CaCl_2$. After several bulb-to-bulb distillations in which only the middle fraction was retained, the bromine was distilled through a trap at -79°C to a trap at -196°C. The fraction remaining in the -79°C trap was retained and stored over P_2O_5.

Nitric Oxide

The nitric oxide (the Matheson Co.) was dried over fused potassium hydroxide and degassed by bulb-to-bulb distillations in which only the middle fraction was kept. The nitric oxide was used immediately after purification and none was stored in the vacuum system.

Sulphurhexafluoride

Sulphurhexafluoride obtained from the Matheson Co. was further purified by distillations through dry ice traps. Initial and final fractions were discarded and the middle fraction was kept in a gas storage bulb attached to a secondary manifold of the main vacuum system.

Ethylene

Research grade ethylene (the Phillips Petroleum Co.) was further purified by drying over P_2O_5 and by bulb-to-bulb distillations. The ethylene was stored as a solid in a liquid nitrogen trap.

Propylene

Research grade propylene (the Phillips Petroleum Co.) was handled in the same manner as described for the ethylene except that the propylene was stored in the gas phase.

3. Dosimetry

Dose rates were determined using the Fricke dosimeter (69). The dosimetry solutions (10^{-3}M Fe^{++}, 10^{-3}M Cl^{-}, and 0.8N H_2SO_4) were made from reagent grade ferrous ammonium sulphate, hydrochloric acid, and sulphuric acid. The water used in preparing these solutions was double distilled with the final distillation being made from alkaline potassium permanganate. The dimensions of the dosimetry tubes were the same as the respective reaction vessels. These tubes were cleaned with permanganic acid followed by successive rinsings with tap water, distilled water, double distilled water, and finally some of the dosimetry solution itself.

The solutions were irradiated for periods of 15, 30, 60, 120, and 180 minutes and the resulting concentrations of Fe^{+++} were determined with a Beckmann D.U. spectrophotometer. The molar extinction coefficient for Fe^{+++} in 0.8N H_2SO_4 at 25°C was taken as 2220 ± 20(+ 0.6% per degree) (70). Since the absorbed dose is a function of the electron density of the absorbing media, the dose rate calculated from the Fricke dosimeter must be corrected in order to give the dose rate for HCl and HBr solutions.

The dose rate from the dosimetry solution is given by expression (i):

$$\text{(i)} \quad \text{DOSE RATE} = \frac{\Delta OD}{\Delta t} \times \frac{N}{\epsilon} \times \frac{100}{G(Fe^{+++})} \times \frac{1}{1000} \quad (\text{ev/ml/time})$$

where $\frac{\Delta OD}{\Delta t}$ is the slope of the optical density versus time plot of the irradiated dosimetry solution, N is Avogadro's number, ϵ is the appropriate molar extinction coefficient of Fe^{+++}, and $G(Fe^{+++})$ is 15.6 (42). The dose rate thus calculated is applicable only to solutions with the same electron density as the 0.8N H_2SO_4 solution. The dose rates calculated in this investigation have been corrected for the ratio of electron densities between the dosimetry solution and the sample to be irradiated. Thus, expression (ii) represents the dose rate for solutions where the solvent is a hydrogen halide.

$$\text{(ii)} \quad \text{DOSE RATE}_{(HX)} = \frac{\Delta OD}{\Delta t} \times \frac{N}{\epsilon} \times \frac{100}{G(Fe^{+++})} \times \frac{1}{1000} \times \frac{1}{d} \times \frac{e_{HX}}{e_{D.Sol'n}}$$

(ev/gm/time)

where d is the density of the dosimetry solution, $\frac{e_{HX}}{e_{D.Sol'n}}$ is the ratio of electrons per gram between the hydrogen halide and the dosimetry solution, and all other symbols have their usual meaning. A sample calculation gives:

$\text{DOSE RATE}_{(Fe^{++} \text{ in } 0.8N\ H_2SO_4)} = 1.094 \times 10^{16}$ ev/gm/min.

$\text{DOSE RATE}_{(HBr)} = 8.782 \times 10^{15}$ ev/gm/min.

$\text{DOSE RATE}_{(HCl)} = 9.740 \times 10^{15}$ ev/gm/min.

Some of the dose rates achieved with the various sources for HBr solutions are given in Table I.

4. Irradiation Techniques

4.1. Cell Preparation

The pyrex irradiation cell to be used was cleaned with permanganic acid. After the usual rinsings the cell was dried in an oven at 110°C. The clean and dry cell was attached to the preparation vacuum line via the $^{10}/_{30}$ ₮ joint and evacuated to 5×10^{-5} mm Hg (or better).

After obtaining a constant pressure, the cell was flamed to the sodium emission temperature and then allowed to cool. A small amount of the appropriate hydrogen halide was distilled into the cell (only HCl was used when HCl-HBr mixtures were to be prepared). The hydrogen halide was allowed to evaporate and remain in contact with the cell for several

TABLE I

Examples of Some of the Dose Rates Employed

Source	Dose Rate	Unit
100 curie Co^{60}	5.80×10^{14}	ev/ml/sec.
1000 curie Co^{60}	5.70×10^{15}	ev/ml/sec.
1000 curie Co^{60}	6.41×10^{13}	ev/ml/sec.
12,000 curie Co^{60}	1.67×10^{16}	ev/ml/sec.
200 curie Co^{60}	8.782×10^{15}	ev/gm/min.
200 curie Co^{60}	6.475×10^{15}	ev/gm/min.

minutes before being pumped off. Before the sample was finally introduced into the cell, the latter was flamed again.

4.2. Sample Preparation

All samples were measured in the gas phase using standard volumes and a mercury manometer with an associated diaphragm gauge. The accuracy of these measurements for HCl and HBr were checked by absorbing a measured sample of the gas in water and titrating with a standard base. The results of the two methods agreed to within 0.5%. The standard bulb used for measuring bromine employed a greaseless stopcock to prevent loss of the bromine by absorption in the silicone grease.

At the termination of any series of runs the vacuum system was re-greased to prevent contamination of subsequent samples.

After being measured, the samples were distilled into the appropriate irradiation cell, subjected to a final degassing, and then sealed off under vacuum.

4.3. Irradiation Procedures

Samples were irradiated at either -79 ± 1 (liquid phase) or -196 ± 2°C (solid phase). These temperatures were obtained by the use of a dry ice-ethanol slurry or liquid nitrogen respectively. Samples which were to be irradiated at -79°C were allowed to stand for several minutes in a dry ice slurry before irradiation to insure proper thermal equilibrium. These samples were also inspected visually for homogeneity.

Samples to be irradiated as solids were melted and refrozen so that the sample formed a continuous solid mass in the bottom of the irradiation cell.

In the radiolysis of HBr and olefin mixtures, the irradiation cells were fixed in a given position inside a small Dewar flask (4 cm outside diameter) by means of a copper spacer. This Dewar flask was then placed at a fixed position inside the radiation source and the irradiation commenced.

When hydrogen or halogen yields were to be determined, the samples were fixed on the trolley (as shown in Figure 8) and the Dewar flask was filled with the desired refrigerant.

5. Analyses

5.1. Hydrogen Yields

After joining the sample vessel to the hydrogen analysis line via the $^{10}/_{30}$ ₮ inner joint and evacuating the system, the tip (B in Figure 8) was broken. The non-condensible gases were transferred from the sample vessel by means of the Toepler pump to the McLeod gauge where the pressure was measured. The palladium thimble was then heated allowing the hydrogen to escape from the McLeod gauge. The pressure was measured until a constant limiting pressure was obtained. The amount of hydrogen originally present was given by the difference between the initial and final pressures.

Approximately 10% of the total hydrogen formed on irradiation was occluded by the solidified sample. A second yield of hydrogen was liberated by a bulb-to-bulb distillation within the irradiation cell. This second yield was then measured and the result combined with the first yield. From the sum of the two, G-values for hydrogen formation were calculated. Attempts to obtain a third yield indicated that virtually all the measurable hydrogen formed had been collected with the first two yields.

5.2. Halogen Yields

Halogen yields were measured spectroscopically using the low temperature apparatus previously described. The irradiated sample was distilled into the quartz cell attached to the side arm of the sample vessel. The spectrum of the unirradiated solution was determined first (using air as a blank), after which the spectrum of the irradiated solution was obtained in the same manner. Spectral measurements were made over the region of $550 m\mu$ to $290 m\mu$. A tungsten lamp was used for wavelengths above $320 m\mu$ and a hydrogen lamp was used for shorter wavelengths.

5.3.1. HBr - Ethylene

The addition reaction between HBr and ethylene was stopped periodically by removing the sample from the source and immediately freezing the mixture in liquid nitrogen. The sample was then returned to the vacuum system. The extent of the reaction was determined by measuring the pressure of products and residual reactants in a standard volume. Reaction rates were calculated from the initial slopes of reaction versus time plots.

5.3.2. HBr - Propylene

In the reaction of HBr with propylene, the sample was allowed to react for a given time and then stopped in the same manner as employed for the ethylene system. The residual HBr was absorbed in water and titrated with a standard silver nitrate solution with Eosin as the indicator. A gas chromatographic column packed with tri-m-cresyl phosphate and helium as the carrier gas was used for product analysis. Comparison standards were prepared from Eastman Organic chemicals in ether solutions.

RESULTS

All the results presented in this chapter, unless otherwise noted, are due solely to the interaction of radiation with the specified systems. The principal mode of studying the radiation induced reactions has been by determining hydrogen yields. Irradiation of an evacuated sample vessel did not produce any detectable hydrogen. Likewise, no hydrogen could be extracted from unirradiated samples which had stood for several hours at either -79°C or -196°C.

1. The Liquid Phase

1.1. HCl

1.1.1.1. Pure HCl: Hydrogen Yields

$G(H_2)$ for the radiolysis of pure liquid HCl was $6.5_3 \pm 0.1_0$. Since this value was in excellent agreement with the value of $6.5_0 \pm 0.1_0$ reported by Armstrong (61), repetition of his dose dependency experiments was deemed unnecessary.

1.1.1.2. Pure HCl: Halogen Yields

The radiolysis of HCl not purified by pre-irradiation failed to produce any chlorine when normal doses were employed. The spectrum showed that bromine was formed by the oxidation of trace impurities of HBr. Samples which had been purified by pre-irradiation (or addition of chlorine) produced only a chlorine spectrum upon irradiation. More detailed results have been presented elsewhere (71) and some of the spectroscopic parameters determined are shown in Table II. From these results, the necessity of employing pre-irradiation (or chlorine addition) in the purification of HCl to remove traces of HBr was readily recognized.

1.1.2. HCl - Bromine

It is known that the hydrogen yields from irradiated HCl are sharply

TABLE II

Absorption Maxima and Extinction Coefficients of Halogen Molecules In Various Solvents

Solute	Solvent	λ Max.	ϵ Max.	Ref.
Br_2	HBr	4000Å	198	
Br_2	HBr (gas)	4190Å	182	72
Br_2	HCl (gas)	4230Å	191	72
Br_2	CCl_4	4110Å	206	73
Cl_2	HCl	3300Å	88	71
Cl_2	CCl_4	3300Å	97	74

reduced by the addition of chlorine (61). The use of bromine as an alternate scavenger is suggested by the similarity in characteristic reactions of the two halogens. The hydrogen yields from irradiated solutions of bromine in HCl were linear with dose (Figure 10) and $G(H_2)$ decreased abruptly with increasing bromine concentration (Table III). The low solubility of bromine in liquid HCl at -79° precluded experiments at higher concentrations and the apparent plateau (see Figure 11) at approximately $G(H_2) = 4.0$ may be due solely to a solubility effect.

It can be seen from Figure 11 that for low concentrations, bromine is a more efficient scavenger than chlorine

1.1.3. HCl - Sulphurhexafluoride

Sulphurhexafluoride is used extensively as a standard in determining appearance potentials for negative ion formation in mass spectrometers (32). Its high cross-section for electron resonance capture and zero energy threshold (75) should make this substance an excellent scavenger for thermal electrons.

The effect of sulphurhexafluoride on the hydrogen yields from irradiated HCl is given in Table IV. No appreciable decrease in $G(H_2)$ was observed until 5.3_1 mole % sulphurhexafluoride was employed. Beyond this concentration the suphurhexafluoride began to crystallize out of solution, thus preventing experiments at higher concentrations.

1.1.4. HCl - Ethylene + Nitric Oxide

Since ethylene should not react with subexcitation electrons, but does react rapidly with hydrogen atoms, this reagent was employed as a discrete hydrogen atom scavenger. In order to inhibit a possible free radical chain addition reaction between the HCl and ethylene, 0.1 mole % nitric oxide was included in each mixture. Nitric oxide alone does not

FIGURE 10

FIGURE 10

The Dependence of Hydrogen Yields on Dose

● -- Br_2 in HCl

▲ -- C_2H_4 and NO in HCl

⊖ -- Br_2 in HBr

△ -- Br_2 in 0.40 Electron Fraction HBr

✕ -- 0.14 Electron Fraction HBr

○ -- 0.34 Electron Fraction HBr

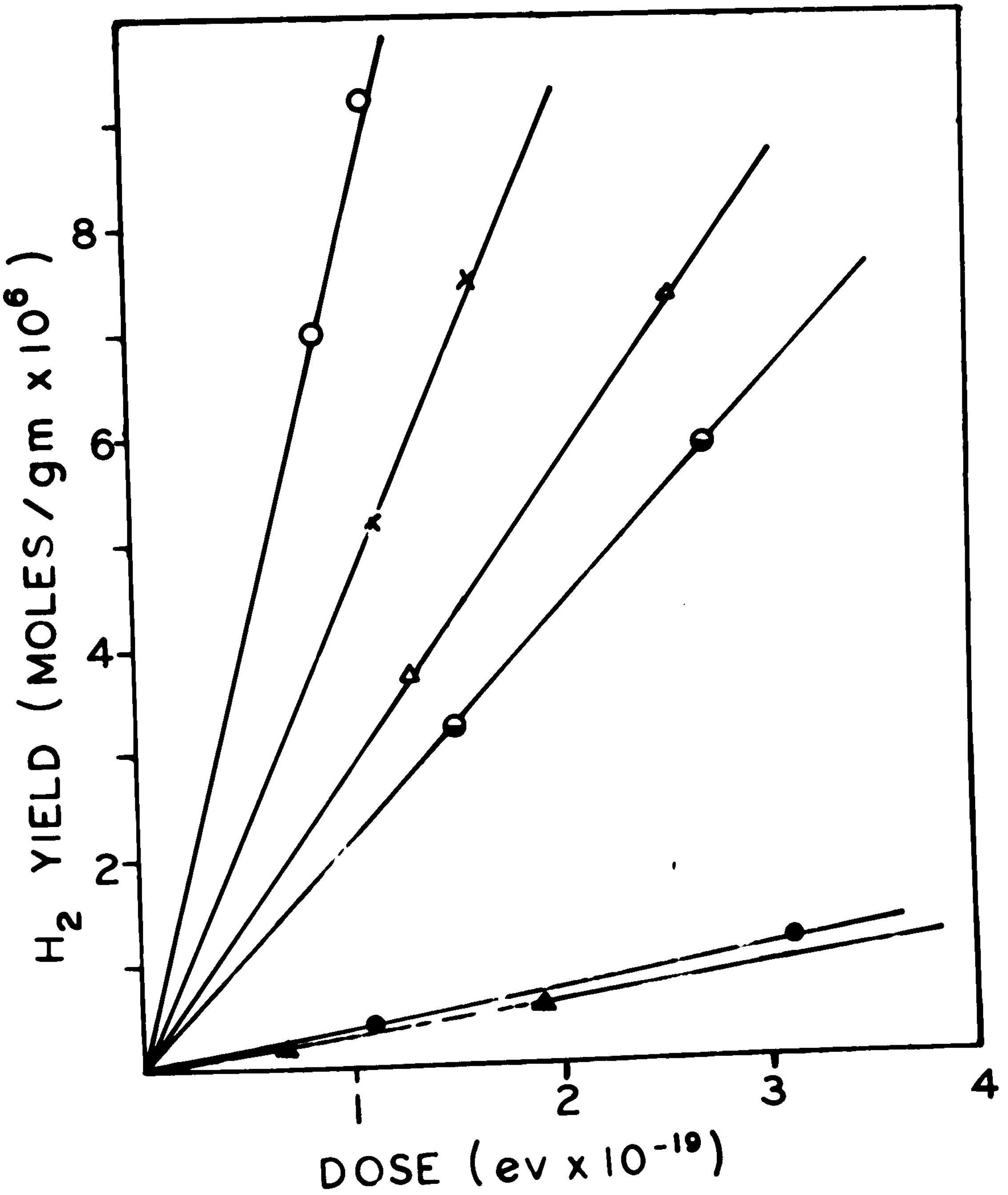
H$_2$ YIELD (MOLES / gm x 10^6)
2
4
6
8
1
2
3
4
DOSE (ev x 10^{-19})

TABLE III

Hydrogen Yields From γ-Irradiated Solutions of Bromine in HCl at -79°C

(Br_2) Moles/gm	$G(H_2)$	$\Delta G(H_2)$
0.000	6.53	0.00
0.118×10^{-4}	5.67	0.86
0.167×10^{-4}	5.50	1.03
0.246×10^{-4}	5.15	1.38
0.345×10^{-4}	5.03	1.50
0.620×10^{-4}	4.72	1.81
0.635×10^{-4}	4.75	1.78
1.143×10^{-4}	4.56	1.97
2.056×10^{-4}	4.14	2.39
$(2.891 \times 10^{-4})^*$	4.13	2.40
$(4.122 \times 10^{-4})^*$	4.08	2.45
$(5.788 \times 10^{-4})^*$	4.05	2.48

*Apparent solubility limit exceeded

FIGURE 11

FIGURE 11

The Variation of G(H_2) from γ- Irradiated HCl (-79°C) With Scavenger Concentration

● -- SF_6

■ -- C_2H_4

▲ -- Br_2

--- -- Cl_2 (see reference (61))

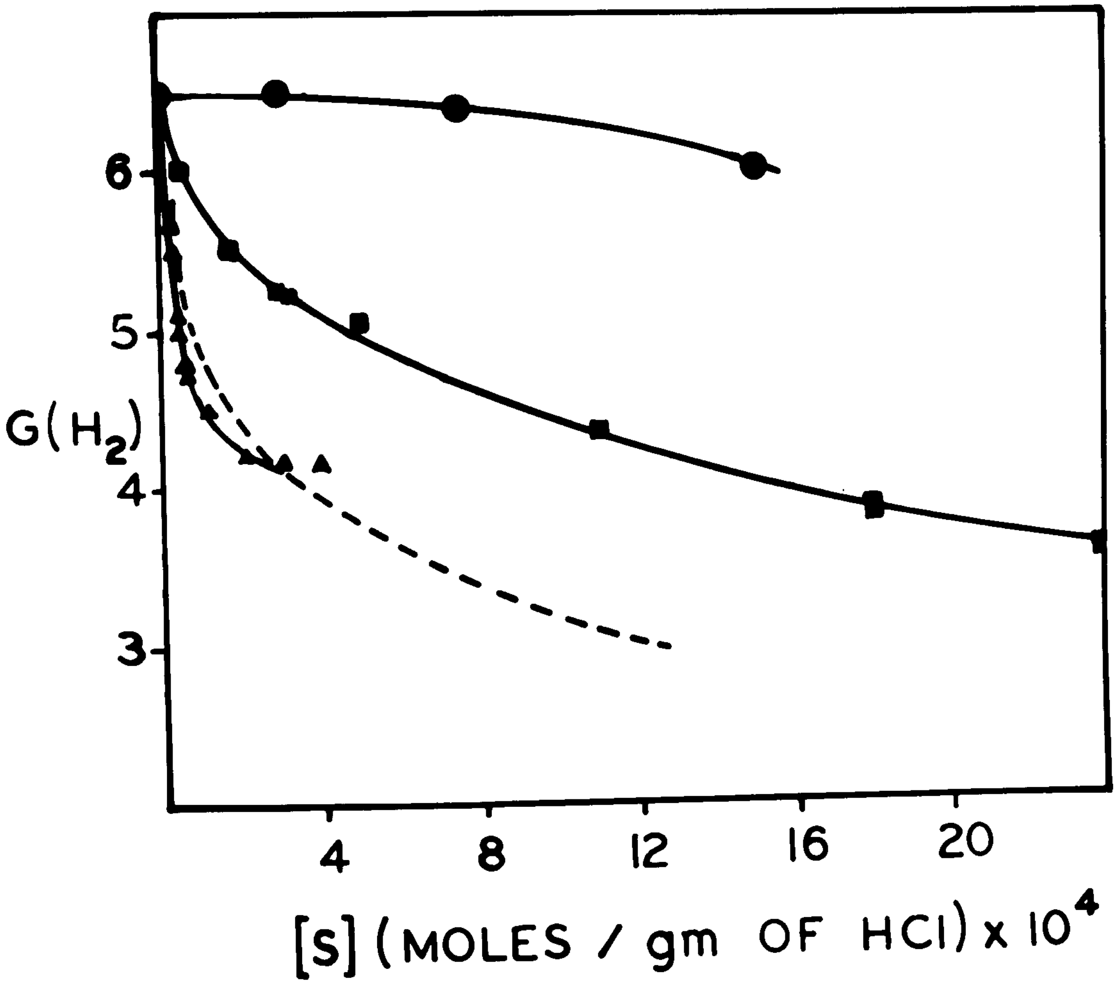
6
5
4
3
G(H_2)
4
8
12
16
20
[S] (MOLES / gm OF HCl) x 10^4

TABLE IV

Hydrogen Yields From γ-Irradiated Solution of Sulphurhexafluoride In HCl at -79°C

SF_6 Moles/gm	$G(H_2)$	$\Delta G(H_2)$
0.000	6.53	0.00
$2.329\text{x}10^{-4}$	6.56	+0.03
$7.365\text{x}10^{-4}$	6.41	0.12
$15.38\text{x}10^{-4}$	5.95	0.58

alter the normal hydrogen yield from HCl (61). The values for $G(H_2)$ from the radiolysis of HCl-ethylene-nitric oxide solutions are given in in Table V. The hydrogen yields were independent of dose over the range of doses used (Figure 10).

The fraction of the total amount of hydrogen formed due to the direct radiolytic decompostion of ethylene was calculated assuming that G_{H_2} from ethylene was 1.2 (76). Thus $G_{H_2}^{HCl}$ represents the yield of hydrogen formed from HCl alone. The total G-value is plotted against ethylene concentration in Figure 11.

1.2. HBr

1.2.1.1. Pure HBr: Hydrogen Yields

The results of the radiolysis of pure liquid HBr are presented in Table VI. The G-value for hydrogen formation was 12.42 ± 0.06. The data indicated that $G(H_2)$ was independent of both sample size and dose absorbed over the range of doses used (i.e. $1.48_4 \mathrm{x} 10^{18}$ to $9.58_1 \mathrm{x} 10^{19}$ ev). No formal dose rate study was made. However, coincidental with the natural decay of the isotope and minor alterations of the sample positioning apparatus, the dose rates involved in these radiolyses varied by as much as 29% but without any subsequent effect on $G(H_2)$.

1.2.1.2. Pure HBr: Bromine Yields

The decomposition products of a hydrogen halide can only be its constituent elements. Thus, an attempt was made to determine the halogen yields spectroscopically and thereby establish a secondary means of examining the effects of radiation on the system.

The spectrum of liquid HBr showed no absorption peaks between 540mμ and 290mμ. With air as a blank, the optical density of the HBr was 0.03_5 at 540mμ and increased gradually to approximately 0.06_5 at 300mμ. Curve A of Figure 12 represents the spectrum of an HBr sample, which had

TABLE V

Hydrogen Yields From γ-Irradiated Solutions of Ethylene (0.1 Mole % Nitric Oxide Added) in HCl at -79°C

(C_2H_4) Moles/gm	$G(H_2)$Observed	$G^{HCl}_{H_2}$	$\Delta G^{HCl}_{H_2}$
0.000	6.53	6.53	0.00
$0.546\text{x}10^{-4}$	5.97	5.97	0.56
$1.67\text{x}10^{-4}$	5.52	5.51	1.02
$2.87\text{x}10^{-4}$	5.27	5.26	1.27
$3.40\text{x}10^{-4}$	5.26	5.25	1.28
$4.90\text{x}10^{-4}$	5.07	5.05	1.48
$11.00\text{x}10^{-4}$	4.38	4.34	2.19
$17.41\text{x}10^{-4}$	3.86	3.80	2.73
$23.9\text{x}10^{-4}$	3.56	3.48	3.05

TABLE VI

Hydrogen Yields From γ-Irradiated HBr at -79°C

HBr (gm)	Dose Rate (ev/gm/min)	Dose (ev)	Molecules of H_2	$G(H_2)$
2.658	9.166×10^{15}	1.303×10^{19}	1.623×10^{18}	12.46
2.742	9.951×10^{15}	5.048×10^{18}	6.272×10^{17}	12.42
2.779	9.166×10^{15}	1.592×10^{19}	1.972×10^{18}	12.39
5.351	7.094×10^{15}	2.149×10^{19}	2.668×10^{18}	12.41
5.708	6.955×10^{15}	1.469×10^{18}	1.827×10^{17}	12.44
5.708	6.955×10^{15}	3.611×10^{18}	4.478×10^{17}	12.40

FIGURE 12

FIGURE 12

Spectra of Solutions of Bromine in HBr (-79°C)

A -- Bromine Produced Radiolytically from an HBr Sample Not Purified by Pre-Irradiation

B -- Synthetic Solution of Bromine in HBr

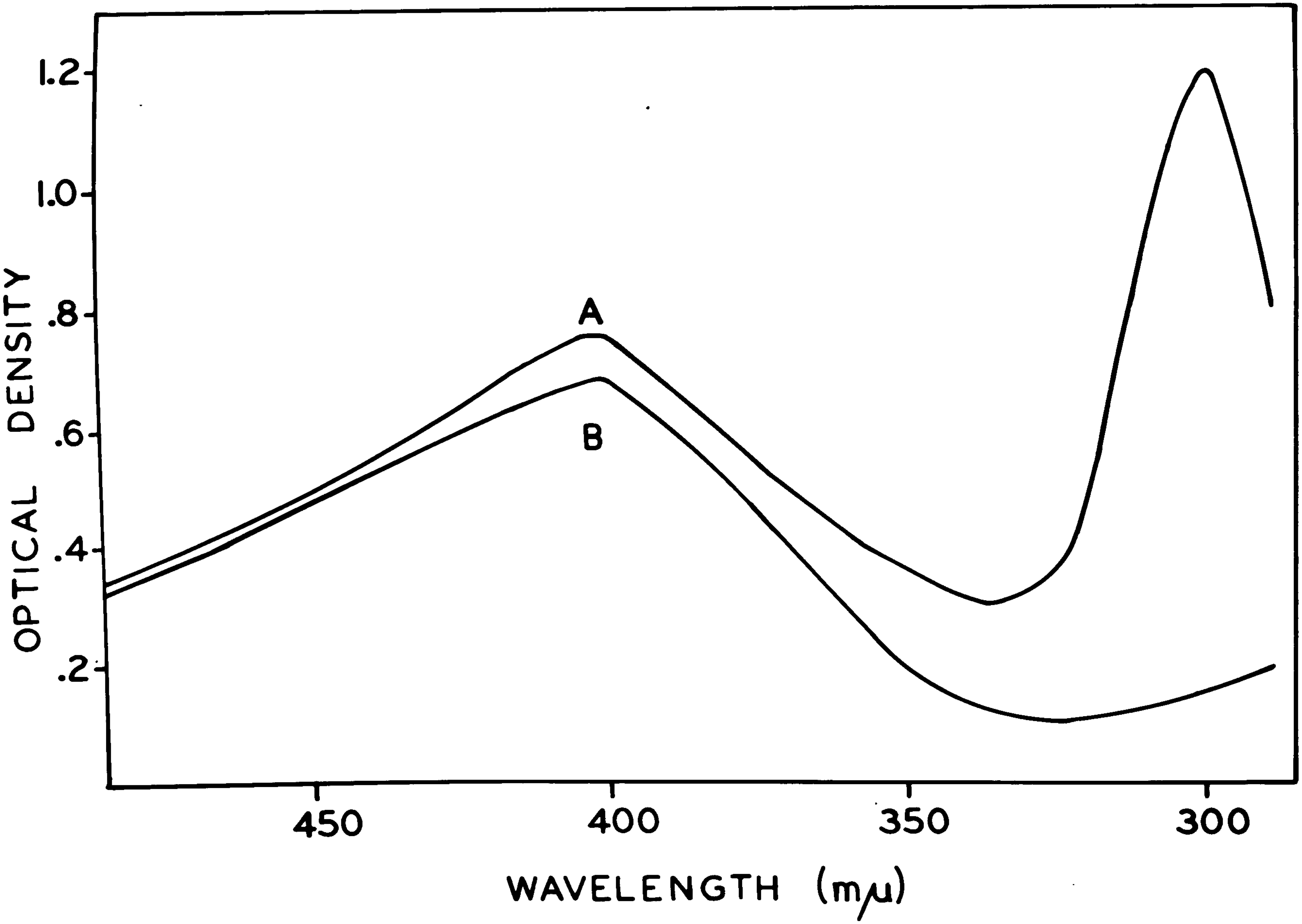

1.2
1.0
.8
.6
.4
.2
OPTICAL DENSITY
A
B
450
400
350
300
WAVELENGTH (mμ)

not been purified by pre-irradiation, after this sample was irradiated for 707 minutes at a dose rate of 8.78_2 x10^{15} ev/gm/min. The optical densities in Figure 12 have been corrected for HBr absorption. Curve B of Figure 12 represents the spectrum of an authentic sample of bromine in HBr. Clearly the 400$m\mu$ peak of the irradiated sample must be due to bromine. The anomalous 300$m\mu$ absorption band is absent from all synthetic solutions and must therefore have been a product of the radiolysis. Since the synthetic solutions were not prepared quantitatively, extinction coefficients could not be calculated from them.

Another sample of HBr was irradiated for a total of 1202 minutes at a dose rate of 8.78_2 x10^{15} ev/gm/min. The spectrum was recorded at 2 hour intervals. The relationship between the 300$m\mu$ peak and the bromine absorption peak is shown by Figure 13. The optical densities of the respective peaks have been plotted against radiation time. It is apparent that little if any bromine is formed in the presence of the precursor to the 300$m\mu$ absorption peak. As the 300$m\mu$ peak approached a limiting absorbance, the bromine yield became linear with radiation time.

Irradiation of liquid HBr which had been purified by pre-irradiation produced a spectrum with only the 400$m\mu$ bromine absorption peak. A plot of optical density against radiation time resulted in a straight line which intersected the origin and had the same slope as curve B in Figure 13. From these data it was possible to calculate the extinction coefficient of bromine in liquid HBr at approximately -79°C. The only assumption necessary is that the hydrogen and halogen yields be identical (i.e. G(Br_2) = 12.4_2). The optical density when the solution was 5.407x10^{-3} M in bromine was 1.07. The extinction coefficient subsequently calculated was 198 and is compared with results from other

FIGURE 13

FIGURE 13

Optical Densities of 300 mμ and 400 mμ Peaks As a Function of Radiation Time

A -- 300 mμ

B -- 400 mμ

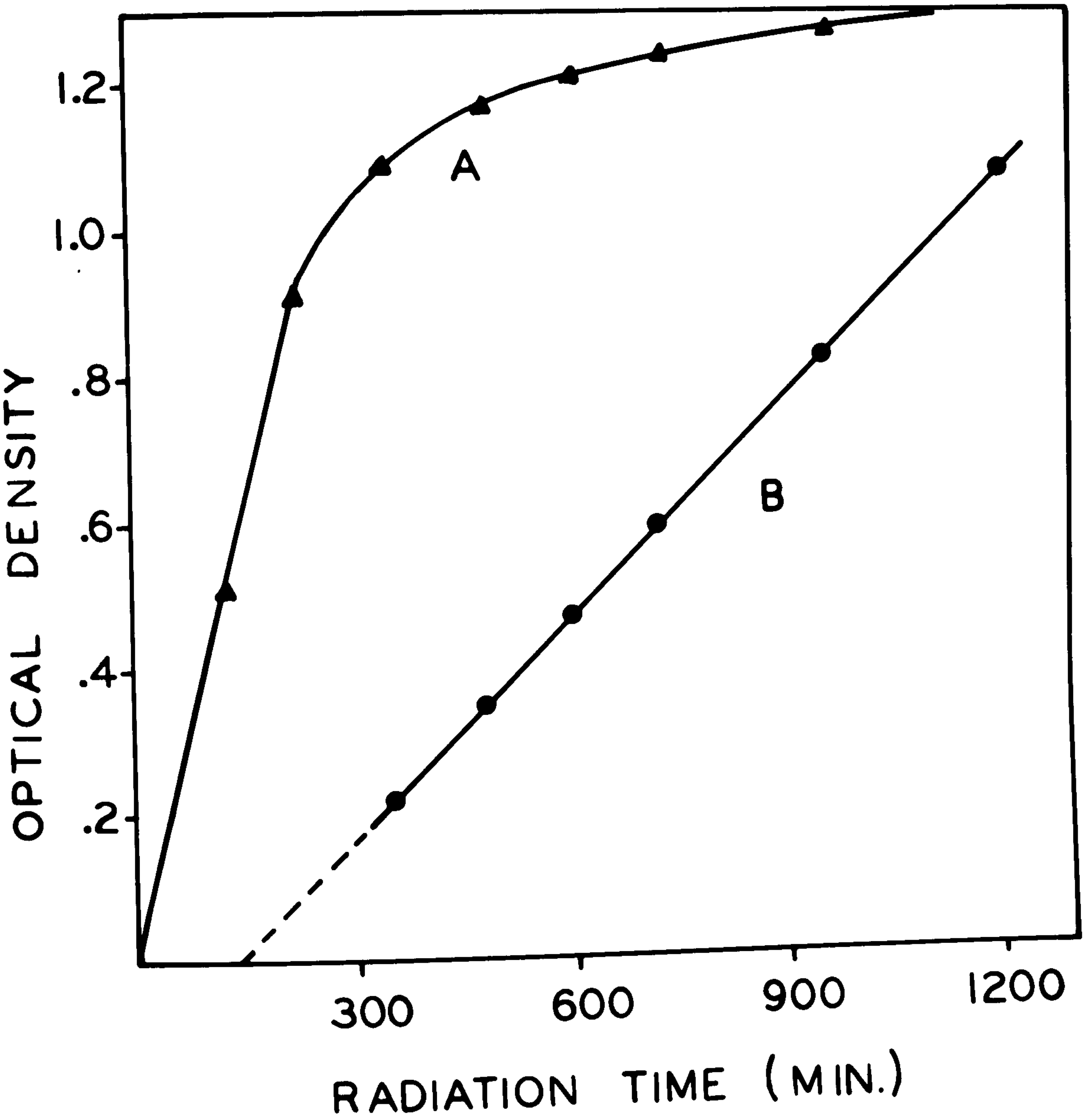
OPTICAL DENSITY
1.2
1.0
.8
.6
.4
.2
A
B
300
600
900
1200
RADIATION TIME (MIN.)

solvent systems in Table II.

1.2.2. HBr - Bromine Mixtures

Molecular bromine is known to react rapidly with hydrogen atoms (77) and mass spectroscopic evidence (32) indicates that it might act as a scavenger for secondary electrons. The lack of a dose dependence for pure HBr suggested that the concentration of bromine attained during radiolysis did not measurably effect the precursors to molecular hydrogen. Irradiation of synthetic solutions of bromine in HBr (the most dilute solution being 60 times more concentrated than any produced radiolytically) caused sizeable decreases in the G-value (Table VII). The practical limit of bromine concentrations was approximately 2M. Beyond this concentration cyrstals, apparently bromine, began to appear.

1.2.3. HBr - Sulphurhexafluoride

Sulphurhexafluoride is an extremely efficient reagent for capturing thermal electrons. Unfortunately, the insolubility of this material in liquid HBr permitted the radiolysis of sulphurhexafluoride in HBr at only one concentration (Table VII). Although the decrease in yield was slight ($\Delta G(H_2) = 0.3 \pm 0.1$) it was too large to be attributed to experimental error. The sulphurhexafluoride appears to be a less efficient scavenger of the molecular hydrogen precursors in HBr than does bromine (Figure 14).

1.2.4. HBr Addition to Ethylene

The photochemically induced free radical addition of HBr to olefins is a familiar reaction in organic chemistry (78). Although large G-values had been reported for both the gas (63) and liquid phase (64) irradiations of HBr-ethylene mixtures, only the gas phase system has been studied kinetically. It was of interest therefore to further investigate the liquid phase radiation-induced reaction and to determine, if possible,

TABLE VII

Hydrogen Yields From γ-Irradiated Solutions of Scavengers in HBr at -79°C

Scavenger	Concentration (Moles/gm)	$G(H_2)$	$\Delta G(H_2)$
--	--	12.40	0.00
Br_2	0.687×10^{-4}	11.70	0.70
Br_2	1.07×10^{-4}	11.45	0.95
Br_2	1.47×10^{-4}	11.23	1.17
Br_2	2.33×10^{-4}	10.72	1.68
Br_2	3.57×10^{-4}	10.32	2.08
Br_2	4.62×10^{-4}	9.81	2.59
Br_2	4.83×10^{-4}	9.56	2.84
Br_2	7.87×10^{-4}	8.54	3.86
Br_2	8.68×10^{-4}	8.49	3.91
SF_6	0.911×10^{-4}	12.13	0.27

FIGURE 14

FIGURE 14

The Variation of $G(H_2)$ From γ-Irradiated HCl - HBr Mixtures (-79°C) with Bromine Concentration

○ -- 1.00 Electron Fraction HBr

■ -- 0.39_8 Electron Fraction HBr

▲ -- 0.14_2 Electron Fraction HBr

◒ -- 0.10_2 Electron Fraction HBr

● -- 1.00 Electron Fraction HCl

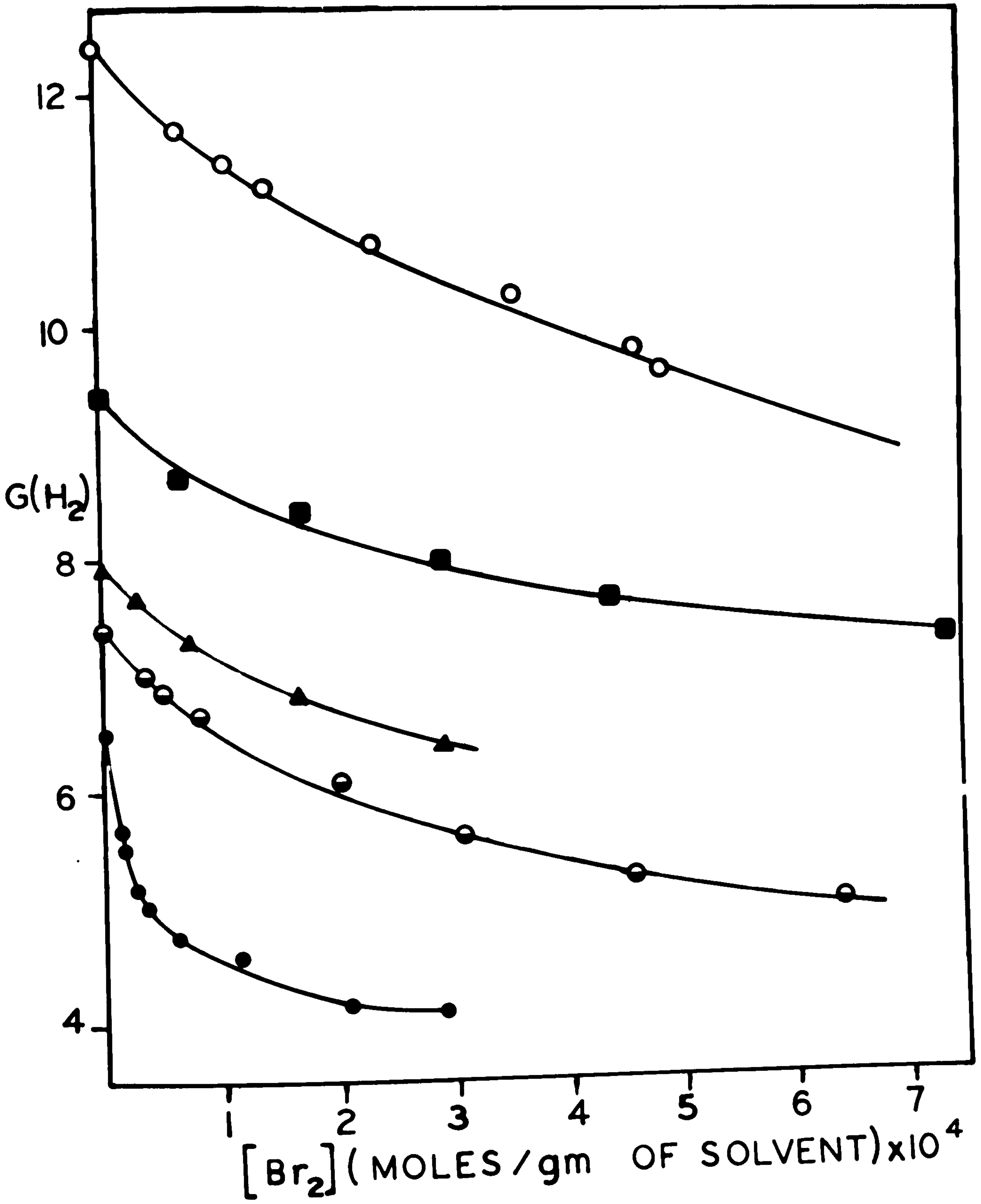
G(H_2)
12
10
8
6
4
1
2
3
4
5
6
7
[Br_2] (MOLES / gm OF SOLVENT) x10^4

whether it proceeded by a similar free radical mechanism.

1.2.4.1. Thermal Reaction

In the presence of a large excess of HBr, only a slight reaction was detected between the HBr and ethylene in the absence of radiation (Tabel VIII A). Only 0.07% and 0.21% of the ethylene had reacted after 420 and 1380 seconds respectively. These rates, which agree with those of Maass (79), can be considered as negligible.

1.2.4.2. Radiation-Induced Reaction

The results of the radiation-induced addition of HBr to ethylene are given in Tables VIII B and IX. The composition of the solutions varied from 5.0 mole % to 15.9 mole % ethylene. First order log plots for ethylene concentration dependence for 15.9 and 5.0 mole % solutions are shown in Figure 15. Solutions of approximately 15 and 5 mole % ethylene were irradiated at several dose rates. The log-log plots of reaction rate against dose rate (Figure 16) indicates a dose rate exponent of 0.6 for both systems.

The initial values of $G(C_2H_5Br)$ varied between $1.03\text{x}10^7$ and $1.04\text{x}10^6$ in the dose rate range of $5.80\text{x}10^{14}$ to $2.27\text{x}10^{15}$ ev/ml/sec. The variation in G-value was proportional to the ethylene concentration.

No reaction was detectable in a 14.3 mole % ethylene solution containing 0.1 mole % nitric oxide after irradiating to a dose of $1.41\text{x}10^{18}$ ev. In this instance, even the thermal reaction was undetected.

1.2.5. HBr - Addition to Propylene

Two distinct products can be formed by the addition of HBr to propylene. The Markownikoff addition product is characteristic of an ionic mechanism, whereas the so-called anti-Markownikoff product suggests

TABLE VIII A

Spontaneous Addition of HBr to Ethylene at -79°C

Moles of C_2H_4	Mole % C_2H_4	Time (sec)	% C_2H_4 Reacted
0.01402	16.8	0	0.00
0.01401	16.8	420	0.07
0.01399	16.8	1300	0.21

TABLE VIIIB

Effect of Nitric Oxide on γ -Irradiated Mixtures of HBr and Ethylene at -79°C

Mole % C_2H_4	Mole % NO	Time (sec)	Dose (ev)	% C_2H_4 Reacted
14.3	0.13	29.9	1.94×10^{16}	0.00
14.3	0.13	2190	1.42×10^{18}	0.00

TABLE IX

Rates of Radiation-Induced Addition of HBr to Ethylene at -79°C

Mole % C_2H_4	Dose Rate ev/ml/sec	Reaction Rate (molec/ml/sec)
5.0	5.80×10^{14}	1.38×10^{19}
5.0	5.80×10^{14}	1.17×10^{19}
5.0	6.41×10^{13}	3.88×10^{18}
15.9	5.80×10^{14}	3.91×10^{19}
15.9	5.80×10^{14}	3.73×10^{19}
14.1	6.41×10^{13}	1.45×10^{19}
15.6	2.27×10^{15}	1.17×10^{20}
15.2	5.70×10^{15}	1.62×10^{20}
15.4	6.48×10^{14}	6.50×10^{19}

FIGURE 15

FIGURE 16

FIGURE 15

First Order Plots For Ethylene Consumption.

A -- 15 mole % C_2H_4

B -- 5 mole % C_2H_4

FIGURE 16

Logarithmic Plots of Reaction Rates Versus Dose Rates

A -- 15 mole % C_2H_4

B -- 5 mole % C_2H_4

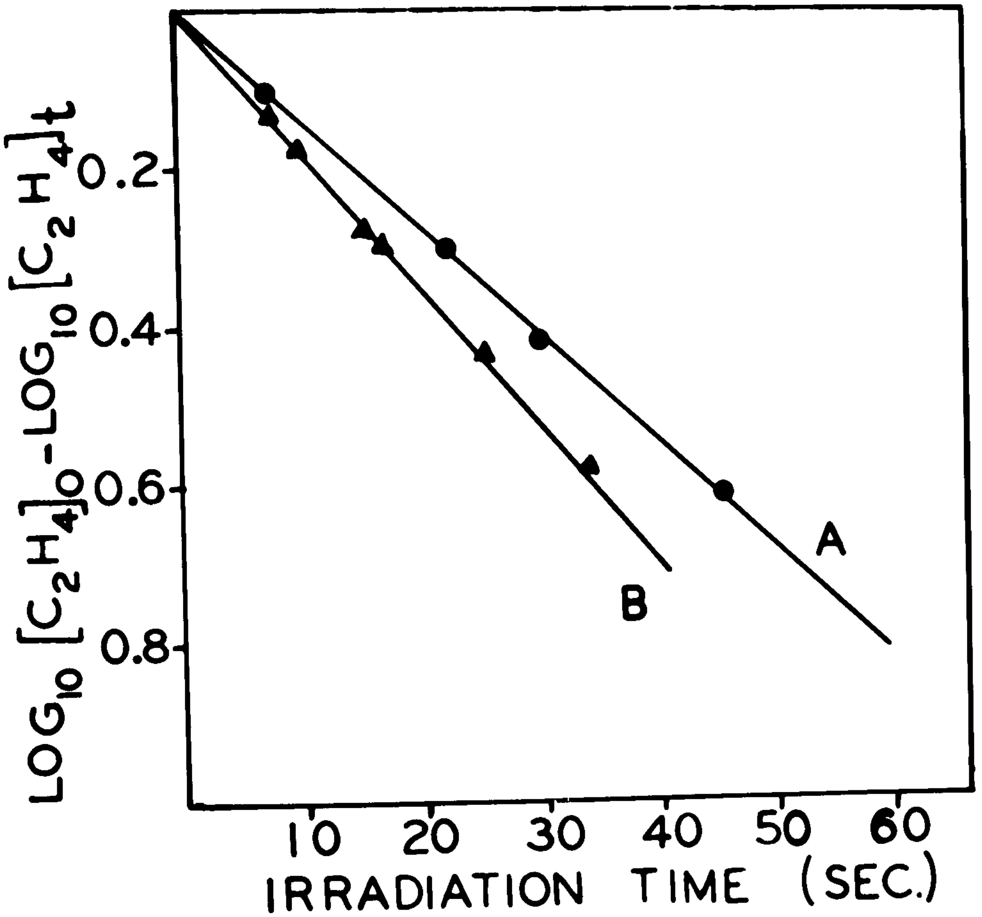
LOG$_{10}$ [C$_2$H$_4$]$_0$ - LOG$_{10}$ [C$_2$H$_4$]$_t$
0.2
0.4
0.6
0.8
A
B
10
20
30
40
50
60
IRRADIATION TIME (SEC.)

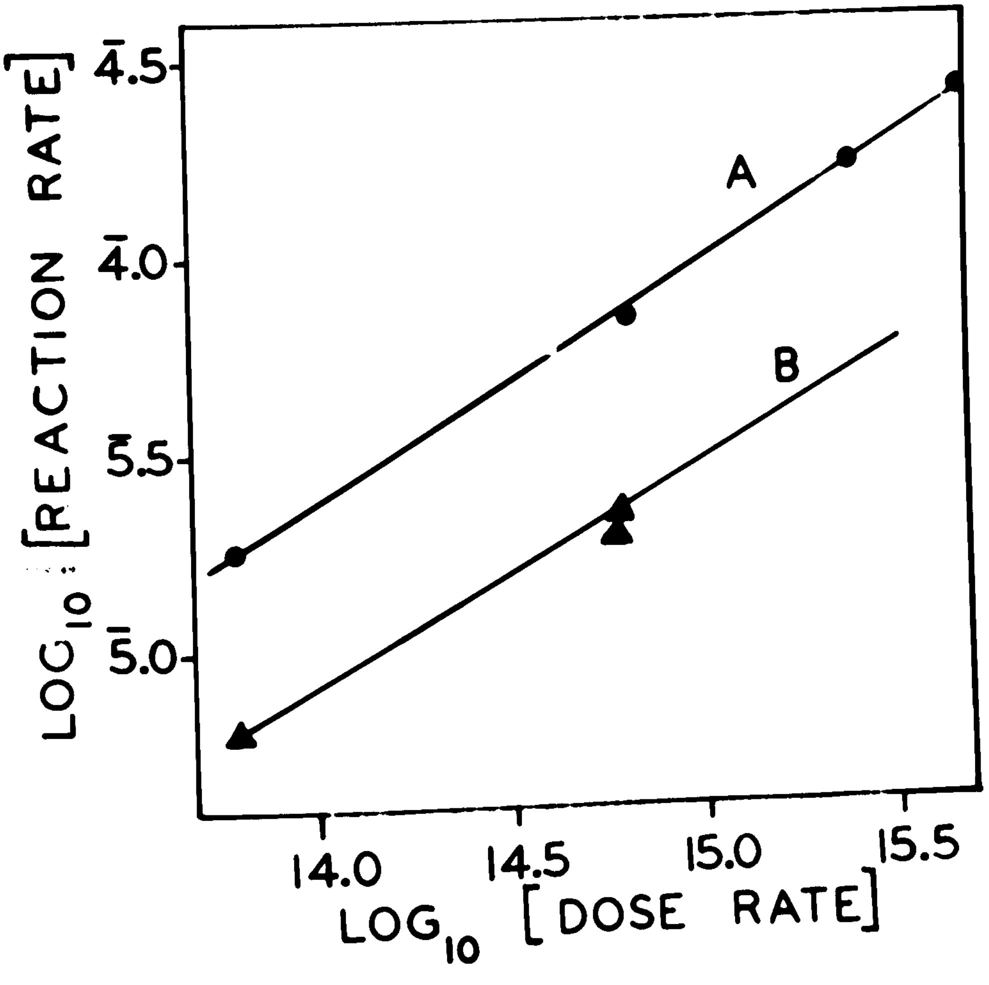
LOG$_{10}$ [REACTION RATE]
$\bar{4}$.5
$\bar{4}$.0
$\bar{5}$.5
$\bar{5}$.0
A
B
14.0
14.5
15.0
15.5
LOG$_{10}$ [DOSE RATE]

a free radical mechanism (80).

1.2.5.1. Thermal Reaction

A slow spontaneous reaction was observed with 27.3 mole % HBr in propylene solutions. The results presented in Table X A indicate an initial rate of 0.1 % per minute. This is in agreement with the value of 0.08 % per minute reported by Maass (81). The addition of nitric oxide did not appear to retard the reaction. Analysis of the reaction products showed that the single major product was 2-bromopropane. Traces of 1-bromopropane and 1-bromohexane were also detected.

1.2.5.1. Radiation Induced Reaction

Solutions of 27.3 mole % HBr in propylene were irradiated at dose rates of 3.48×10^{15} and $1.0_0 \times 10^{18}$ ev/ml/min. The results shown in Table XI suggest a chain reaction (i.e. $G(C_3H_7Br) > 10^3$), however a kinetic analysis was precluded by what appeared to be a variable induction period. 1-Bromopropane was the only significant compound found by the gas chromatographic analysis of the reaction products.

Nitric oxide appeared to appreciably inhibit the radiation-induced reaction (Table X B). A long irradiation in the Gamma-cell with nitric oxide present did effect a greater consumption of HBr than could be accounted for by the thermal reaction, however no attempt was made to analyse the reaction products.

1.3. HCl - HBr Mixtures

1.3.1. Hydrogen Yields

$G(H_2)$ for the radiolysis of HBr is approximately twice that for HCl. Mixtures of the two were irradiated to see if HBr would increase the sensitivity of HCl to radiation. The linearity of the yields with dose is shown in Figure 10. The variation of $G(H_2)$ with composition is illustrated by the solid curve A in Figure 17 (see also Table XII).

TABLE X A

Spontaneous Addition of HBr to Propylene at -79°C

Mole % HBr	Time (min)	Residual HBr (Millimoles)
27.3	0	2.81
27.3	15	2.76
27.3	45	2.76
27.3	120	2.78
27.3	169	2.73
27.3	335	2.69
27.3	1018	2.69

TABLE X B

Effect of Nitric Oxide on γ- Irradiated Mixtures of HBr and Propylene at -79°C

Moles % HBr	Mole % NO	Time (min)	Dose (ev)	Residual HBr (Millimoles)
27.3	0.10	0	0.0	2.81
27.3	0.10	35.5	3.6×10^{19}	2.73
27.3	0.10	240	0.0	2.73
27.3	0.10	215	2.2×10^{20}	2.45

TABLE XI

1-Bromopropane Yields From γ-Irradiated Mixtures of HBr and Propylene at -79°C

Mole % HBr	Time (mins)	Dose (ev)	Residual HBr (millimoles)	$G(n\text{-}C_3H_7Br)$
27.3	0	0.0	2.81	
27.3	0.12	1.2×10^{18}	2.56	1.25×10^{5}
27.3	0.30	3.0×10^{18}	2.59	4.40×10^{4}
27.3	0.50	5.0×10^{18}	2.43	4.56×10^{4}
27.3	1.00	1.0×10^{19}	2.08	4.40×10^{4}
27.3	0.73	7.3×10^{18}	0.00	$>2.31\times10^{4}$
27.3	1.30	1.30×10^{19}	0.00	$>1.30\times10^{4}$
27.3	2.00	2.0×10^{19}	0.00	$>8.45\times10^{3}$

FIGURE 17

FIGURE 17

The Variation of $G(H_2)$ From γ-Irradiated HCl - HBr Mixtures As a Function of Electron Fraction HBr

A -- Observed Values of $G(H_2)$ at -79°C

A′-- G-Values Anticipated From a Simple Additivity Law

B -- Observed Values of $G(H_2)$ at -196°C

B′-- G-Values Anticipated From a Simple Additivity Law

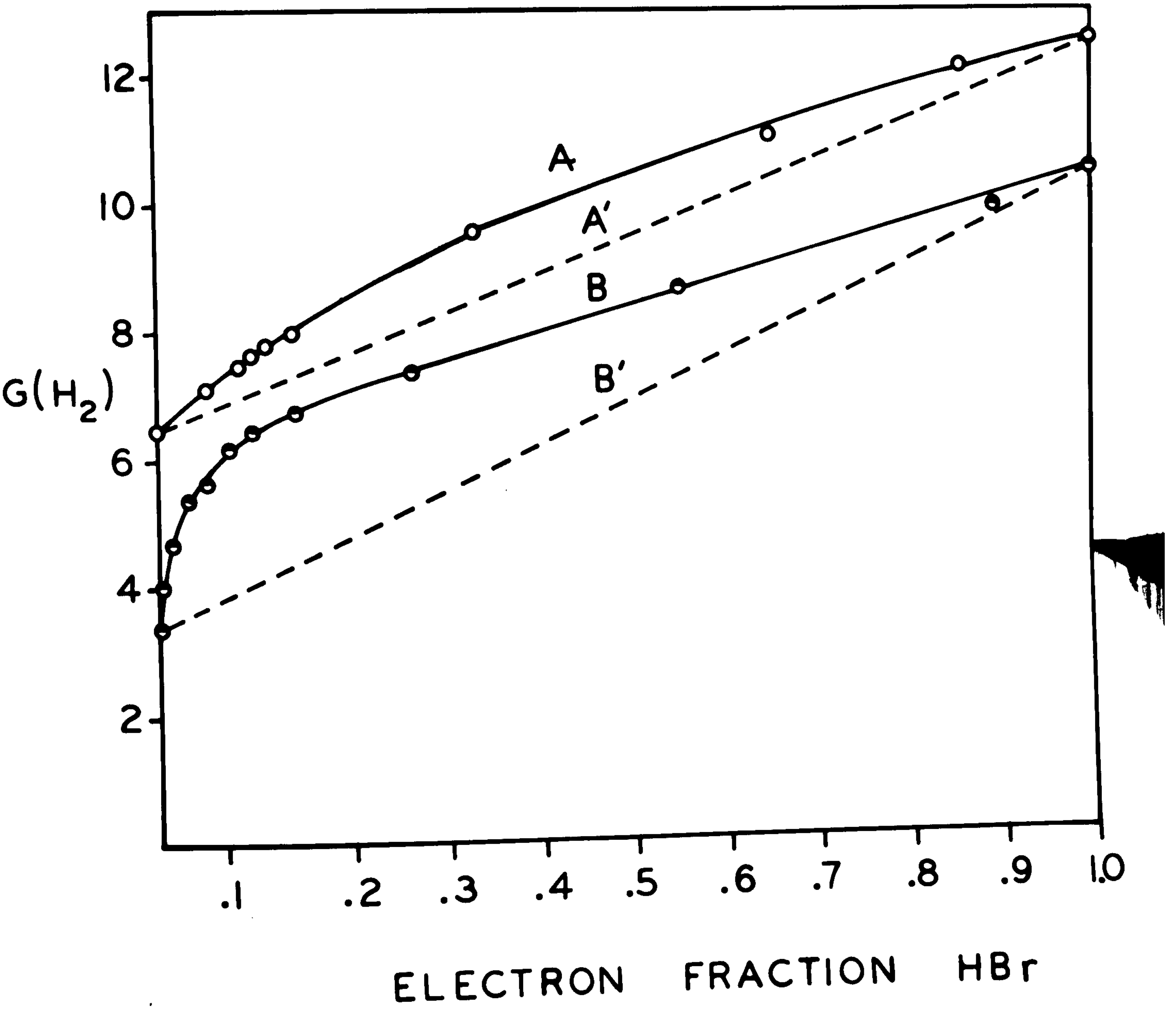
12
10
8
6
4
2
G(H_2)
A
A′
B
B′
.1
.2
.3
.4
.5
.6
.7
.8
.9
1.0
ELECTRON FRACTION HBr

TABLE XII

Hydrogen Yields From γ-Irradiated HCl - HBr Mixtures at -79°C

Electron Fraction		Temp	$G(H_2)$
HBr	HCl		
0.000	1.000	-79°	6.53
0.052	0.948	-79°	7.18
0.092	0.908	-79°	7.37
0.102	0.848	-79°	7.43
0.114	0.886	-79°	7.75
0.142	0.858	-79°	7.95
0.335	0.665	-79°	9.46
0.646	0.354	-79°	11.00
0.857	0.143	-79°	12.12
1.000	0.000	-79°	12.40

The abscissa, electron fraction HBr, represents the fraction of the total dose which is absorbed by the HBr. The broken line (Figure 17 curve A^1) is the expectation value given by the sum of the yields from each pure component assuming that they maintain their normal G-values for hydrogen formation. The maximum difference between $G(H_2)$ observed and that predicted by curve A^1 is one G-unit.

1.3.2. HCl - HBr - Bromine

The effect of bromine as a scavenger in HCl - HBr mixtures was compared with the analogous results with pure HCl and HBr. The linearity of the yields is represented in Figure 10. The decrease in $G(H_2)$ with increasing bromine concentration for solutions of bromine in 0.10_2, 0.14_2, and 0.39_8 electron fraction HBr in HCl is given in Table XIII. In all cases the concentration of bromine was less than the respective solubility limits. A direct comparison of the effect of bromine on the rate of hydrogen formation from HCl, HBr, and the three HCl - HBr mixtures is given in Figure 14.

2. The Solid Phase

2.1. HCl

2.1.1. Hydrogen Yields

The hydrogen yields from irradiated pure solid HCl are dose dependent. As shown in Figure 18 as the dose approaches zero, $G(H_2)$ approaches the value for liquid HCl. For doses greater than approximately 3×10^{18} ev/gm, $G(H_2)$ becomes almost constant at $3.3_6 \pm 0.1$. This plateau value agrees with Armstrong's result (61) of $3.3_0 \pm 0.1$. Although Armstrong also noted a dose dependence, he chose to work at doses higher than 2×10^{18} ev/gm; thus, his G-value would lie on the plateau. The concentration of chlorine at the initial part of the plateau is approximately

TABLE XIII

Hydrogen Yields From γ-Irradiated Solutions of Bromine in HCl - HBr Mixtures at -79°C

Electron Fraction HBr	(Br_2) Moles/gm of solvent	$G(H_2)$	$\Delta G(H_2)$
0.102	0.000	7.43	0.00
0.102	0.344×10^{-4}	6.98	0.45
0.102	0.514×10^{-4}	6.80	0.63
0.102	0.698×10^{-4}	6.66	0.77
0.102	2.023×10^{-4}	6.06	1.37
0.102	3.049×10^{-4}	5.34	2.09
0.102	4.559×10^{-4}	5.26	2.17
0.102	6.409×10^{-4}	5.02	2.41
0.142	0.000	7.95	0.00
0.142	0.263×10^{-4}	7.68	0.27
0.142	0.741×10^{-4}	7.31	0.64
0.142	1.663×10^{-4}	6.83	1.12
0.142	2.930×10^{-4}	6.43	1.52
0.398	0.000	9.40	0.00
0.398	0.664×10^{-4}	8.67	0.73
0.398	1.669×10^{-4}	8.52	0.88
0.398	2.878×10^{-4}	7.97	1.43
0.398	4.327×10^{-4}	7.65	1.75
0.398	7.417×10^{-4}	7.31	2.09

FIGURE 18

FIGURE 18

The Variation of G(H_2) From γ-Irradiated Solid Samples (-196°C) As a Function of Dose

○ -- HBr

● -- 0.14_2 Electron Fraction HBr

◐ -- 0.05 Electron Fraction HBr

◓ -- HCl

■ -- Intermittent

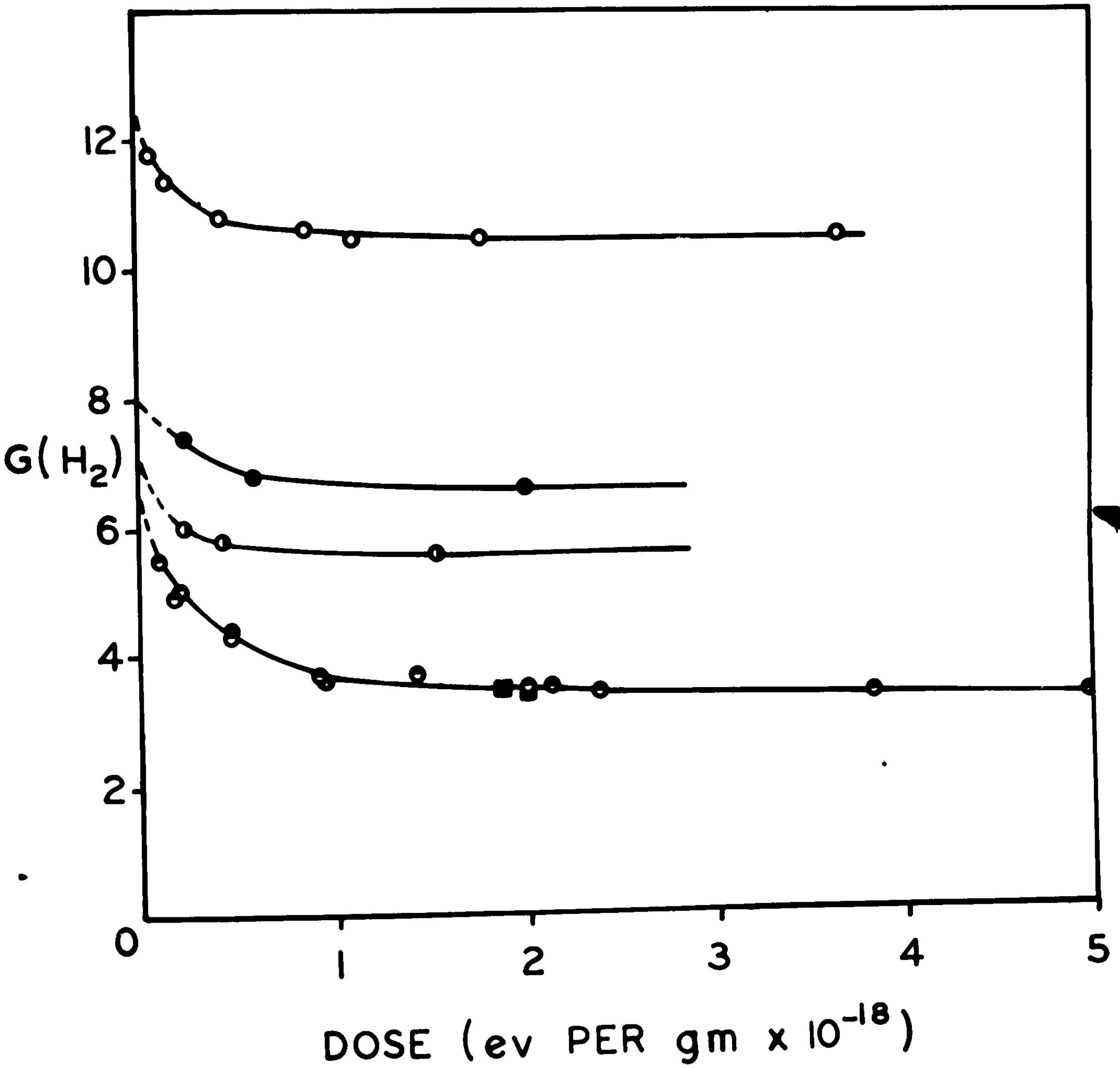

12
10
8
6
4
2
G(H$_2$)
0
1
2
3
4
5
DOSE (ev PER gm x 10^{-18})

1.2×10^{-7} moles/gm.

A distinct green color which was produced in the solid sample during the radiolysis disappeared upon melting. The color did not appear again when the sample was refrozen.

Intermittent irradiations in which the sample was irradiated to a dose of about 0.24×10^{18} ev/gm, melted, refrozen, and re-irradiated successively up to a total dose of approximately 1.9×10^{18} ev/gm gave a yield which was identical with that obtained from a continuous irradiation to the same total dose.

2.1.2. Hot Filament Reaction

The filament technique of Klein and Scheer (67) was employed to ascertain whether or not thermal hydrogen atoms would react with HCl at -196°C. A thin film of HCl (approximately one gram) was frozen uniformly over the walls of the reaction vessel. Hydrogen was admitted to the system until a pressure of 0.10 mm Hg was reached. Continuous heating of the filament for at least 1800 seconds failed to cause any increase in the initial hydrogen pressure. Increasing both the filament voltage to approximately 10 v and doubling the initial hydrogen pressure also failed to initiate any observable reaction.

2.2. HBr

2.2.1. Hydrogen Yields

The hydrogen yields from irradiated HBr are dose dependent (Figure 18). Beyond a dose of approximately 1.2×10^{18} ev/gm, the yield becomes linear with dose and can be expressed as $G(H_2) = 10.5\pm0.1$. For smaller doses, $G(H_2)$ increases rapidly with decreasing dose. As the dose approaches zero $G(H_2)$ approaches 12.4_0 or the G-value for hydrogen formation in the liquid phase. The concentration of hydrogen and thus of bromine at the initial part of the plateau is approximately $2.1_0\times10^{-7}$ moles/gm. A definite green color which grew in intensity with increasing dose was produced on irradiation of the solid sample. The color did not reappear after melting and refreezing.

2.2.2. Hot Filament Reaction

The initial conditions were the same as those employed for HCl. Curve A of Figure 19 represents a plot of hydrogen pressure against reaction time. Although there is a sharp initial decrease in the apparent reaction rate, the increase in hydrogen pressure becomes linear with time after approximately 100 seconds. The linear portion of curve A has a slope of 0.08_1.

At a reaction time of approximately 5 seconds the ratio of moles of hydrogen formed to the weight of HBr (i.e. $\sim 1.5\text{x}10^{-6}$ moles/gm) is approximately the same as the ratio obtained from the radiolysis of solid HBr at a dose of $0.9\text{x}10^{18}$ ev/gm.

2.3. HCl - HBr Mixtures

Solid mixtures of HCl and HBr were irradiated to compare the sensitizing effects of HBr in solid HCl with the analogous liquid systems.

$G(H_2)$ for the radiolysis of HCl - HBr mixtures is dose dependent. The results for 0.14_2 and 0.05_1 electron fraction HBr in HCl are shown in Figure 18. The variation of $G(H_2)$ obtained by relatively long irradiations (therefore plateau values of $G(H_2)$) as a function of composition is represented by the solid curve B in Figure 17 (see also Table XIV). The broken line (curve B^1) represents the theoretical values of $G(H_2)$ derived from the sum of the yields of each pure component multiplied by its electron fraction.

G-values for the mixtures were extremely sensitive to composition for very low concentration. The trace amounts of HBr in HCl not purified by pre-irradiation caused the G-value to be 3.8 ± 0.1 instead of $3.3_6 \pm 0.1$

FIGURE 19

FIGURE 19

The Variation of Hydrogen Pressure (P_{H_2}) With Reaction Time

▲ -- HBr

● -- HCl

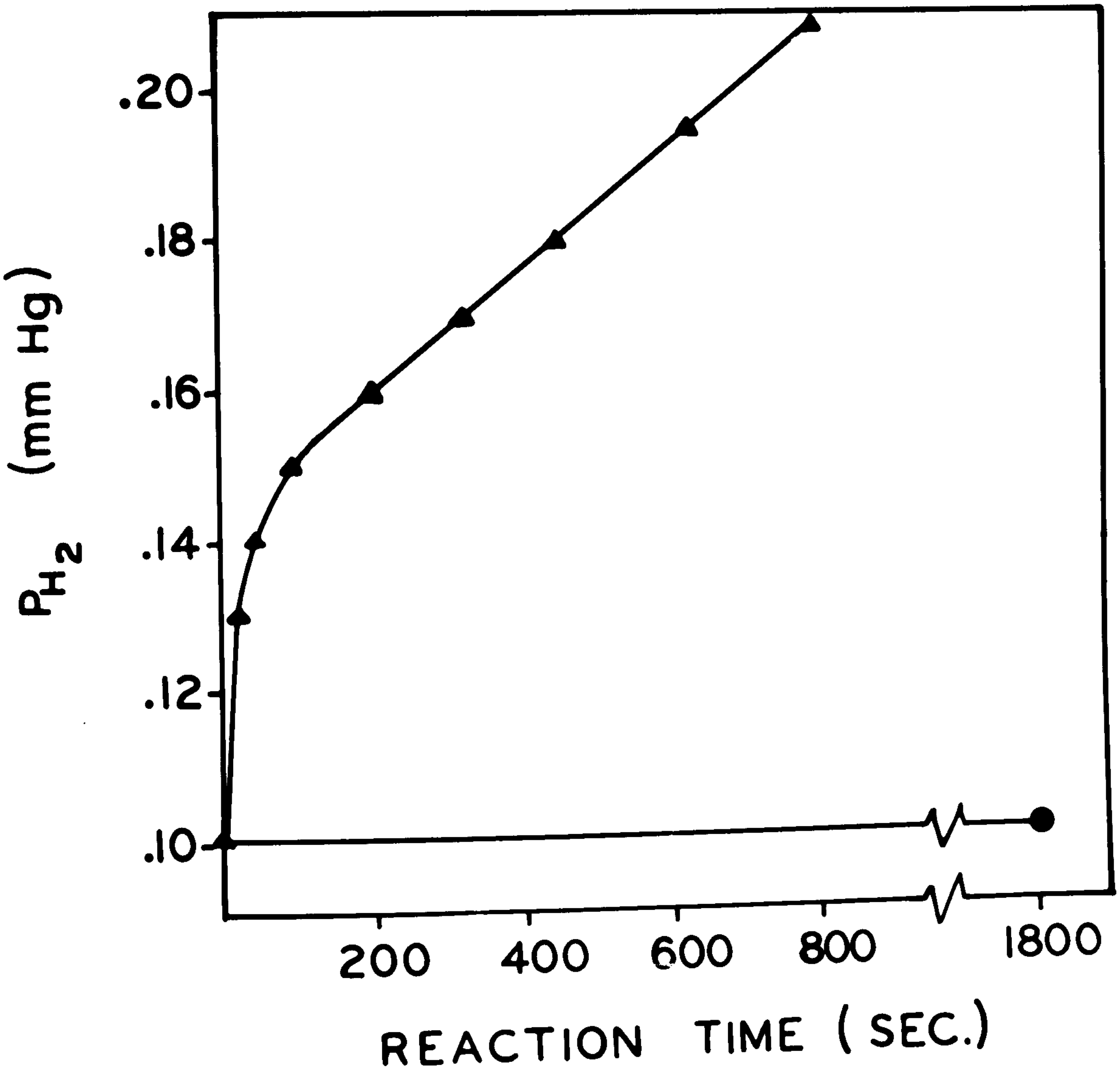
P_{H_2} (mm Hg)
.20
.18
.16
.14
.12
.10
200
400
600
800
1800
REACTION TIME (SEC.)

TABLE XIV

Hydrogen Yields From γ-Irradiated Solid HCl - HBr Mixtures at -196°C

Electron Fraction		Temp	$G(H_2)$
HBr	HCl		
0.000	1.000	-196°	3.36
0.003	0.997	-196°	4.06
0.013	0.987	-196°	4.72
0.034	0.966	-196°	5.44
0.052	0.948	-196°	5.70
0.075	0.925	-196°	6.21
0.102	0.898	-196°	6.47
0.142	0.858	-196°	6.69
0.261	0.739	-196°	7.35
(0.475)*	0.525	-196°	7.38
0.549	0.451	-196°	8.58
0.881	0.119	-196°	9.89

*Heterogeneous Sample

as observed for HCl purified by pre-irradiation. For the lowest concentration of HBr used, 0.003 electron fraction HBr, $G(H_2)$ was 4.06 which constitutes an increase of 0.7 G-units over the yield from pure HCl. At approximately 0.10 electron fraction HBr, $G(H_2)$ is equal to that of pure liquid HCl.

The solid mixtures were prepared by rapidly refreezing a thoroughly mixed liquid sample. The infrared spectra of solid HCl - HBr mixtures prepared by a like technique indicated a homogeneous sample (82). Thus the solid mixtures irradiated in this investigation were assumed to be homogeneous. However, to test the effect of heterogeneity a sample was prepared by freezing HBr over solid HCl. Some interfacial mixing would be inevitable but it is unlikely that this would exceed 20 %. $G(H_2)$ for the radiolysis of a two phase mixture of 0.47_5 electron fraction HBr was $7.4_0 \pm 0.1$. This is only 0.7 G-units larger than the value predicted by curve B^1 of Figure 17.

DISCUSSION

This chapter is divided into two main sections. The first deals with the radiolysis of HCl, HBr, and HCl - HBr mixtures in the liquid phase. The second section deals with essentially the same systems, however, here they are irradiated as solids.

The convention adopted for expressing G-values throughout this chapter employs the use of brackets for total yields whether measured of calculated. Thus, the total number of hydrogen molecules produced in an irradiation multiplied by one hundred and divided by the total absorbed dose would be expressed as $G(H_2)$. Partial yields are distinquished by the use of a subscript. If the hydrogen measured was formed from two different intermediates, then the yields of these would be expressed as G_A and G_B. The over-all representation might then be

$$G(H_2) = G_A + G_B$$

or

$$G(H_2) = G_{H_2} + G_{H_2}'$$

1. The Radiation Chemistry of Hydrogen Halides: The Liquid Phase

The primary products formed in the tracks of the Compton recoil electrons are ions and electronically excited molecules. Before considering the results observed in this investigation, it would seem advantageous to briefly review the reactions which are likely to involve these reactive intermediates.

1.1. Ionic Reactions

Mass spectrometric studies of HCl and HBr indicate that the principal ions formed by electron bombardment are HX^+, HX^{++}, X^+, and X^{++} (83, 84, 85). Molecular ions of charge higher than two have not been found (83). At an electron impact energy of 150v, the relative abundances are~100:7:46:10. In both cases HX^+ is the predominant ionic species formed. It is not possible to predict the exact abundances and types of ions which would be formed in irradiated liquid hydrogen halides. However, solvent stabilization would likely tend to reduce fragmentation in the liquid phase ionizations. In any case if X^+ were formed from a highly excited molecular ion:

$$(HX^+)^* \longrightarrow H + X^+ + \text{energy} \qquad [1a]$$

the charge transfer process:

$$X^+ + HX \text{ —— } HX^+ + X \qquad [2]$$

should be energetically allowed and should occur rapidly. Thus, neglecting the low apparent yield of multiple charge ions, the initial ionizing act would be:

$$HX \rightsquigarrow HX^+ + e \qquad [3]$$

$$HX \rightsquigarrow (HX^+)^* \longrightarrow H + X^+ + e + \text{energy} \qquad [1b]$$

$$X^+ + HX \longrightarrow HX^+ + X \qquad [2]$$

It will thus be assumed that the only primary positive ion of consequence in the irradiated liquid is HX^+.

By using the Bethe equation (see p.5) to calculate the collisional energy loss and choosing $W^{\beta}_{HX} \approx 25$ev, it may be shown that the distribution of ions along the tracks should be similar to that exhibited in irradiated (Co^{60} γ -rays) water. The effect of overlapping spurs can be neglected for both HCl and HBr under the present experimental conditions.

Subexcitation electrons from the ionized molecules will lose energy rapidly by excitation of oscillational modes of the molecules of the medium and by dipole interactions. Frohlich and Platzman (28) predict that the rate of energy loss will be directly proportional to the dielectric constant and inversely proportional to the dielectric relaxation time. No experimental data are available on the dielectric relaxation times of liquid HCl and HBr which are likely to be shorter than that of water. However, any increase in the rate of energy loss because of this would be at least partially compensated by the comparatively low static dielectric constants ($\epsilon_{HCl} \approx 10$ and $\epsilon_{HBr} \approx 7$) (86). The rate of energy loss should therefore be comparable to that in water. Simple calculations from a formula given by Samuel and Magee (29) show that the electron would have to travel beyond a critical intercharge distance of approximately 200Å before it could be considered as free. The possibility then exists that the electron will be thermalized while still in the field of the parent positive ion. Neutralization could then ensue giving rise to energetic radical fragments:

$$e + HX^+ \rightarrow HX^* \rightarrow H + X + \text{energy}. \qquad [4]$$

The time necessary for such a process is uncertain although it should not be very different from that predicted by Samuel and Magee for electrons in liquid water ($\sim 10^{-13}$ sec).

Other processes involving both the electron and ion can occur within this apparent neutralization time. For instance, Schissler and Stevenson (26) have observed the gas phase ion-molecule reaction:

$$HX + HX^+ \longrightarrow H_2X^+ + X \qquad [5]$$

for which the calculated rate constants for HCl and HBr were 4.4×10^{-10} and 5×10^{-10} cc/molecule sec. respectively. Assuming the same rate constants for the liquid phase and concentrations of $1.9_7 \times 10^{22}$ and $1.6_8 \times 10^{22}$ molecules/ml for HCl and HBr respectively, it can be shown that the lifetime for HX^+ is also of the order of 10^{-13} sec. or less. Thus, reaction [5] followed by either reaction [6a] or [6b] :

$$e + H_2X^+ \longrightarrow H + HX + \text{energy} \qquad [6a]$$

$$\longrightarrow H + H + X + \text{energy} \qquad [6b]$$

must be considered as alternatives to reaction [4].

Recent studies (32, 75, 87) with hydrogen halides in the gas phase indicate the high efficiency of the reaction:

$$e + HX \text{———} H + X^- \qquad [7]$$

for electrons in the energy range 0.1 - 1.5 ev.

In gaseous HCl, electron capture occurs over the energy range 0.65ev to 1.5ev with a maximum at 0.8ev which lies above the first vibrational level of the HCl (0.36ev) (88). Energy loss to vibrational excitation can thus compete with reaction [7] and hence reduce the probability of the electron attachment process. On the other hand, the maximum capture cross-section for HBr (0.2ev) is below the lowest vibrational level (0.31ev) (88), thus moderation processes should not seriously affect the capture probability.

The infrared absorption spectra of HX systems offers convincing evidence for hydrogen bonding in the condensed phases (82) and it is also known that X^- will be strongly associated with HX molecules (89). In the liquid phase reaction [7] can be replaced by the reaction:

$$e + H\text{-}X\text{--}H\text{-}X \longrightarrow H + X^-\text{--}H\text{-}X \qquad [7a]$$

Accordingly, the energy of stabilization of $[X^-\text{--}H\text{-}X]$ must be considered as part of the over-all free energy change of the capture reaction in the liquid phase. Davies (90) has calculated a bond energy of approximately 2ev for the hydrogen bond in $[F^-\text{--}H\text{-}F]$. Although the chloride and bromide analogues are not expected to be so strongly bound, the energy of the hydrogen bonds thus formed may be sufficient to make the capture reaction exothermal. A further ramification of this "solvent effect" may be an alteration in the position of the potential energy curve for electron resonance capture (see curve G in Figure 3). If the resonance energy required to form the repulsive negative molecular-ion is sufficiently reduced such that capture would occur over an energy range where thermalization becomes a very slow process, then reaction [7a] may be the exclusive fate of the secondary electrons in liquid HCl and HBr. On the basis of the gas phase values of the mean capture cross-sections (i.e. $2x10^{-18}$ and $6x10^{-17}$ cm^2/molecule for HCl and HBr respectively (75)) and the concentration of molecules in the liquid hydrogen halides, the lifetime with respect to resonance capture of the subexcitation electrons should be less than 10^{-13} seconds.

The kinetic energy of the products of reaction [7a] will depend upon the energy of the electron which is captured. Since the kinetic energy of the fragments will be divided in the inverse ratio of their masses (91), hydrogen atoms formed by the capture of energetic electrons may possess sufficient kinetic energy to exhibit hot-atom characteristics. But electron attachment reactions are only efficient for low energy electrons, thus reaction [7a] should lead to the formation of hydrogen atoms with close to thermal energies.

The diffusion coefficient for $[X^{-}--H-X]$ would certainly be much smaller than for an electron. If reaction [7a] does occur, there can be little doubt that reaction [5] would precede neutralization. The fact that both liquid HCl and HBr have measurable conductivities plus the recent work of Peach and Waddington (92) on acid-base reactions involving HCl suggests that neutralization would occur according to the reaction:

$$H_2X^+ + X^- \text{--}H\text{-}X \rightleftharpoons 3HX \qquad [8]$$

This is the reverse of the autoprotolysis reaction.

The sequences given by reactions [3] - [4] , reactions [3] - [5] - [6a], and reactions [3] - [5] - [6b] are all of the "Samuel-Magee" type and predict the formation of hot hydrogen atoms. The alternate "Platzman" reaction path is given by the reactions [3] - [5]-[7a] . The latter sequence predicts the formation of only thermal or low energy hydrogen atoms.

1.2. Free Radical Reactions

The ultra-violet absorption spectra of gaseous HCl and HBr reveal the existence of many highly excited states (93, 94). Subsequent decomposition of most of these states appears to give rise to hydrogen and halogen atoms in their ground states (94). These fragments would be formed with considerable excess kinetic energy (up to 2ev) of which most would be acquired by the hydrogen atom:

$$HX \rightsquigarrow HX^* \longrightarrow H + X + \text{energy} \qquad [9]$$
$$\longrightarrow H^* + X$$

Reaction [9] differs from other hot atom forming reactions (viz. reaction [4]) in that it does not presuppose an ionic precursor.

The product-forming or forward reactions of hydrogen and halogen atoms in the liquid hydrogen halides are:

$$H + HX \longrightarrow H_2 + X \qquad [10]$$
$$H^* + HX \longrightarrow H_2 + X \qquad [10^*]$$

$$H + H + M \longrightarrow H_2 + M \qquad [11]$$

and

$$X + X + M \longrightarrow X_2 + M \qquad [12]$$

Since the activation energy for reaction [10] is low ($E_{10}(HCl) \approx 5$Kcal/mole and $E_{10}(HBr) \approx 1$Kcal/mole) (95) and the concentration of HX molecules will be high, it can be assumed that very few hydrogen atoms will disappear by reaction [11] or the recombination reaction:

$$H + X + M \longrightarrow HX + M \qquad [13]$$

As the products accumulate in the system the reactions:

$$X + H_2 \longrightarrow HX + H \qquad [14]$$

and

$$H + X_2 \longrightarrow HX + X \qquad |15|$$

become probable. Although reaction [14] may be neglected principally on energetic grounds (95), reaction [15] should be quite rapid. In the present investigation, the yields reported for the radiolysis of the pure hydrogen halides were linear with dose. Thus the concentration of X_2 produced radiolytically was too small to cause a detectable competition between reaction [15] and either reaction [10] or [10*]. The liquid phase yields reported here can thus be regarded as true initial yields.

1.3. Pure Hydrogen Halide

The discussions in the preceding sections might best be summarized in terms of a modified form of the Erying, Hirschfelder, and Taylor (5) mechanism:

$$HX \rightsquigarrow HX^+ + e \qquad [3]$$

$$HX \rightsquigarrow HX^* \longrightarrow H^* + X \qquad [9]$$

$$HX^+ + HX \longrightarrow H_2X^+ + X \qquad [5]$$

$$e + H_2X^+ \longrightarrow H + HX + \text{energy} \qquad [6a]$$

$$e + \text{H-X--H-X} \longrightarrow H + X^-\text{--H-X} \qquad [7a]$$

$$H_2X^+ + X^-\text{--H-X} \rightleftharpoons 3HX \qquad [8]$$

$$H + HX \longrightarrow H_2 + X \qquad [10]$$

$$H^* + HX \longrightarrow H_2 + X \qquad |10^*|$$

Excluding reaction [9] the maximum ion pair yield predicted by this mechanism is 2.0. The higher yield predicted by the Erying, Hirschfelder, and Taylor mechanism (i.e. $-M_{HX}/_N = 4.0$) arises from the difference between reaction [8] and reaction [16]

$$\text{i.e.} \quad HX^+ + X^- \longrightarrow H + 2X \qquad [16]$$

as the choice of ion-recombination reaction.

Ordinarily a reduction in yield upon going from the gas phase to the liquid phase would be expected. However, if the suggested value of $W_{HBr} = 26.5$ (57) is used to calculate G-values from the observed ion-pair yield of the gas phase radiolysis of HBr, the results of this investigation indicate that the yields for both the liquid ($G(H_2) = 12.4$) and solid (plateau $G(H_2) = 10.5$) phases are in fact larger than the gas phase yield ($G(H_2) = 9.4$). This apparently low G-value for the gas phase could be attributable to back reactions or to the choice of an erroneously high value of W_{HBr}. Regardless of the source of the discrepancy it is obvious that the radiation sensitivity of HBr is not seriously affected by the gas to liquid phase transition.

Using the observed value of $-M_{HCl}/_N = 3.3$ (55) and the approximate value of $W_{HCl} = 25$, $G(H_2)$ for gaseous HCl would be 6.6 as compared with $G(H_2) = 6.5 \pm 0.1$ observed in this investigation for the liquid phase. Once again the qualitative nature of the G-value for the gas phase yield permits only the conclusion that the radiation sensitivity of HCl is not markedly affected by a gas to liquid phase transition.

In order to correlate the liquid phase G-values with the ion-pair yield of 2.0 predicted on the basis of the modified Eyring, Hirschfelder, and Taylor mechanism, the values for W_{HX} would have to be 8.1 and 15.4 for HBr and HCl respectively. Since such values seem too low (particularly in the case of HBr) reaction [9] must also contribute significantly to the primary act. Although for different reasons, a similar conclusion regarding the occurrence of reaction [9] has also been expressed by Zubler, Hamill, and Williams (57).

1.4. Scavenger Studies: HCl

Armstrong (61) has employed chlorine as a scavenger in liquid HCl (-79°C). His results indicate that at least two hydrogen forming species are produced during the radiolysis. The G-value for the more readily scavenged species was 2.3 and for the second species was 4.2. Armstrong preferred to interpret his results as a competition between HCl and chlorine for thermal and hot hydrogen atoms.

i.e.

$$H + HCl \longrightarrow H_2 + Cl \qquad [10]$$

$$H + Cl_2 \longrightarrow HCl + Cl \qquad [15]$$

$$H^* + HCl \longrightarrow H_2 + Cl \qquad [10^*]$$

$$H^* + Cl_2 \longrightarrow HCl + Cl \qquad [15^*]$$

The values for k_{10}/k_{15} and k_{10^*}/k_{15^*} were estimated to be 1.7×10^{-3} and 0.10 respectively. These values are in substantial agreement with results determined by Klein and Wolfsberg (96) from more conventional studies. Thus, the hydrogen atom scavenging mechanism is strongly supported.

On the other hand the reactions:

$$e + Cl_2 \longrightarrow Cl + Cl^- \qquad [17]$$

and

$$HCl^* + Cl_2 \longrightarrow HCl + Cl_2^* \qquad [18]$$

might also occur and cause equivalent reductions in $G(H_2)$. The agreement between Armstrong's results and those of Klein and Wolfsberg would then only be fortuitous.

In the present investigation these scavenger studies have been extended to include the following systems: HCl and bromine, HCl and ethylene-nitric oxide, and HCl and sulphurhexafluoride. Assuming that the reduction in hydrogen yield arises from the competition between:

$$H + HCl \longrightarrow H_2 + Cl \qquad [10]$$

and

$$H + S \longrightarrow \text{product(s)} \qquad [15]$$

where S represents any of the above scavengers, then the usual steady state approximation leads to the equation:

$$\frac{1}{\Delta G(H_2)} = \frac{1}{G_H}\left[1 + \frac{k_{10}(HCl)}{k_{15}(S)}\right] \qquad [1.1]$$

$\Delta G(H_2)$ is the difference between $G(H_2)$ in the absence of a scavenger and $G(H_2)$ at a scavenger concentration (S).

A competition for the second hydrogen producing species will also exist:

$$H^* + HX \longrightarrow H_2 + X \qquad [10^*]$$

$$H^* + S \longrightarrow \text{product(s)} \qquad [15^*]$$

The sum of the two yields:

$$G_{H_2} + G_{H_2^*} = G(H_2) \qquad [1.2]$$

will obviously be equal to the observed hydrogen yield. The total should then be given by:

$$G(H_2) = G_{H_2} + G_{H_2^*} \qquad [1.3]$$

$$= G_H\left[\frac{1}{1 + k_{15}(S)/k_{10}(HCl)}\right] + G_{H^*}\left[\frac{1}{1 + k_{15^*}(S)/k_{10^*}(HCl)}\right]$$

Provided that the difference between the values of the two rate constant ratios is sufficiently large then it is possible to separate equation [1.3] into two expressions similar to equation [1.1].

Figure 20 represents a plot of $1/\Delta G(H_2)$ against $1/(X_2)$ where X_2 is bromine in curve A and curve B is Armstrong's (61) curve for chlorine. The intercept for the linear portion of curve A gives a value of 2.4±0.2 for G_H. From the slope

i.e. $$\frac{1}{G_H}\left[\frac{k_{10}(HCl)}{k_{15}}\right]$$

FIGURE 20

FIGURE 21

FIGURE 20

Kinetic Plot of the Effect of Halogens on the Hydrogen Yield From γ-Irradiated HCl (-79°C)

The reciprocal of the reduction in the hydrogen yield ($1/\Delta G(H_2)$) plotted against the reciprocal of the halogen concentration ($1/(X_2)$) measure in moles/gm HCl.

— — — $X_2 = Cl_2$ (see reference (61))

● $X_2 = Br_2$

FIGURE 21

Kinetic Plot of the Effect of Ethylene on the Hydrogen Yield From γ-Irradiated HCl (-79°C)

$1/\Delta G(H_2)$ plotted against the reciprocal of the ethylene concentration ($1/(C_2H_4)$) measured in moles/gm HCl.

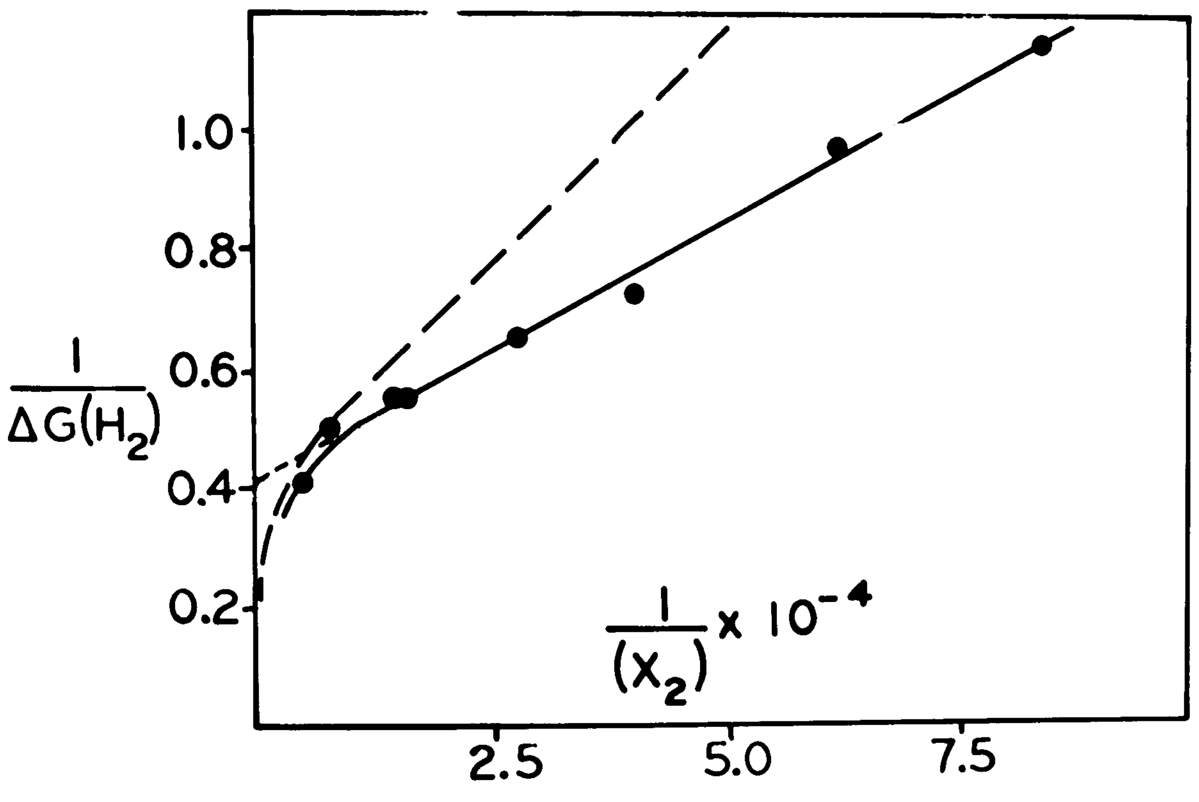
1.0
0.8
0.6
0.4
0.2
$\frac{1}{\Delta G(H_2)}$
$\frac{1}{(X_2)} \times 10^{-4}$
2.5
5.0
7.5

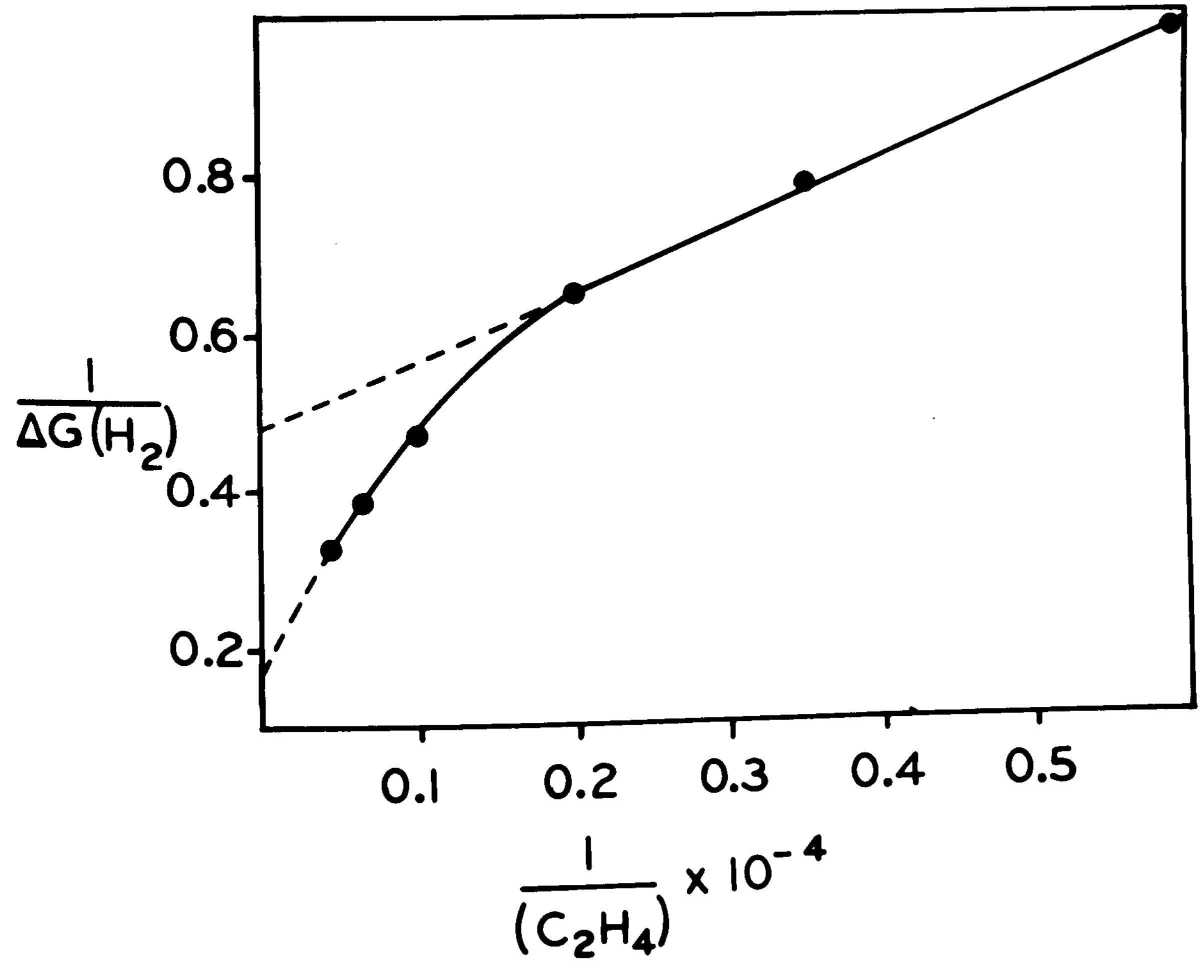
0.8
0.6
0.4
0.2
$\frac{1}{\Delta G(H_2)}$
0.1
0.2
0.3
0.4
0.5
$\frac{1}{(C_2H_4)} \times 10^{-4}$

a value of $7.9 \pm 0.2 \times 10^{-4}$ was calculated for the ratio

$$k_{10(H + HCl)}/k_{15(H + Br_2)}$$

From independent kinetic data on hydrogen atom reactions (95, 97, 98), a value of $6 \pm 3 \times 10^{-4}$ was estimated for the same ratio (see Appendix I).

The value obtained for G_H is in substantial agreement with that observed by Armstrong (see Table XV) and strongly suggests that both chlorine and bromine scavenged the same species.

Comparison of the rate constant ratios obtained by the use of chlorine and bromine as scavengers leads to a calculated value of 0.46 for the ratio

$$k_{(H + Cl_2)}/k_{(H + Br_2)}.$$

Values between 0.26 and 0.72 can be calculated for the same ratio from more conventional kinetic data (95, 96) (Appendix I). From the data illustrated in Figures 1 and 2, the relatively large difference in appearance potentials suggests that the observed value of 0.46 is too large to represent a ratio of rate constants for electron scavenging by chlorine and bromine respectively. However, the arguments advanced with respect to solvent effects on the capture of electrons by HCl should also apply to chlorine, thus electron scavenging by the halogens cannot be categorically excluded on this basis alone.

Ethylene is known to react readily with hydrogen atoms (67, 99):

$$H + C_2H_4 + M \longrightarrow C_2H_5 + M \qquad [19]$$

It is unlikely that the presence of ethylene would alter the normal reactions of secondary electrons. A plot of $1/\Delta G(H_2)$ against $1/(C_2H_4)$ is shown in Figure 21. The values for $G(H_2)$ have been corrected for the contribution from the direct radiolytic reaction:

$$C_2H_4 \rightsquigarrow C_2H_2 + H_2 \qquad [20]$$

TABLE XV

Values of Kinetic Parameters Obtained from Scavenger Studies of γ-Irradiated HCl at -79°C

Scavenger	k_{HCl}/k_S	k_{HCl^*}/k_{S^*}	G_H	G_{H^*}
Cl_2	$1.7\text{x}10^{-3}$	0.10	2.3	4.2
Br_2	$7.9\text{x}10^{-4}$	----	2.4	4.1
C_2H_4	$6.3\text{x}10^{-3}$	~0.14	2.1	4.4

The plot resolves into two parts. From the linear portion corresponding to low ethylene concentrations a value of 2.1 ± 0.2 for G_H is obtained and the calculated value for

$$k_{10}(H + HCl)/k_{19}(H + C_2H_4)$$

is 6.3×10^{-3}.

However the charge transfer reactions

$$HCl^+ + C_2H_4 \longrightarrow HCl + C_2H_4^+ \qquad [21a]$$

$$HCl^+ + C_2H_4 \longrightarrow Cl + C_2H_5^+ \qquad [21b]$$

$$H_2Cl^+ + C_2H_4 \longrightarrow C_2H_5^+ + HCl \qquad [22]$$

might also occur (24). It is unlikely that reactions [21a] and [21b] could precede reaction [5] due to resonance requirements, thus reaction [22] is the most probable charge transfer reaction. If formed, the ethyl carbonium ion could only reduce the hydrogen yield by capturing electrons:

$$C_2H_5^+ + e \longrightarrow C_2H_5^* \qquad [23]$$

Since the resultant excited ethyl radical would have a high probability of decomposing,

i.e. $$C_2H_5^* \longrightarrow C_2H_4 + H + \text{energy} \qquad [24]$$

such a scavenging mechanism would not be expected to exhibit the efficiency suggested by the observed value of 6.3×10^{-3} for the rate constant ratio.

When the rate data of Kang Yang (99) for the addition of hydrogen atoms to ethylene and kinetic data (95) for reaction [10] are used to calculate (see Appendix I)

$$k_{10}(H + HCl)/k_{19}(H + C_2H_4)$$

a mean value of 10×10^{-3} is obtained. The agreement between this value and that obtained experimentally in this work is further evidence for the existence of thermal or low energy hydrogen atoms in irradiated liquid HCl.

Extrapolation of the second or more steeply sloped portion of the curve in Figure 21 intersects the ordinate at $1/\Delta G(H_2) = 0.15$ (i.e. $\Delta G(H_2) = 6.5$). Thus at sufficiently high ethylene concentrations all the precursors to molecular hydrogen formed in irradiated HCl would be scavenged. From equation [1.2] G_{H*} must be 4.4. By substituting values of ΔG_{H_2*} for higher ethylene concentrations into the expression:

$$\frac{1}{\Delta G_{H_2*}} = \frac{1}{G_{H*}}\left[1 + \frac{k_{10*}(\mathrm{HCl})}{k_{19*}(C_2H_4)}\right]$$

the rate constant ratio

$$k_{10*}(\mathrm{H} + \mathrm{HCl})/k_{19*}(\mathrm{H} + C_2H_4)$$

was calculated and found to be ~ 0.14.

As a first approximation the ratio of rate constants for hot-atom reactions should be approximately equal to the ratio of the pre-exponential factors. Using

$$\log_{10}(A/T^{1/2})_{\mathrm{H} + \mathrm{HCl}} = 9.40 \qquad (95)$$

and

$$\log_{10}(A/T^{1/2})_{\mathrm{H} + C_2H_4} = 9.10 \qquad (99)$$

the predicted value of

$$k_{10*}(\mathrm{H}^* + \mathrm{HCl})/k_{19*}(\mathrm{H}^* + C_2H_4)$$

would be approximately 2 as opposed to the observed value of ~ 0.14. Since ethyl radicals formed by the reaction:

$$\mathrm{H}^* + C_2H_4 \longrightarrow C_2H_5^* \qquad [19^*]$$

would be in a highly excited vibrational state, the back reaction

$$C_2H_5^* \longrightarrow C_2H_4^* + \mathrm{H} + \text{energy} \qquad [23]$$

may lead to the spontaneous reformation of hydrogen atoms. Likewise the abstraction reaction:

$$\mathrm{H}^* + C_2H_4 \longrightarrow C_2H_3\cdot + H_2 \qquad [24]$$

would compete with reaction [19*]. In view of these competing reactions a value of

$$k_{10}*(H* + HCl)/k_{19}*(H* + C_2H_4)$$

much larger than that predicted would be anticipated. Thus the relatively small observed value indicates that ethylene was scavenging the "hot-yield" by reacting with some species other than a hot hydrogen atom.

An alternate mechanism, that of energy transfer:

$$HCl* + C_2H_4 \longrightarrow C_2H_4* + HCl \tag*{[25]}$$

might then be suggested. Indeed, as a corollary, the question may be asked as to whether or not there is a real hot atom yield. The second species may simply be an excited molecule forming hydrogen by the bimolecular process:

$$HCl* + HCl \longrightarrow H_2 + Cl_2 \tag*{[26]}$$

It is outside the scope of this investigation to attempt an unambiguous identification of the second hydrogen producing species. For the sake of clarity this species will continue to be referred to as a hot hydrogen atom.

The values of G_H and G_{H*} obtained by the use of the three scavengers are all in substantial agreement with each other (Table XV), Since G_H determined from the ethylene scavenging experiments must certainly represent thermal hydrogen atoms, then bromine and chlorine must have been reacting with thermal hydrogen atoms also or their stoichiometric equivalent (i.e. secondary electrons).

Sulphurhexafluoride is known to have an extremely high cross-section for electron capture with a zero energy threshold (75). Thus, it should be an extremely effective scavenger of thermal electrons. At 5 mole %, sulphurhexafluoride caused a decrease of only 0.5 in the G-value. However, at comparable concentrations other scavengers had reduced the yield by as much as 3.7 G-units, thus it seems unlikely that thermalized electrons could be the principal precursors to hydrogen via reactions [4] or [6].

The results of the scavenging experiments with liquid HCl leads to the conclusion that the first hydrogen forming species is a thermal hydrogen atom. The second species is either a hot hydrogen atom or an electronically excited molecule. The latter entity could certainly be the precursor to hot atoms if they were formed in the system. These excited molecules must be produced by a direct interaction with the primary ionizing particle or the delta-rays. The alternate ion-electron recombination reaction (i.e. reaction [6a] or [6b]) presupposes the formation of thermalized electrons which should then have been (but were not) detected.

1.5. HCl - HBr Mixtures

The marked difference in yields between irradiated HCl and HBr is not readily explained on the basis of either the difference in ionization potentials ($I_{HCl} = 12.6$ev, $I_{HBr} = 11.7$ev) (100) or bond dissociation energies ($D_{HCl} = 4.43$ev, $D_{HBr} = 3.75$ev) (88). It was hoped that by irradiating HCl - HBr mixtures an explanation for the large difference in radiation sensitivities of the two compounds could be obtained.

Possible sources of this difference could be (a) that a significant number of hydrogen atoms in irradiated HCl are reacting by reactions [11] and [13] , (b) that ion-recombination in liquid HBr produces radicals,

i.e. $H_2Br^+ + Br^- \text{--} H\text{-}Br \longrightarrow H + Br + 2\ HBr$ [27]

or $H_2Br^+ + e \longrightarrow H + H + Br^-$ [6b]

and (c) that a greater number of ions and/or dissociative excited molecules are formed in HBr.

Since irradiation of liquid HCl and water should result in about the same ion density, an estimate of the extent of track recombination in HCl can be obtained from calculations based on the diffusion kinetic model of irradiated water. The hydrogen atom scavenging efficiency of HCl in pure liquid HCl at -79°C is approximately equivalent to a 5×10^{-5} moles/ℓ aqueous solution of a solute of maximum hydrogen atom scavenging efficiency (i.e. unit steric factor and zero activiation energy). From tables computed by Kuppermann and Belford (101), the number of hydrogen atoms undergoing recombination in HCl should range from between G = 1.5 to G = 0.3 depending upon the choice of initial spur dimensions. From this analogy it seems highly improbable that recombinations could account for more than a difference of one G-unit between the hydrogen yields from HCl and HBr.

From the slopes of the plots in Figure 22, rate constant ratios can be calculated using the expression:

$$\frac{1}{\Delta G(H_2)} = \frac{1}{G_H} + \frac{1}{G_H}\left[\frac{k_{10(H + HCl)}(HCl)}{k_{15(H + Br_2)}(Br_2)} + \frac{k_{10(H + HBr)}(HBr)}{k_{15(H + Br_2)}(Br_2)}\right] \qquad [1.4]$$

Using the experimentally determined value of 7.9×10^{-4} for

$$k_{10(H + HCl)}/k_{15(H + Br_2)}$$

values for

$$k_{10(H + HBr)}/k_{15(H + Br_2)}$$

were calculated (Table XVI). At low concentrations of HBr in HCl, the calculated value of 0.10±0.02 for

$$k_{10(H + HBr)}/k_{15(H + Br_2)}$$

is in excellent agreement with the temperature independent value of 0.12 for the same ratio which has been reported by several authors (97, 102). It seems, however, that at the higher HBr concentration the value of this rate constant ratio decreases. This apparent trend to lower values of the rate constant ratio is discussed more fully in section [1.6].

From the above data a value of 7.9×10^{-3} for the ratio

FIGURE 22

FIGURE 22

Kinetic Plot of the Effect of Bromine on the Hydrogen Yield from γ-Irradiated HCl - HBr Mixtures

$1/\Delta G(H_2)$ plotted against the reciprocal of the bromine concentration $(1/(Br_2)$ measured in moles/gm solvent.

■ -- 0.39_8 Electron Fraction HBr
○ -- 0.14_2 Electron Fraction HBr
● -- 0.10_2 Electron Fraction HBr

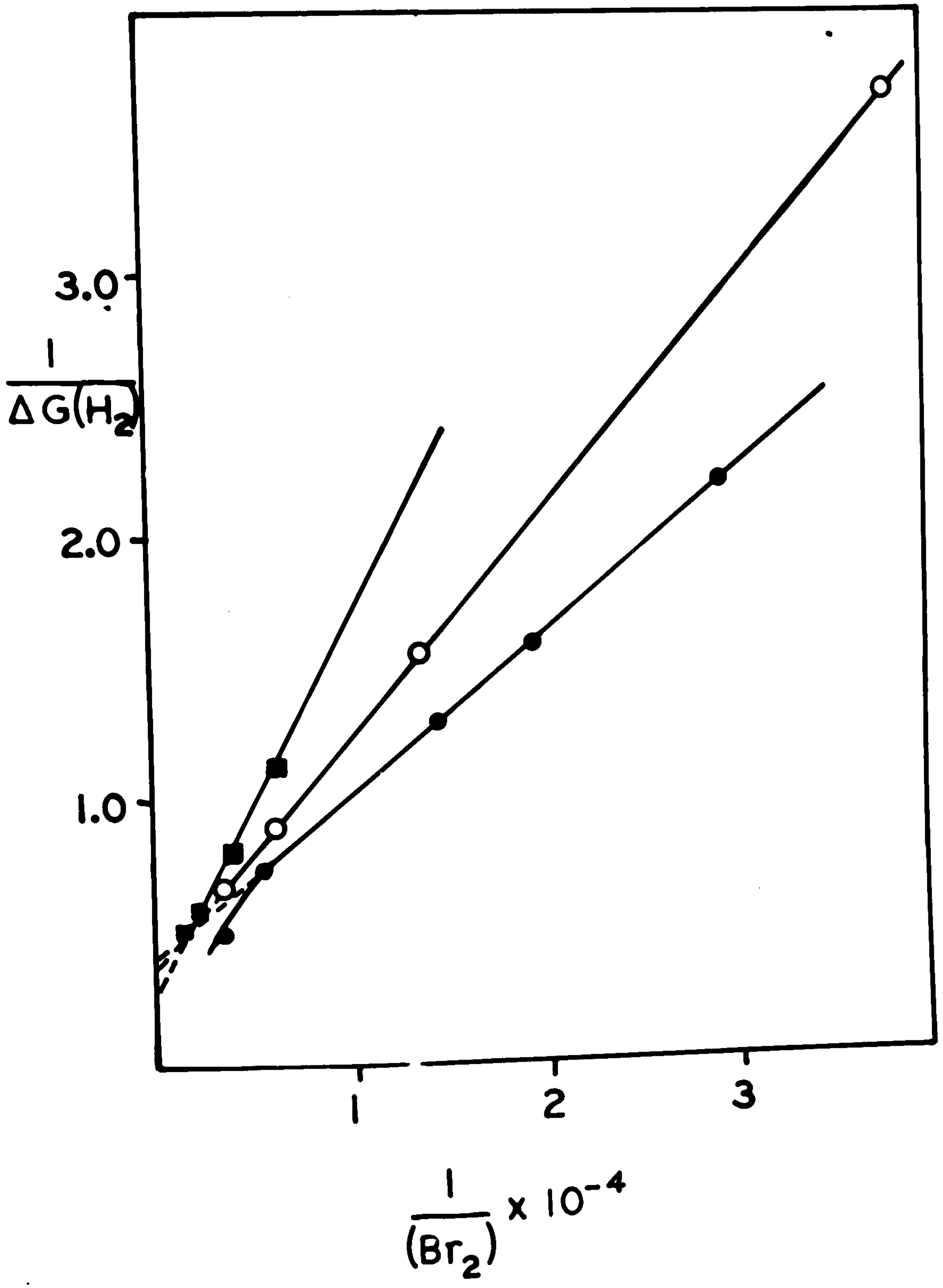

3.0
2.0
1.0
$\frac{1}{\Delta G(H_2)}$
1
2
3
$\frac{1}{(Br_2)} \times 10^{-4}$

TABLE XVI

Values of Kinetic Parameters Obtained from Scavenger (bromine) Studies of γ-Irradiated HCl - HBr Mixtures at -79°C

Composition Electron Fraction HBr	k_{HBr}/k_{Br_2}	G_H	G_{H^*}
0.000 (1.00 HCl)	----	2.4	4.2
0.102	1.00×10^{-1}	2.5	4.9
0.142	1.05×10^{-1}	2.6	5.4
0.398	6.38×10^{-2}	3.0	6.4
1.000	----	(4.0)[a]	---

(a) extrapolated

$$k_{10(H + HCl)}/k_{10(H + HBr)}$$

was calculated. If the experimental data of Ogg and Williams (98) is used to calculate the same ratio, a value of $5 \pm 3 \times 10^{-3}$ is obtained (Appendix I).

On the basis of this ratio, it can be assumed that at sufficiently high concentrations, HBr should readily scavenge the majority of hydrogen atoms undergoing recombination in HCl. From curve A in Figure 17 it can be seen that the maximum increase in hydrogen yield (over the expected yield) is only about one G-unit. It is obvious then that reactions [11] and [13] cannot adequately explain the large difference between G(-HCl) and G(-HBr).

The G-values for the formation of the first hydrogen forming species in the HCl - HBr mixtures increase with increasing concentrations of HBr (see Table XVI). From this apparent linear trend an approximate value of $G_H = 4.0$ for pure HBr can be obtained by extrapolation. Thus, it can be concluded that the curvature of curve A in Figure 17 is principally due to an increase in the hot-hydrogen atom yield. This conclusion also implies that track recombination reactions in liquid HCl do not occur to a significant extent. A probable source of the slight increase in hot-hydrogen atom yield could be a competition between the energy transfer reactions:

$$HCl^* + HCl \longrightarrow HCl + HCl^{\dagger}\text{(NON DISSOCIATE STATE)} \qquad [28]$$

$$HCl^* + HBr \longrightarrow HCl + HBr^* \qquad [29]$$

followed by:

$$HBr^* \longrightarrow H + Br + \text{energy} \qquad [9a]$$

Thus far it has been assumed that only one hydrogen atom is formed from each ion-pair produced in either HCl or HBr. If the ion-recombination reactions in HBr produce radicals then the ionic yield could be doubled.

i.e. $e + H_2Br^+ \longrightarrow H + H + Br + \text{energy}$ [6b]

or $H_2Br^+ + Br^- \text{--} H\text{-}Br \longrightarrow H + Br + 2HBr$ [27]

For reasons already proposed it is unlikely that reaction [27] would produce free radicals. Reaction [6b] involves the unlikely assumption that the electron in liquid HBr will be thermalized without undergoing dissociative electron capture by a neutral HBr molecule. Furthermore, an increased yield due to reaction [6b] presumes that all three radicals produced within the same solvent cage must survive recombination reactions. Thus the occurrence of reactions [6b] and [27] seems improbable. It appears then that there is a genuine difference in the number of ions and/or dissociative excited states produced in the radiolysis of liquid HCl from those produced in liquid HBr.

1.6. Scavenger Studies: HBr

As discussed in the previous section, it was possible to determine the value of

$$k_{10(H + HBr)}/k_{15(H + Br_2)}$$

and obtain an estimate of G_H (for HBr) from the HCl - HBr mixtures. However, the apparent trend to lower values of the rate constant ratio at higher HBr concentrations and the approximate nature of the value of G_H suggested the advisability of directly investigating the effects of bromine in pure HBr.

Figure 23 represents a plot of $1/\Delta G(H_2)$ against $1/(Br_2)$. The initial portion of the plot (low bromine concentrations) shows a definite curvature unlike the analogous cases of chlorine or bromine in HCl. At higher concentrations of bromine (i.e. greater than $\sim 4\times10^{-4}$ moles/gm. HBr) the plot becomes linear and extrapolation leads to a value of $1/\Delta G(H_2)$ of 0.08_0 (see insert Figure 23). This corresponds to complete scavenging

FIGURE 23

FIGURE 23

Kinetic Plot of the Effect of Bromine on the Hydrogen Yield From γ-Irradiated HBr (-79°C)

$1/\Delta G(H_2)$ plotted against the reciprocal of the bromine concentration $(1/(Br_2))$ measured moles/gm.

INSERT -- high concentrations of bromine

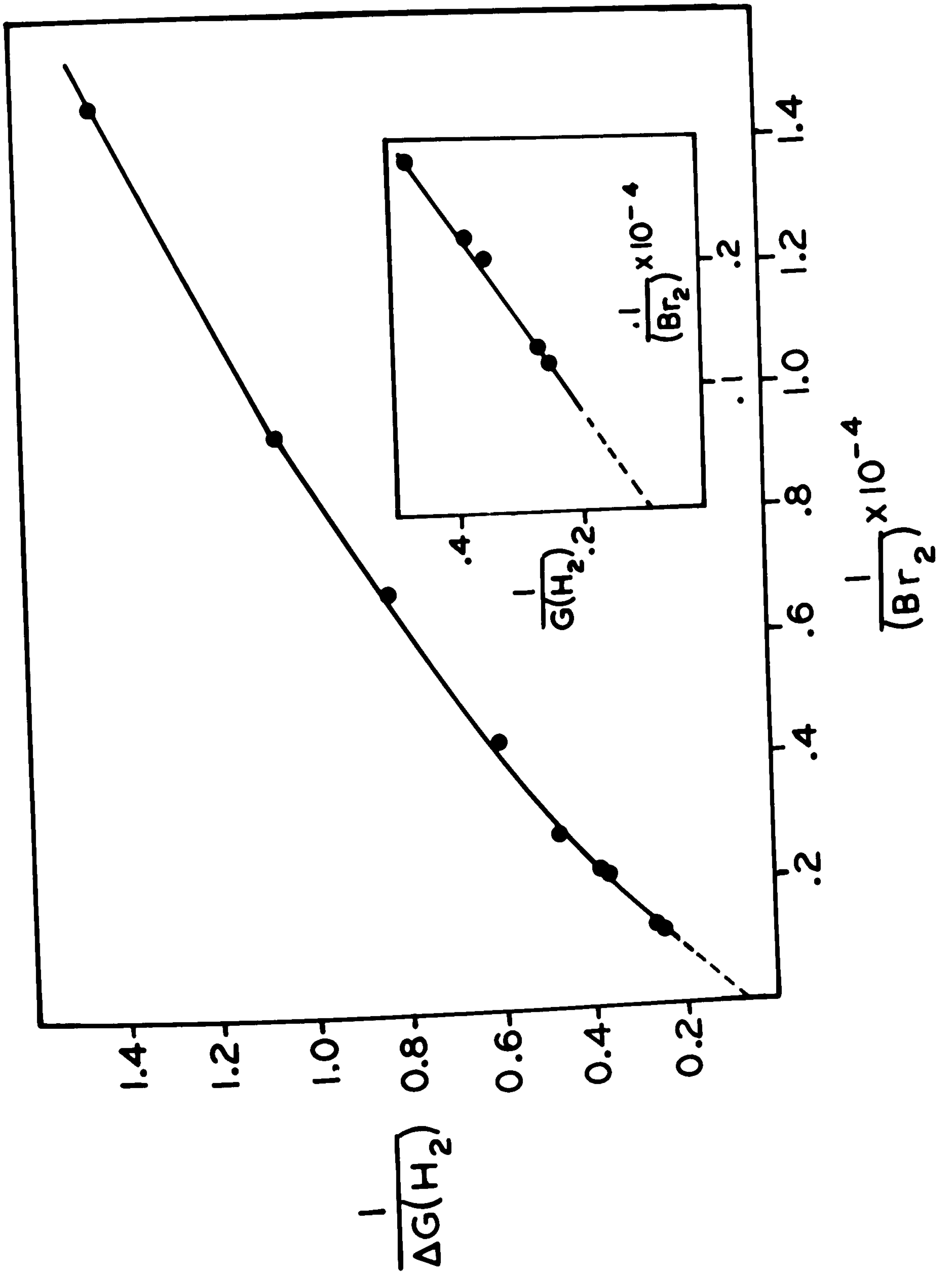
1/ΔG(H2)
0.2
0.4
0.6
0.8
1.0
1.2
1.4
1/(Br2) x10-4
.2
.4
.6
.8
1.0
1.2
1.4
1/G(H2)
.2
.4
1/(Br2) x10-4
.1
.2

of all hydrogen forming species by bromine.

Examination of the plot in Figure 23 shows that it is impossible to obtain a value of 0.10 for

$$k_{10(H + HBr)}/k_{15(H + Br_2)}$$

using $G_H = 4.0$. Indeed, it is impossible to obtain this value of the rate constant ratio for any real value of G_H. Thus, it must be concluded that bromine does not reduce the hydrogen yield in irradiated HBr by a mechanism involving only hydrogen atoms.

An alternate mechanism can be proposed assuming the three sets of concurrent reactions:

$$e + Br_2 \longrightarrow Br + Br^- \qquad [17]$$

$$e + HBr\text{--}HBr \longrightarrow H + Br^-\text{--}H\text{-}Br \qquad [7a]$$

$$H + Br_2 \longrightarrow HBr + Br \qquad [15]$$

$$H + HBr \longrightarrow H_2 + Br \qquad [10]$$

$$H^* + Br_2 \longrightarrow HBr + Br \qquad [15^*]$$

$$H^* + HBr \longrightarrow H_2 + Br \qquad [10^*]$$

The usual steady state treatment leads to the following equation:

$$G(H_2) = G_{H_2} + G_{H_2^*} = G_e\left[\frac{1}{1 + \frac{k_{17}(Br_2)}{k_{7a}(HBr)} + \frac{k_{15}(Br_2)}{k_{10}(HBr)} + \frac{k_{17}k_{15}(Br_2)^2}{k_{7a}k_{10}(HBr)^2}}\right] + G_{H^*}\left[\frac{1}{1 + \frac{k_{15^*}(Br_2)}{k_{10^*}(HBr)}}\right] \qquad [1.5]$$

Although such a mechanism must be construed as hypothetical due to lack of experimental evidence, it can be employed to explain several otherwise anomalous results. Thus for instance, from equation [1.5] it can be shown that $1/\Delta G(H_2)$ will not become a linear function of $1/(Br_2)$ until all the thermal hydrogen atoms and electrons have been scavenged. This conclusion agrees with the qualitative features of the plot in

Figure 23.

The trend to lower values of

$$k_{10(H + HBr)}/k_{15(H + Br_2)}$$

observed in the HCl - HBr mixtures as the HBr concentration was increased can also be explained on the basis of this mechanism. As indicated in section [1.4], the electron capture reaction (reaction [7a]) in pure HCl occurs prior to thermalization of the electron. Since in dilute solutions of HBr in HCl reaction [7a] should still predominate, added bromine should act only as a hydrogen atom scavenger. The results listed in Table XVI substantiate this conclusion. As the concentration of HBr is increased the probability of electron capture by HCl is decreased. Since both HBr and bromine capture electrons over approximately the same energy range, a trend towards electron scavenging by bromine would be predicted with increasing HBr concentration. Although the low value of

$$k_{10(H + HBr)}/k_{15(H + Br_2)}$$

calculated at 0.40 electron fraction HBr in HCl (Table XVI) cannot explicitly be attributed to electron scavenging by bromine, it is clearly too small to be consistent with hydrogen atom scavenging exclusively.

Regretably, sulphurhexafluoride was only slightly soluble in liquid HBr at -79°C. Nonetheless, at a concentration of 0.911×10^{-4} moles/gm HBr, $\Delta G(H_2)$ was 0.3, whereas at an equivalent concentration in HCl, sulphurhexafluoride caused no apparent change in $G(H_2)$. Since both sulphurhexafluoride and bromine have zero energy capture thresholds (32), these results qualitatively support the proposed electron scavenging mechanism for bromine in HBr.

1.7. Hydrobromination of Ethylene

The value of $G(n\text{-}C_2H_5Br)$ for the radiolysis of liquid phase mixtures of ethylene in HBr exceeded 10^6 molecules per 100ev. This can only be interpreted as a chain reaction between HBr and ethylene.

Following the free radical mechanism proposed by Vaughan (103) and others (104), the initiation step would be:

$$HBr \overset{I}{\rightsquigarrow} H + Br \qquad [1]$$

$$Br + C_2H_4 \longrightarrow C_2H_4Br \qquad [30]$$

Ethylene would also react with hydrogen atoms and subsequently produce more bromine atoms:

$$H + C_2H_4 \longrightarrow C_2H_5\cdot \qquad [19]$$

$$C_2H_5\cdot + HBr \longrightarrow C_2H_6 + Br \qquad [31]$$

The alternate reaction:

$$C_2H_5\cdot + HBr \longrightarrow C_2H_5Br + H \qquad [32]$$

would be endothermic and would not act as a propagating step in the mechanism. Propagation should proceed via:

$$C_2H_4Br\cdot + HBr \longrightarrow C_2H_5Br + Br \qquad [33]$$

and be followed by one or more of the three termination reactions:

$$Br + Br + M \longrightarrow Br_2 + M \qquad [12]$$

$$Br + C_2H_4Br \longrightarrow C_2H_4Br_2 \qquad [34]$$

$$2C_2H_4Br \longrightarrow C_4H_8Br_2 \qquad [35]$$

$$\longrightarrow C_2H_4 + C_2H_4Br_2 \qquad [35a]$$

For low concentrations of ethylene, as employed in this investigation, bromine radicals would be present in a much higher concentration than bromoethyl radicals. Thus termination via reaction [12] should predominate.

Application of the steady state approximation for the reaction sequence [1] - [30] - [33] -[12] leads to the rate equation:

$$\frac{d(C_2H_5Br)}{dt} = \frac{k_{30}}{k_{13}^{1/2}} I^{1/2}(C_2H_4) \qquad [1.6]$$

This corresponds to the first order dependence on ethylene concentration observed experimentally. The approximate half-order dose rate exponent (i.e. 0.6) observed also confirms the choice of reaction [12] as the main terminating step.

Nitric oxide completely inhibited the reaction. This fact is consistent with the free radical character of the reaction.

1.8. Hydrobromination of Propylene

Unlike ethylene, hydrobromination of propylene can result in two distinct major products. A Markownikoff or ionic mechanism would lead to 2-bromopropane as the product, whereas an anti-Markownikoff or free radical mechanism would yield exclusively 1-bromopropane (80). Since the radiation times were generally less than five minutes, any 2-bromopropane formed in appreciable quantity would have resulted from a radiation-induced ionic mechanism. Analysis of the products showed that the single major product was 1-bromopropane indicating a free radical mechanism.

In the presence of nitric oxide, the reaction was greatly inhibited. The consumption of HBr was however larger than was anticipated from the spontaneous reaction.

Although a mechanism for the thermal addition of HBr to propylene has not been established, the over-all process is consistent with the following reaction sequence:

$$HBr + C_3H_6 \rightleftharpoons HBr \cdot C_3H_6 \qquad [36]$$

$$3HBr \rightleftharpoons H_2Br^+ + Br^- \text{--} H\text{-}Br \qquad [9]$$

$$H_2Br^+ + HBr \cdot C_3H_6 \rightleftharpoons C_3H_7 \cdot HBr^+ + HBr \qquad [37]$$

$$C_3H_7 \cdot HBr^+ + Br^- \text{--} H\text{-}Br \rightleftharpoons C_3H_7Br + 2HBr \qquad [38]$$

2. The Solid Phase

2.1. Pure Hydrogen Halide

The hydrogen yields previously reported for the radiolysis of solid HCl ($G(H_2) = 3.3$) (61) and solid HBr ($G(H_2) = 10.5$) (71) do not represent the true initial yields. Figure 18 clearly indicates that the G-values are dose dependent and reach an apparent plateau after a dose of approximately 2×10^{18} ev/gm. The values given above correspond to the yields in the plateau region.

The true initial G-values can only be obtained by extrapolating the $G(H_2)$ against dose curves to zero dose. Although the values obtained involve some uncertainty it can be seen from Figure 18 that $G(H_2)$ at zero dose should be very nearly equal to $G(H_2)$ for the corresponding liquid phase radiolyses. Thus:

$$G(-HCl)_{-79^\circ} \approx G_0(-HCl)_{-196^\circ}$$

$$G(-HBr)_{-79^\circ} \approx G_0(-HBr)_{-196^\circ}$$

It is apparent from these results that the initial formation of ions and excited molecules in the solid phase must be virtually the same as in the liquid phase. It cannot be concluded however that the ratio of ionization to excitation will also be identical.

Two possibilities can be postulated to explain the observed dose dependency: (1) hydrogen is formed on melting of the sample and the reduced yields result from an increase in radical recombination reactions due to the high radical concentration accumulated prior to melting, and (2) a product of the radiolysis is reacting with the precursor(s) to hydrogen in the solid matrix during the course of the irradiation.

If the reactions:

$$H + H + M \longrightarrow H_2 + M \qquad [11]$$

$$\mathrm{H + X + M \longrightarrow HX + M} \qquad [13]$$

were able to compete with:

$$\mathrm{H + HX \longrightarrow H_2 + X} \qquad [10]$$

only because of the accumulation of hydrogen and halogen atoms in the solid medium, then the G-value obtained by intermittent irradiation should be greater than an equivalent continuous irradiation. After each melting no radicals would remain; therefore, $G(H_2)$ obtained for a series of thirty minute irradiations should be the same as a single thirty minute irradiation. Since $G(H_2)$ for intermittent irradiations (for HCl at least) was identical to that for a continuous irradiation, molecular hydrogen must have been formed directly during the radiolysis. Thus, neither the recombination reactions proposed above nor:

$$\mathrm{H_2 + X \longrightarrow HX + H} \qquad [14]$$

can account for the dose dependency.

This conclusion requires that either hydrogen atoms or their precursors are being scavenged by a species produced during the irradiation. Quite obviously this product could only be atomic or molecular halogen. The results of the intermittent irradiations indicated that it was unlikely that atomic halogen was the scavenger.

Since the molecular halogen was being produced 'in situ' it would have been homogeneously distributed in the medium. Under these conditions it is possible to analyse the data by an equation of the general form:

$$\frac{1}{\Delta G(H_2)} = \frac{1}{G_{H'}} + \frac{1}{G_{H'}}\left[\frac{\alpha(A)}{\beta(X_2)}\right] \qquad |2.1|$$

where A represents the species (initially assumed to be HX) with which the scavengeable entity H' reacts to form molecular hydrogen or a product which leads directly to hydrogen. The usual rate constants have been replaced by more general proportionality constants α and β, the reasons for which will become obvious later. In order for this expression to be applicable the G-values used in determining $\Delta G(H_2)$ must be equivalent to the rates of hydrogen formation at each concentration of halogen. The G-values shown in Figure 18 were calculated from the total amount of hydrogen formed from a given dose. Since the rate of hydrogen formation decreases as the halogen accumulates in the system, these integrated values will be larger than the instantaneous values. The true values of $G(H_2)$ at various concentrations of halogen were calculated from tangents to a plot of total hydrogen formed against dose. The true G-values are compared to the integrated values in Table XVII. HBr reached the plateau region after relatively short irradiation times and it was only possible to calculate true G-values for three concentrations of bromine. The data are therefore less accurate in this case.

From the data in Table XVII and equation [2.1] the plots shown in Figure 24 were obtained. The values of G_H' from the intercepts for both HCl ($G_H' = 3.8$) and HBr ($G_H' = 2.3$) are considerably less than $G(H_2)$. It is noted that Armstrong (61) observed a limiting G-value of 2.7 in the radiolysis of solid solutions of chlorine in HCl. This corresponds to the value anticipated from the relationship:

$$G_o(H_2) = G_H' + G_{H*} \qquad [2.2]$$

where $G_o(H_2) = 6.5$ and $G_H' = 3.8$. As was the case in the liquid phase, at least two hydrogen forming species must be produced in the solid phase irradiations.

2.2. The Identity of H'

Thermal hydrogen atoms produced by the hot filament technique failed to react with HCl at -196°C. This result was consistent with that anticipated from existing gas kinetic data (95). It is unlikely therefore that

TABLE XVII

True G-values for γ-Irradiated Solid (-196°C) HCl and HBr

HCl		HBr	
$G(H_2)$ Observed	$G(H_2)$ True	$G(H_2)$ Observed	$G(H_2)$ True
5.5	4.8	11.6	11.1
5.0	4.5	11.2	10.7
4.8	4.1	10.8	10.5
4.3	3.7		
3.8	3.3		
3.6	3.2		

FIGURE 24

FIGURE 24

Kinetic Plot of the Effect of Halogen on the Hydrogen Yield From γ-Irradiated Solid Hydrogen Halide (-196°C)

The reciprocal of the reduction in the rate of hydrogen formation ($1/\Delta G(H_2)$) plotted against the reciprocal of the halogen concentration ($1/(X_2)$) measured in moles/gm. The top scale is for HBr (i.e. ○). The bottom scale is for HCl (i.e. ●).

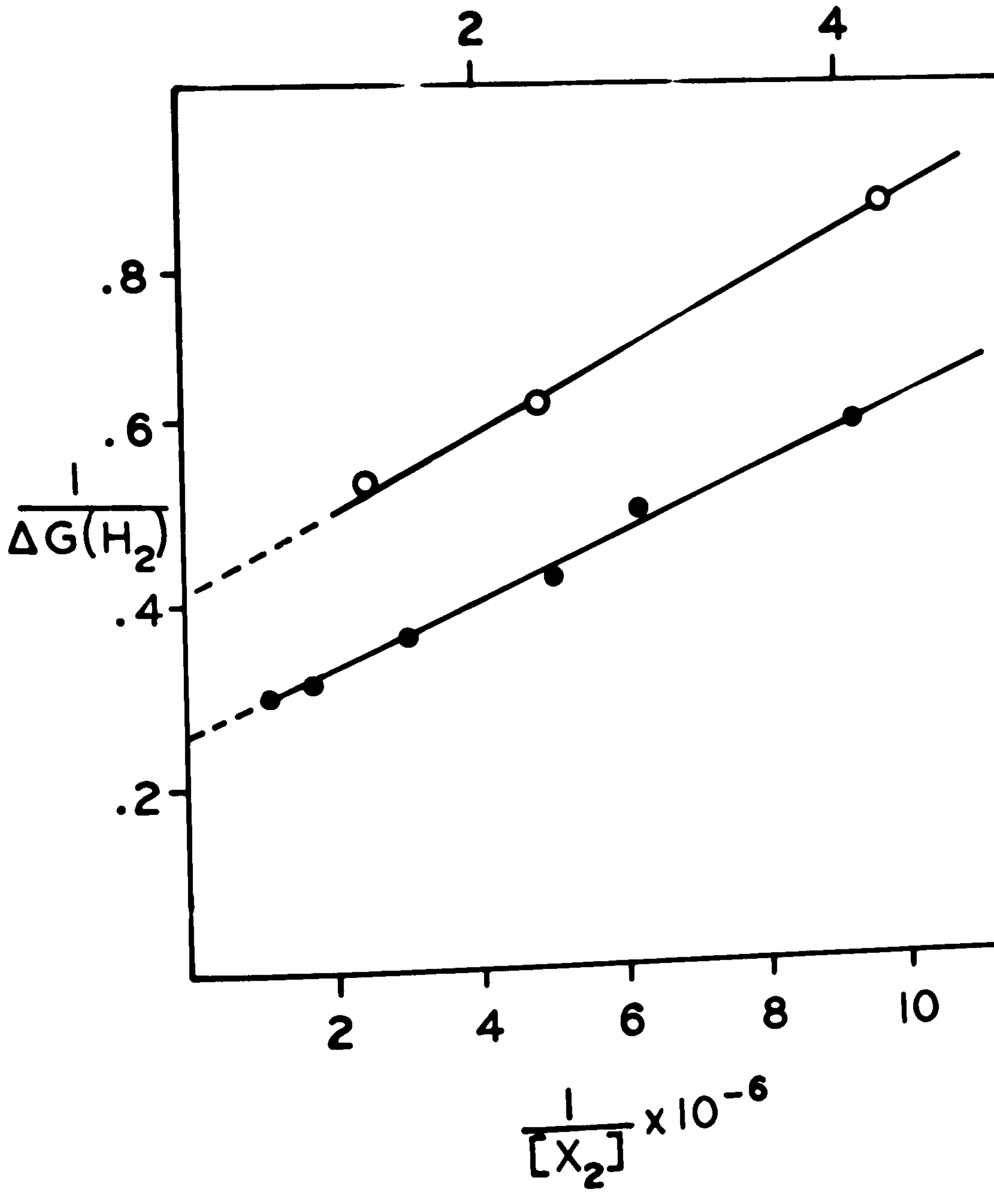

2
4
.8
.6
.4
.2
$\frac{1}{\Delta G(H_2)}$
2
4
6
8
10
$\frac{1}{[X_2]} \times 10^{-6}$

H' in irradiated HCl would be a thermal hydrogen atom. A reasonable alternative would be to identify H' with the secondary electron. The mechanism of hydrogen production would involve the ion-molecule condensation:

$$HCl^{+} + HCl \longrightarrow H_2Cl^{+} + Cl \qquad [5]$$

followed by the recombination reactions:

$$e + H_2Cl^{+} \longrightarrow H_2 + Cl \qquad [6]$$

$$Cl + Cl \longrightarrow Cl_2 \qquad [12]$$

This mechanism predicts both the direct formation of molecular hydrogen and halogen. The chlorine atoms will be formed in close proximity to each other and this would favor reaction [12] rather than radical trapping by the solid matrix. By analogy with the liquid phase the second species is probably a hot hydrogen atom. Molecular hydrogen would be readily formed by this precursor:

i.e. $$HCl^{*} \longrightarrow H^{*} + Cl \qquad [9]$$

$$H^{*} + HCl \longrightarrow H_2 + Cl \qquad [10^{*}]$$

since phase and temperature changes are not expected to seriously affect such epithermal reactions. Furthermore, the abstraction reaction should occur within a short distance of the dissociation of the excited molecule, then once again the two chlorine atoms could react to form molecular chlorine. Other considerations such as local heating (melting) and the fact that the chlorine atoms will also have some kinetic energy likewise favor the formation of molecular chlorine in the solid phase radiolysis of HCl.

Unlike HCl, solid HBr at -196°C reacts with hydrogen atoms produced by the Klein and Scheer (67) technique. The results of this reaction show a qualitative resemblance to the radiation-induced reaction. Hydrogen formation by the Klein and Scheer method can be interpreted by the following reaction sequence:

$$\mathrm{H_2} \xrightarrow[\text{Filament}]{\Delta} \mathrm{H + H} \qquad [39]$$

$$\mathrm{H + HBr_{(S)}} \longrightarrow \mathrm{H_2 + Br_{(S)}} \qquad [10]$$

$$\mathrm{H + Br_{(S)}} \longrightarrow \mathrm{HBr_{(S)}} \qquad [13]$$

It is improbable that molecular bromine would be formed in a significant yield over the initial portion of the reaction due to the restricted diffusion of the bromine radicals through solid HBr at -196°C.

An approximate value of

$$k_{10(\mathrm{H + HBr})}/k_{13(\mathrm{H + Br})} \qquad \text{(in HBr at -196°C)}$$

was calculated using slopes measured from the initial portion of the reaction-time curve and the concentrations of HBr and bromine atoms ($1/2\,(\mathrm{Br\cdot}) = (\mathrm{H_2})_t - (\mathrm{H_2})_o$). The value of the ratio thus calculated was $5\mathrm{x}10^{-4}$. From the liquid phase results it would appear that

$$k_{10(\mathrm{H + HBr})}/k_{15(\mathrm{H + Br_2})} \qquad \text{(in HBr at -196°C)}$$

must be greater than this and of the order of 10^{-1}.

Using the equation:

$$\frac{1}{\Delta G(\mathrm{H_2})} = \frac{1}{G_H} + \frac{1}{G_H}\left[\frac{k_{10}\ (\mathrm{HBr})}{k_{(\mathrm{H + Br_N})}(\mathrm{Br_N})}\right] \qquad [2.3]$$

where $(\mathrm{Br_N}) = 3 - \mathrm{N(H_2)}$, for the radiation-induced reaction leads to values for the rate constant ratio of $1.3\mathrm{x}10^{-5}$ when $N = 2$ and $0.65\mathrm{x}10^{-5}$ when $N = 1$. Clearly neither of the competitions for hydrogen atoms offers satisfactory agreement. Since H' fails to show the characteristics of thermal hydrogen atoms alone, it must be concluded as it was in the case of HCl that H' is either an electron or both an electron and a thermal hydrogen atom.

2.3. The Electron Return Model

The previous discussion has presented evidence to suggest that the secondary electrons in irradiated solid hydrogen halides return to the positive ion. In order that the electron would escape the coulombic attraction of the parent ion it must travel beyond the critical inter-charge distance r_c. From the equation proposed by Samuel and Magee (29):

$$\frac{e^2}{D r_c} = k T \qquad [2.4]$$

it can be shown that r_c will exceed 600Å for HCl at -196°C and for HBr at -196°C it will be of the order of 400Å. If the electron did migrate beyond this distance it could enter the coulombic field of the positive ions of adjacent spurs (the mean separation of the spurs should be approximately 1000Å).

From the relationship developed by Platzman and Frohlich (28),

$$-\frac{dw}{dt} = \frac{\pi}{4d} \frac{\epsilon_s - \epsilon_{ir}}{\tau n^4} \qquad [2.5]$$

(where d is the intermolecular distance, ϵ_s is the static dielectric constant, ϵ_{ir} is the low frequency dielectric, τ is the dielectric relaxation time, and n is the refractive index) the rate of energy loss ($-\frac{dw}{dt}$) due to dielectric interactions for electrons within the range of 1 - 10ev can be calculated. Using the dielectric data of Cole et al. (86) the values of $-\frac{dw}{dt}$ for HCl and HBr are 3.6×10^6 ev/sec and 2.2×10^8 ev/sec respectively. These can be compared with

$$-\frac{dw}{dt} \approx 10^{13} \text{ ev/sec}$$

for water at 20°C. Although other processes are probably also important, the trend indicates that an electron should travel relatively further in the solid hydrogen halide than in liquid water.

Both HCl and HBr at -196°C form long "zig-zag" hydrogen bonded chains (82). Secondary electrons produced in these systems should therefore have preferred migration paths and thus should travel much further from the parent ion than if a random walk diffusion path were followed. Dainton and Jones (53) have demonstrated that in systems where such preferred paths exist the electron can migrate distances of at least 50Å from the parent ion.

After being thermalized, the electron should return to neutralize the parent ion and form molecular hydrogen and halogen. As the radiolysis progresses the concentration of halogen will increase. The infrared spectra of HCl and HBr have shown that the presence of a geometrically odd oscillator such as chlorine will terminate the chain (82). Thus, an electron encountering this terminal would be forced either to alter its path or be captured.

i.e. $e + X_2 \longrightarrow X_2^-$ [40]

It was observed that a greenish color was produced in the solid hydrogen halide by the radiolysis. A similar observation has been reported (105) for the radiolysis of solid potassium chloride and identified as Cl_2^- by electron spin resonance. Recent data (106) on the radiolysis of aqueous systems also supports the existence of these species.

The dose dependence of $G(H_2)$ in the radiolysis of solid HCl and HBr would thus arise from the competition between:

$e + H_2X^+_{(HX)_n} \longrightarrow H_2 + X_{(HX)_n}$ [6c]

and $e + X_{2(HX)_n} \longrightarrow X^-_{2(HX)_n}$ [40a]

If it is assumed that the electron reacts with equal efficiency with either the positive ion or the halogen molecule, then the relative rates of electron capture by either entity should depend only on the respective collision probabilities. These probabilities will be proportional to the distance which an electron can travel before encountering a scavenger. Such a distance will in turn be proportional to the ratio of the concentrations of hydrogen halide and halogen molecules in the medium. Therefore:

$$\frac{d(H_2X^+_2(HX)_n + e)}{dt} = \alpha\,(HX) \qquad [2.6]$$

and

$$\frac{d(e + X_{2(HX)_n})}{dt} = \beta\,(X_2) \qquad [2.7]$$

Equation [2.1] then becomes:

$$\frac{1}{\Delta G(H_2)} = \frac{1}{G_e} + \frac{1}{G_e}\left[\frac{\alpha\,(HX)}{\beta\,(X_2)}\right] \qquad [2.8]$$

A value of 5×10^{-4} was calculated for α/β for solid HCl using equation [2.8] and the slope in Figure 24. The same calculation leads to a value of 1.3×10^{-5} for solid HBr. If the electron returns to the positive ion, then it must effectively traverse each HX molecule twice; therefore,

$$\alpha = 2\alpha'$$

and α'/β will be proportional to the distance the electron travels in the solid medium.

When

$$\frac{\alpha'(HX)}{\beta\,(X_2)}$$

is unity the rate of electron return will be equal to the rate of scavenging. Since the rates are proportional to the distance that the electron travels, then this equilibrium distance can be calculated. Using the appropriate values of α'/β and the volume occupied by one HX molecule (which is known from X-ray data (107)), the values calculated for the equilibrium distances were 30Å and 100Å for HCl and HBr respectively.

Inherent in the above calculations is the assumption that the system is homogeneous. This is not strictly true since there will be high local concentrations along the original primary particle track. Thus, it is quite possible that the equilibrium distances are much greater than those given above. Nonetheless, the evidence supports the proposal that the secondary electrons do diffuse further from the parent ion than the 10 to 20Å usually assumed in liquid water. Furthermore, it may be inferred that the large difference in the equilibrium distances between HCl and HBr is an indication that electrons are freer to diffuse in HBr than in HCl. This view is consistent with the trend in dielectric constants. HCl at -196°C has a low dielectric constant ($\epsilon = 3.8$) (86) and would not be a very effective insulator of the interionic forces. On the other hand HBr at -196°C has a much larger dielectric constant ($\epsilon = 41.8$) (86), thus the secondary electron should be less influenced by the parent ion. Since longer migration distances would be anticipated for electrons in HBr, the probability of electron capture at lower halogen concentrations would be increased.

From the preceding discussion it is evident that hydrogen was produced by at least two mechanisms in the radiolysis of solid HCl and HBr. For both hydrogen halides, the data are consistent with the proposal that the first hydrogen forming process involved ion-electron recombination. Although the second species (assuming that there is only one other species) was not identified, analogy with the liquid phase leads to the conclusion that this intermediate resulted from a direct excitation process.

2.4. HCl - HBr Mixtures

The large difference in yields between HCl and HBr which was observed in the liquid phase irradiations is also a feature of the solid phase radiolyses. The variation of $G(H_2)$ with composition is shown in Figure 17. The G-values used in this plot are the integrated plateau values.

A dose dependency similar to that exhibited by solid HCl and HBr was also observed for the mixtures (see Figure 18). The lack of experimental data does not justify the determination of the true initial G-values by extrapolation, but in view of the behaviour observed with pure

HCl and HBr, it seems reasonable to assume that the true initial G-values should correspond to the liquid phase G-values. It is unlikely that they could exceed this value and the curve for the 0.14 electron fraction HBr mixture indicates that it could not be much less than this.

As seen in Figure 17, the plateau yields increased sharply until a concentration of approximately 5 mole % HBr (i.e. 0.1 electron fraction HBr) had been reached. Thereafter $G(H_2)$ increased gradually. If it is assumed (as seems reasonable from the previous section) that these plateau values of $G(H_2)$ represent hydrogen formed in processes other than the ion-electron recombination reaction and thermal hydrogen atom reactions then the abrupt increase in $G(H_2)$ must be attributed to an increase in the formation of dissociative excited molecules. Further, it is clear that the yield does not follow a simple additivity law.

The insertion of an HBr molecule into a hydrogen bonded HCl chain will terminate that chain (82). If the initial excitation energy does not transfer from chain to chain, then the addition of the HBr will tend to localize this energy on fewer molecules (20) (for instance, at 5 mole % HBr the length of the hydrogen bonded chains should not exceed 60Å) and generally result in energy transfer to the HBr. This alteration in the state of aggregation of the molecules of the medium could conceivably also effect the ratio of ionization to excitation. It appears from Figure 25 (where the difference between $G(H_2)_{-79°C}$ and the plateau value of $G(H_2)_{-196°C}$ has been plotted against composition) that this must be the case if the condition $G_o(H_2)_{-196°C} \leq G(H_2)_{-79°C}$ is to be fulfilled. Thus it appears that HBr precludes ionization in HCl and preferentially forms excited states with the scavenged energy.

i.e.

$$HCl^{**}(HCl)_n \longrightarrow HCl^{+}(HCl)_n + e \qquad [41]$$

FIGURE 25

FIGURE 25

Effect of Phase Transition on the Hydrogen Yields From γ-Irradiated HCl - HBr Mixtures

The difference between the integrated plateau yields (-196°C) and the corresponding liquid phase yields (-79°C) is plotted against electron fraction HBr.

— — — linear interpolation

—●— observed values

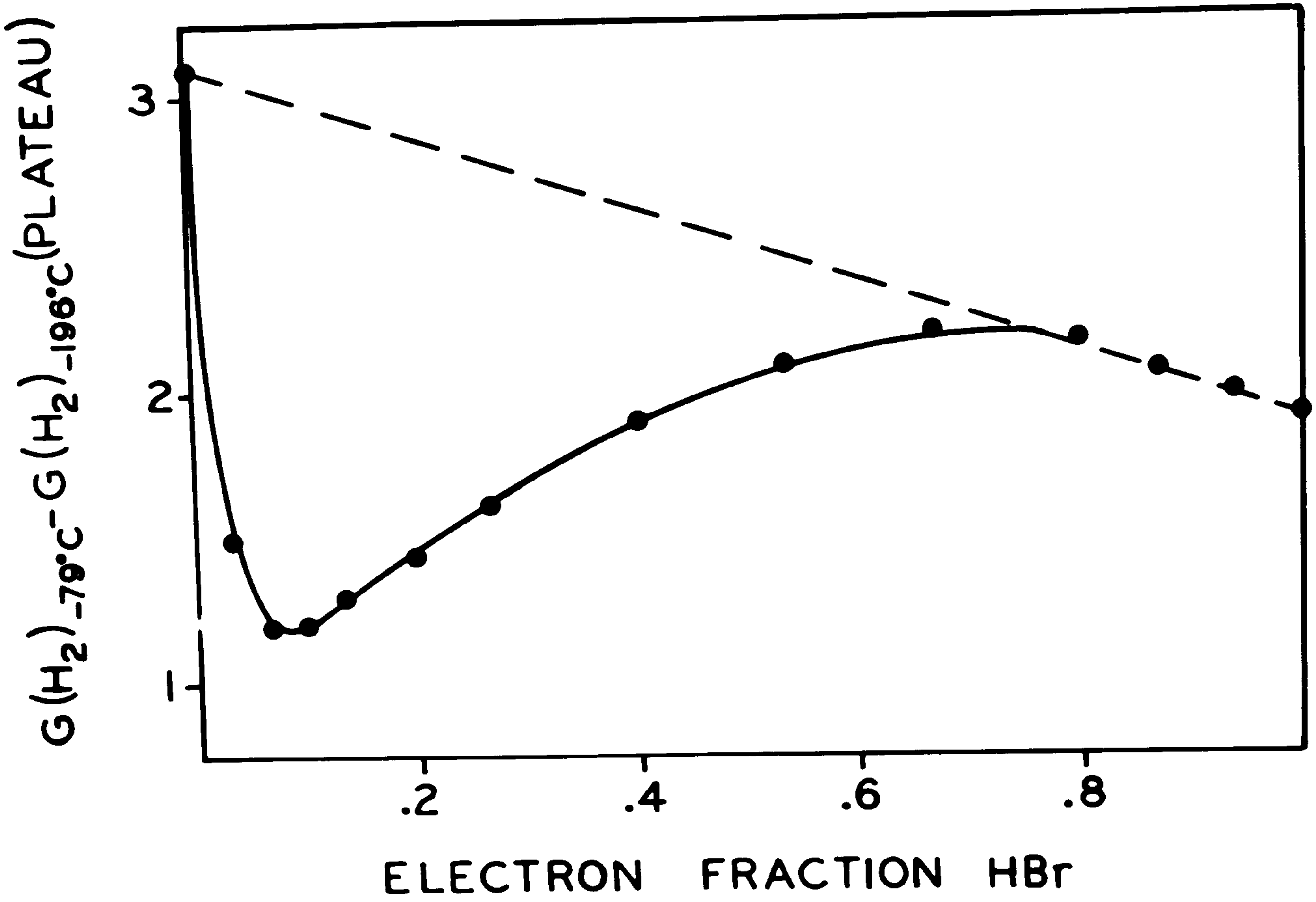

$G(H_2)_{-79°C} - G(H_2)_{-196°C}$(PLATEAU)
3
2
1
.2
.4
.6
.8
ELECTRON FRACTION HBr

$$\left[HBr(HCl)_n\right]^{**} \longrightarrow HBr^{*}(HCl)_n \qquad [42]$$

where the notation ** represents the initial electronic excitation and * represents a dissociative excited state.

The lack of more adequate theoretical and experimental data prevents the development of a more definitive mechanism. Further experiments could substantiate several of the critical assumptions. For instance, it would be useful to examine both the irradiated pure components as well as the mixtures by electron spin resonance spectroscopy to establish more conclusively the presence of the proposed entity X_2^-. Further, the addition of DCl to HCl should produce interesting isotope effects if chain shortening is an important feature of the excitation mechanism.

BIBLIOGRAPHY

(1) H. Becquerel, cf. La Radioactivite, Chapter 1, Paris (1924) (Quoted from "The Radiation Chemistry of Gases", S.C. Lind, Reinhold Publ. Corp., New York (1961)).

(2) F. Giesel, Verhandl. deut. physik Ges., 2, 9 (1900) (Quoted from Lind's book as in Ref. (1)).

(3) P. Curie and A Debierne, Compt. rend., 132, 770 (1901).

(4) S.C. Lind, "The Chemical Effects of Alpha Particles and Electrons," Chemical Catalogue Co., Inc., New York (1928).

(5) H. Eyring, J.O. Hirschfelder, and H.S. Taylor, J. Chem. Phys., 4, 570 (1936).

(6) F.W. Spiers, Discussions Faraday Soc., 12, 13 (1952).

(7) G.J. Hine and G.L. Brownell, "Radiation Dosimetry", Academic Press Inc., New York (1958).

(8) F. Hutchinson and E. Pollard, Vol 1, Chapter 1, "Mechanisms in Radiobiology," (M. Errera and A. Forssberg, Eds.) Academic Press Inc., New York (1961).

(9) C.M. Davidson and R.D. Evans, Revs. Mod. Phys., 24, 79 (1952).

(10) B. Rossi, "High Energy Particles," Prentice-Hall, New York (1952).

(11) F. Bloch, Ann. Physik 16, 285 (1933).

(12) R.D. Kleeman, Proc. Roy. Soc., A79, 220 (1907).

(13) H.S.W. Massey and E.H.S. Burhop, "Electronic and Ionic Impact Phenomena," Osford University Press, London (1952).

(14) D.E. Lee, "Actions of Radiations on Living Cells," Cambridge University Press (1947).

(15) C.J. Hochanadel, Chapter VIII, "Comparative Effects of Radiation", (M Burton et al., Eds.) Wiley, New York (1960).

(16) R.L. Platxman, Radiation Research, 17, 419 (1962).

(17) C. Reid, Quart. Rev. Chem. Soc., 12, 205 (1958).

(18) M. Kasha, Discussions Faraday Soc., 9, 14 (1950).

(19) (a) Th. Forster, Radiation Research Suppl., 2, 326 (1960).

(b) Th. Forster, Chapter XIII, "Comparative Effects of Radiation," (M. Burton et al., Eds.) Wiley, New York (1960).

(20) J.L. Magee, Chapter VII, "Comparative Effects of Radiation," (M. Burton et al., Eds.) Wiley, New York (1960).

(b) J.L. Magee and K. Funabashi, J. Chem. Phys., 34 1715 (1961).

(21) (a) G.E. McRae and M. Kasha, J. Chem. Phys., 28, 727 (1958).

(b) G.E. McRae, Aust. J. Chem., 14, 329, 344, 354 (1961).

(22) R.J. Carter, W.H. Hamill, and R.R. Williams, J.Am. Chem. Soc., 77, 6457 (1955).

(23) J. Franck and E. Rabinowitch, Trans, Faraday Soc., 30, 120 (1934).

(24) J.H. Beynon, "Mass Spectrometry and Its Application to Organic Chemistry", Elsevier Publ., New York (1960).

(25) D.P. Stevenson and D.O. Schissler, Vol. V, Chapter IV, "The Chemical and Biological Action of Radiations", (M. Haissinsky, Ed.) Academic Press, New York (1961).

(26) D.O. Schissler and D.P. Stevenson, J. Chem. Phys., 24, 926 (1956).

(27) J.L. Franklin and F.H. Field, J. Am. Chem. Soc., 83, 3555 (1961).

(28) H. Frohlich and R.L. Platzman, Phys. Rev., 91, 1152 (1953).

(29) A.H. Samuel and J.L. Magee, J. Chem. Phys., 21, 1080 (1953).

(30) J.L. Magee and M. Burton, J. Am. Chem. Soc., 72, 1965 (1950).

(31) W. Person, J. Chem. Phys., 38, 109 (1963).

(32) (a) D.C. Frost and C.A. McDowell, J. Chem. Phys., 29, 1424 (1958).

(b) D.C. Frost and C.A. McDowell, Can. J. Chem., 38, 407 (1960).

(33) H.S. Massey, Discussions Faraday Soc., 12, 24 (1952).

(34) E.J. Hart and R.L. Platzman, Vol. 1 Chapter 2, "Mechanisms in Radiobiology", (M. Errera and A. Forssberg, Eds.) Academic

Press Inc., New York (1961).

(35) W. Duane and O. Scheuer, Le Radium, 10, 33 (1913).

(36) H. Fricke and E.R. Brownscombe, Phys. Rev., 44, 240 (1933).

(37) P. Guenther and L. Holzapfel, Z. Phys. Chem., 44B, 374 (1939).

(38) H. Fricke, E.J. Hart, and H.P. Smith, J. Chem. Phys., 6, 229, (1938).

(39) H. Fricke and E.J. Hart, J. Chem. Phys., 4, 418 (1936).

(40) A.O. Allen, "The Radiation Chemistry of Water and Aqueous Solutions," Van Nostrand, New York (1961).

(41) H.A. Schwarz, J.P. Losee, and A.O. Allen, J. Am. Chem. Soc., 76, 4693 (1954).

(42) (a) R.H. Schuler and A.O. Allen, J. Chem. Phys., 24, 56 (1956).

(b) C.J. Hochanadel and J.A. Ghormley, J. Chem. Phys., 21, 880 (1953).

(c) R.M. Lazo, H.A. Dewhurst, and M. Burton, J. Chem. Phys., 22, 1370 (1954).

(43) D.A. Flanders and H. Fricke, J. Chem. Phys., 28, 1126 (1958).

(44) P.J. Dyne and J.M. Kennedy, Can. J. Chem., 36, 1518 (1958).

(45) A Kuppermann, Vol. V, Chapter III, "The Chemical and Biological Action of Radiation," (M. Haissinsky, Ed.) Academic Press, New York (1961).

(46) C.J. Hochanadel, J. Chem. Phys,, 56, 587 (1952).

(47) A.O. Allen and H.A. Schwarz, Proc. 2nd Int. Conf. Peaceful Uses of Atomic Energy, Geneva, 29, 30 (1958).

(48) C.J. Hochanadel, J. Phys, Chem., 56, 587 (1952).

(49) E. Collinson, F.S. Dainton, D.R. Smith, and S. Tazule, Proc. Chem. Soc., 140 April (1962).

(50) F.S. Dainton and D.B. Peterson, Nature, 186, 878 (1960); Proc. Roy. Soc., A267, 443 (1962).

(51) M.S. Matheson and B. Smaller, J. Chem. Phys,, 23, 521 (1955).

(52) M. Haissinsky and M. Magat, Compt. Rend., 233, 954 (1951).

(53) F.S. Dainton and F.T. Jones, Radiation Research, 17, 388 (1962).

(54) S.C. Lind, Le Radium, 8, 289 (1911); J. Phys. Chem., 16, 586 (1912).

(55) J. Vandamme, Bulle. soc. chim. Belg., 41, 597 (1932).

(56) R. Gillerot, Bull. soc. shim. Belg., 39, 503 (1930).

(57) E.G. Zubler, W.H. Hamill, and R.R. Williams, J. Chem. Phys., 23, 1263 (1955).

(58) (a) J. Vandamme, Bull. soc. chim. Belg., 41, 597 (1932)
(b) K.G. Brattain, J. Phys. Chem., 42, 617 (1938).

(59) D.A. Armstrong and R.A. Lee, Paper to be given at the Annual Chem. Inst. Can. Conference, Toronto (1963).

(60) S.C. Lind and R. Livingston, J. Am. Chem. Soc., 58, 612 (1936).

(61) D.A. Armstrong, Can. J. Chem., 40, 1385 (1962).

(62) W.H. Hamilland J.A. Young, J. Chem. Phys., 20, 888 (1952).

(63) D.A. Armstrong and J.W.T. Spinks, Can. J. Chem., 37, 1210 (1959).

(64) D.A. Armstrong and J.W.T. Spinks, Can. J. Chem., 37, 1003 (1959)

(65) F. Mitchell, B. Green, and J.W.T. Spinks, Can. J. Chem., 38, 689 (1960).

(66) H.A. Dewhurst and E.H. Winslow, J. Chem. Phys., 26, 969 (1957).

(67) M.D. Scheer and R. Klein, J. Phys. Chem., 65, 375 (1961).

(68) E.R. Johnson and A.O. Allen, J. Am. Chem. Soc., 74, 4147 (1952).

(69) N. Miller and J. Wilkinson, Discussions Faraday Soc., 12, 50 (1952).

(70) J.W. Boyle and H.A. Mahlman, Radiation Research, 16, 416 (1962).

(71) R.C. Rumfeldt and D.A. Armstrong, Can. J. Chem., 41, 1104 (1963).

(72) N.S. Bayliss and A. Rees, Trans. Faraday Soc., 35, 792 (1939).

(73) A.I. Popov and J.J. Mannion, J. Am. Chem. Soc., 74, 222 (1952)

(74) R.E. Buckles and J.F. Mills, J. Am. Chem. Soc., 75, 552 (1953).

(75) N.S. Buchnelnikova, Soviet Phys.-Tech. Phys., 35, 783 (1959).

(76) (a) R.A. Back, T.W. Woodward, and K.A. McLauchlin, Can. J. Chem., 40, 1380 (1962).

(b) P. Ausloos and R. Gordon, J. Chem. Phys., 36, 5 (1962).

(c) M.C. Sauer and L.M. Dorfman, J. Phys. Chem., 66, 322 (1962).

(77) A.A. Frost and R.G. Pearson, "Kinetics and Mechanisms," 2nd Edition, Wiley, New York (1961).

(78) E.W.R. Steacie, "Atomic and Free Radical Reactions," Reinhold Publ. Corp., New York (1954).

(79) O. Maass and C.H. Wright, J.Am. Chem. Soc., 46, 2664 (1924).

(80) (a) F.R. Mayo and C. Walling, Chem. Reviews, 27, 351.

(b) F.R. Mayo and M.G. Savoy, J. Am. Chem. Soc., 69, 1339 (1947).

(c) F.R. Mayo and J.J. Katz, J. Am. Chem. Soc., 69, 1339 (1947).

(81) (a) C. Coffin and O. Maass, Can. J. Research, 3, 526 (1930)

(b) C. Coffin, H. Sutherland, and O. Maass, Can. J. Research, 2, 267 (1930).

(82) (a) D.F. Hornig and W.E. Osberg, J. Chem. Phys., 23, 662 (1955).

(b) D.F. Hornig and G.L. Hiebert, J. Chem. Phys., 27, 752 (1957); 28, 316 (1958).

(83) W.H. Johnson and J.R. Arnold, J. Chem. Phys., 21, 1499 (1953).

(84) A.O. Nier and E.E. Hanson, Phys. Rev., 50, 722 (1936).

(85) Manufacturing Chemists Association Research Project, Mass Spectral Data, Serial No. 9 (1959).

(86) (a) N.L. Brown and R.H. Cole, J. Chem. Phys., 21, 1920 (1953).

(b) R.W. Swenson and R.H. Cole, J. Chem. Phys., 22, 284 (1954).

(c) S. Havriliak and R.H. Cole, J. Chem. Phys., 23, 2455 (1955); Discussions Faraday Soc., 23, 31 (1957).

(87) (a) R. Fox, J. Chem. Phys., 26, 1281 (1957).

(b) H. Guthier and H. Neuert, Z. Naturforsch, 9a, 335 (1954).

(88) G. Herzberg, "Molecular Spectra and Molecular Structure", (I. Spectra of Diatomic Molecules) Van Nostrand, New York (1955).

(89) (a) A. Allerhand and P. von R. Schleyer, J. Am. Chem. Soc., 85, 1233 (1963).

(b) D W. Sharp, J. Chem. Soc., 2558 (1958).

(c) G. Glockler and R.E. Peck, J. Chem. Phys., 4, 658 (1936).

(d) See also reference (86a).

(90) M. Davies, J. Chem. Phys., 15, 739 (1947).

(91 H.A. Schwarz, R.R. Williams, and W.H. Hamill, J. Am. Chem. Soc., 74, 6008 (1952).

(92) M.E. Peach and T.C. Waddington, J. Chem. Soc., 2329 (1960); 1238 (1961).

(93) J.K. Jacques and R.F. Barrow, Proc. Phys. Soc., 73, 538 (1959).

(94) R.F. Barrow and J.G. Stamper, Proc. Roy. Soc., A263, 259, 277 (1961

(95) S.W. Benson, "The Foundations of Chemical Kinetics," McGraw-Hill, Toronto (1960).

(96) F.S. Klein and M. Wolfsberg, J. Chem. Phys, 24, 1494 (1961).

(97) D. Britton and R.M. Cole, J. Phys. Chem., 65, 1302 (1961).

(98) R.R. Williams and R.A. Ogg, J. Chem. Phys., 15, 691 (1947).

(99) Kang Yang, J. Am. Chem. Soc., 84, 3795 (1962).

(100) J.E. Collin, Can. J..Chem., 40, 2172 (1962).

(101) A. Kuppermann and G.G. Belford, J. Chem. Phys., 36, 1412 (1962).

(102) M. Bodenstein and G. Jung, Z. phys. chem., 121, 127 (1926). (see also references (91), (95), and (97))

(103) W. Vaughan, F. Rust, and T. Evans, J. Org. Chém., 7, 477, 491 (1942).

(104) (a) H. Schmitz, H.Schumachker, and A. Jager, Z. phys. chem., B51, 281 (1942).

(b) G.B. Kistiakowski and J.C. Sternberg, J. Chem. Phys, 21, 2218 (1953).

(105) T.G. Castner and W. Kanzig, J. Phys. Chem. Solids, 3, 178 (1957).

(106) L.I. Grossweiner and M.S. Matheson, J. Phys. Chem., 61, 1089 (1957).

(107) R.W.G. Wyckoff, "Crystal Structures", Interscience Publ., New York (1948).

APPENDIX I

The Calculation of Rate Constant Ratios for Competing Atom Reactions

With tne exception of

$$k_{10(H + HBr)}/k_{15(H + Br_2)},$$

which has been determined directly and is reported to be temperature independent (see reference 97), all values of rate constant ratios used for comparison with the ratios determined in this investigation have been calculated using the data presented in Table XVIII. In the case of the values from Ogg and Williams (98), rate constant ratio data was calculated directly from tables presented by them. (The expression for the rate constant ratio

$$k_{(H + HBr)}/k_{(H + HI)}$$

reported by Ogg and Williams is erroneous due to the apparent omission of R, the gas constant, in determining the activation energy term.)

TABLE XVIII

Some Kinetic Parameters of Hydrogen Atom Reactions

Competing Species	Pre-Exponential Factors $\log_{10}(A/T^{1/2})$ liters/mole-sec	Activation Energy Difference Kcal/mole	Ref.
HCl/Cl_2	9.40/10.26	1.5	95, 96
HCl/Br_2	9.40/9.83	2.4	95, 98
HCl/C_2H_4	9.40/9.10	2.2	95, 99
HCl/HBr	9.40/8.91	2.4	95, 98
Cl_2/Br_2	10.26/9.83	0.8	95, 96, 98